nagra.

Technical Report 13-02

An Assessment of the Impact of the Long Term Evolution of Engineered Structures on the Safety-Relevant Functions of the Bentonite Buffer in a HLW Repository

July 2014

D. Savage

Savage Earth Associates Ltd, UK

National Cooperative
for the Disposal of
Radioactive Waste

Hardstrasse 73
CH-5430 Wettingen
Switzerland
Tel. +41 56 437 11 11

www.nagra.ch

nagra.

Technical Report 13-02

An Assessment of the Impact of the Long Term Evolution of Engineered Structures on the Safety-Relevant Functions of the Bentonite Buffer in a HLW Repository

July 2014

D. Savage

Savage Earth Associates Ltd, UK

National Cooperative
for the Disposal of
Radioactive Waste

Hardstrasse 73
CH-5430 Wettingen
Switzerland
Tel. +41 56 437 11 11

www.nagra.ch

This report was prepared on behalf of Nagra. The viewpoints presented and conclusions reached are those of the author(s) and do not necessarily represent those of Nagra.

ISSN 1015-2636

Summary

Bentonite is important as a near-field buffer and backfill for a SF/HLW repository in Opalinus Clay in Switzerland, with desirable properties of this (compacted) material including swelling, low solute transport rates, inter alia. Intrinsic to these properties is that they should be preserved in the long-term, i.e. over safety-relevant timescales (up to a million years). Although evidence from natural analogues can be used to demonstrate the potential stability of bentonite in the repository environment, there are a number of processes which could potentially perturb its long-term performance, such as thermal gradients from the decay heat of waste packages and chemical gradients due to the presence of thermodynamically unstable materials (steel, concrete) used as engineering structures.

These potential interactions of bentonite with engineered components (canister metals, concrete tunnel liner, steel support mesh, and arches, plus transport rails) in a geological repository for SF/HLW in Opalinus Clay have been assessed. These interactions are likely to be strongly non-linear, with a complex interplay between fluid transport, clay ion exchange and dissolution, secondary mineral growth, and consequent changes in physical properties (porosity, permeability, swelling pressure) of the clay. Despite the differing nature of the chemical interactions of bentonite with concrete and steel, it is considered that the timescales of alteration will be very similar due to the similar rates of key processes in the bentonite (montmorillonite dissolution at alkaline pH and the growth of zeolite and sheet silicate minerals). Although timescales of a million years are considered for this alteration, it is envisaged that near-field evolution will be curtailed well within this timeframe by mass transport constraints (porosity decreasing to zero) or mass balance limitations (reactants completely consumed). The time-dependent nature of some of these processes means that not all are readily amenable to study by conventional laboratory experimental procedures. Consequently, the results of published reaction-transport simulations have been important in defining key properties at performance assessment-relevant timescales.

This evaluation suggests that for an optimistic estimate of bentonite alteration at 100 ka limited by mass transport constraints (porosity decreasing to zero), there will be a thin (0.05 m thick; 1 vol.-% total bentonite) alteration layer around the canister, derived partly through thermal redistribution of minerals and aqueous solutes, and partly due to interaction of the steel canister with bentonite. This results in a thin zone with zero porosity and zero swelling pressure (montmorillonite totally altered) around the canister, but with a hydraulic conductivity the same as the initial value (potential minor fracturing is assumed to cancel out the effects of decreased porosity). The mineralogical composition of the thin zone is assumed to consist of a thin layer of calcite, gypsum/anhydrite and magnetite on the canister, with montmorillonite in the altered bentonite replaced by Fe-silicates such as cronstedtite, berthierine and chlorite. Beyond this inner alteration zone is an annulus of 0.68 m (92 vol.-% total) of unaltered bentonite.

The potential interaction of metallic engineered structures other than the canister with bentonite is relatively minor. Even using a mass balance constraint with no kinetic or mass transport limitations for conversion of montmorillonite to chlorite, then only 2 vol.-% of the total bentonite in the canister zone would be transformed by reaction with these structures. Removing the rails prior to closure would reduce this effect to 1 vol.-%.

At the external margin of the bentonite, alteration of the buffer and sealing element adjacent to the concrete liner is optimistically estimated to be 0.02 m in thickness (4 vol.-% total) at 100 ka after closure (note that there is no concrete along the sealing element interface, so this estimate is unrealistic). The hydraulic conductivity of this zone is estimated to be decreased in compari-

son with the initial state. The porosity and swelling pressure of this zone are likely to decrease to zero over a timescale of a few hundreds to a thousand years due to alteration of montmorillonite. The mineralogical composition of this zone is likely to be characterised by a sequence of calcite, C-(A)-S-H minerals, Ca-zeolites, sepiolite and saponite clays, with C-S-H minerals forming nearest the cement contact, and other minerals such as zeolites and clays forming further towards the canister.

The concrete liner itself may degrade via conversion of portlandite and C-S-H gel to ettringite with a consequent increase in porosity. Reaction-transport simulations suggest that porosity may increase a few percent over 100 ka as an optimistic estimate of degradation.

For the sealing element, there are no canisters present, but there are steel reinforcement arches, along with steel mesh, steel anchors and steel rails. Using the conversion of montmorillonite to chlorite mass balance constraint described above, a maximum of 5 vol.-% of bentonite could be transformed to non-swelling silicates. Removing the rails prior to closure would reduce this effect to 4 vol.-%.

For a pessimistic estimate of bentonite alteration at 100 ka after closure, it is assumed that the canister is entirely corroded and degraded to iron oxyhydroxides and in the surrounding bentonite, montmorillonite is considered to be totally converted to non-swelling Fe-silicates such as cronstedtite, berthierine and chlorite (mass balance estimate). This transformation is expected to preserve the original porosity and hydraulic conductivity, but to decrease swelling pressure to zero. This altered zone is estimated to be 0.45 m thick and to extend to the bentonite zone altered by interaction with the concrete liner.

Similarly, alteration of the buffer and sealing element adjacent to the concrete liner is pessimistically estimated to be 0.2 m thick (35 vol.-% total bentonite) at 100 ka after closure. The porosity and hydraulic conductivity of this zone are estimated to be unchanged with regard to the initial state, but with zero swelling pressure due to removal of montmorillonite. The mineralogical composition of this zone is likely to be characterised by a sequence of calcite, C-(A)-S-H minerals, Ca-zeolites, sepiolite and saponite clays, with C-S-H minerals forming nearest the cement contact, and other minerals such as zeolites and clays forming further away. A zone of exchange of Ca for Na ions in montmorillonite a few tens of cm thick will advance in front of the mineral dissolution-precipitation reactions. Corresponding estimates for an OPC concrete liner indicate that the amount of bentonite mass altered is increased by a factor of 2.5 and alteration thicknesses are increased by a factor of between 2.5 and 3 for the tunnel diameters considered (~ 60 vol.-% total bentonite).

The concrete liner is estimated to be totally degraded in terms of physical properties as a pessimistic estimate at 100 ka after closure, but a zone of ettringite, calcite and tobermorite may exist marking its former presence.

The state of the bentonite barrier at 1 Ma after closure is estimated to be similar to that at 100 ka, albeit with more crystalline degradation products of clay and concrete.

The interactions of a copper canister with bentonite are predicted to be restricted to minor amounts of cation exchange in montmorillonite (Cu for Na), resulting in no changes to safety-relevant properties over the lifetime of the repository.

Zusammenfassung

Bentonit spielt sowohl als Barrierenmaterial im Nahfeld als auch als Verfüllmaterial im Schweizerischen BE/HAA-Lagerkonzept im Opalinuston eine wichtige Rolle. Die gewünschten Eigenschaften dieses (kompaktierten) Materials umfassen unter anderem seine Quellfähigkeit und die niedrige hydraulische Leitfähigkeit bei Vollsättigung. Wichtig ist, dass diese Eigenschaften langfristig erhalten bleiben, das heisst über den Betrachtungszeitraum von bis zu einer Million Jahren. Obwohl Erkenntnisse von natürlichen Analoga benutzt werden können, um die potenzielle Integrität von Bentonit unter Lagerbedingungen zu demonstrieren, gibt es eine Anzahl von Prozessen, die seine Integrität möglicherweise beeinträchtigen. Hierzu gehören zum Beispiel die Wärmeabgabe der Endlagerbehälter und chemische Wechselwirkungen mit thermodynamisch instabilen Materialien (Zement und Stahl).

Diese möglichen Wechselwirkungen von Bentonit mit Behältern und Einbauten (Tunnelsegmenten aus Beton, Stahlnetzen, Stahlbögen und Schienen) wurden für ein geologisches Tiefenlager BE/HAA im Opalinuston abgeschätzt. Nicht-lineare und komplexe Wechselwirkungen, welche unter anderem zu Mineralumwandlungen, zu Mineralauflösungs- bzw. Mineralausfällungsreaktionen und zum Ionenaustausch führen, resultieren in einer Änderung der physikalischen Eigenschaften des Bentonits, wie die des Quelldrucks, der Permeabilität und der Porosität. Auch wenn sich die chemischen Wechselwirkungen von Bentonit mit Stahl bzw. zementhaltigen Materialien grundlegend unterscheiden, sind die Reaktionsraten aufgrund des Verhaltens von Bentonit ähnlich (Umwandlung von Montmorillonit zu Zeolithen und Schichtsilikaten bei hohem pH). Obwohl für diese Veränderungen ein Zeitfenster von einer Million Jahren betrachtet wird, nimmt man an, dass sich die Entwicklung im Nahfeld aufgrund von Einschränkungen bei Massentransport (Porosität geht gegen null) oder Massenbilanzen (Reaktant ist aufgebraucht) innerhalb einer kürzeren Periode abspielen wird. Die zeitabhängige Natur einiger dieser Prozesse bedeutet, dass nicht alle mit konventionellen Methoden im Labor untersucht werden können. Deshalb waren Resultate von publizierten Transportmodellierungen wichtig, um Schlüsseleigenschaften auf der für die Sicherheitsanalyse relevanten Zeitskala zu definieren.

Diese Auswertung zeigt auf, dass es bei einer optimistischen Abschätzung von Veränderungen im Bentonit nach 100'000 Jahren, limitiert durch Einschränkungen bei Massentransport (Porosität geht gegen null), eine geringmächtige (0.05 m dünn; 1 Vol.-% des Bentonits) veränderte Schicht um den Behälter herum geben wird. Diese rührt teilweise von thermischen Auflösungs- und Ausfällungsreaktionen von Mineralen und teilweise von Wechselwirkungen der Stahlbehälter mit dem Bentonit her. So entsteht eine geringmächtige Zone um den Behälter ohne Porosität und Quelldruck (wo der Montmorillonit völlig umgewandelt ist). Die hydraulische Leitfähigkeit entspricht aber weiterhin dem Anfangswert, da davon ausgegangen wird, dass mögliche kleine Risse den Effekt verminderter Porosität ausgleichen werden. Es wird angenommen, dass die mineralogische Zusammensetzung der geringmächtigen Zone aus einer dünnen Schicht Calcit, Gips / Anhydrit und Magnetit (auf der Behälteroberfläche) besteht, während der Montmorillonit im umgewandelten Bentonit durch Fe-Schichtsilikate wie Cronstedtit, Berthierin und Chlorit ersetzt wird. Jenseits dieser inneren alterierten Zone besteht weiterhin ein 0.68 m mächtiger (92 Vol.-%) Bereich von unverändertem Bentonit.

Abgesehen vom Behälter sind die möglichen Wechselwirkungen von Bentonit mit weiteren Stahlelementen von geringer Bedeutung. Auch wenn man Massenbilanzen ohne kinetische oder transportbedingte Limitierungen betrachtet, würden maximal 2 Vol.-% des gesamten Bentonits in Chlorit umgewandelt werden. Werden die Schienen vor der Verfüllung des Nahfelds entfernt, wird 1 Vol.-% des Bentonits in Chlorit umgewandelt werden.

Am Kontakt zwischen Bentonit und Zementausbau wird die veränderte Zone in der Bentonitverfüllung und der hydraulischen Barriere, welche an die Betonauskleidung anschliesst, optimistisch auf eine Mächtigkeit von 0.02 m (4 Vol.-%) 100'000 Jahre nach Verschluss geschätzt. (Man beachte, dass kein Beton entlang der Berührungsfläche mit der hydraulischen Barriere vorhanden ist, deshalb ist diese Schätzung unrealistisch).

Die hydraulische Leitfähigkeit dieser Zone wird im Vergleich mit dem Ausgangszustand vermutlich abnehmen. Die Porosität und der Quelldruck dieser Zone werden wahrscheinlich über einen Zeitraum von ein paar hundert bis tausend Jahren auf null abnehmen, aufgrund der Umwandlung des Montmorillonits. Die mineralogische Zusammensetzung dieser Zone wird vermutlich durch eine Sequenz von Calcit, C(-A)-S-H-Phasen, Ca-Zeolithen, Sepioliten sowie Saponiten charakterisiert, wobei sich C-S-H-Phasen beim Kontakt zum Zement und andere Minerale, wie Zeolithe und Tone, näher am Behälter bilden.

Der Betonausbau selbst könnte via Umwandlung zu Portlandit und C-S-H-Gel zu Ettringit degradieren, woraus eine Zunahme der Porosität resultieren würde. Transportmodellierungen lassen vermuten, dass die Porosität, bei einer optimistischen Schätzung dieser Umwandlung über 100'000 Jahre, einige wenige Prozente zunehmen wird.

Bei der hydraulischen Barriere gibt es keine Behälter, aber es gibt stahlverstärkte Bögen zusammen mit Stahlnetzen, Stahlankern und Stahlschienen. Wenn man die oben beschriebenen Massenbilanz-Auflagen zur Umwandlung von Montmorillonit zu Chlorit benutzt, könnte ein Maximum von 5 Vol.-% Bentonit in nicht-quellende Silikatminerale umgewandelt werden. Würde man die Schienen vor Verschluss entfernen, würde sich dieser Effekt auf 4 Vol.-% reduzieren.

Für eine pessimistische Schätzung der Bentonitumwandlung 100'000 Jahre nach Verschluss wird angenommen, dass der Behälter vollständig korrodiert und zu Eisenoxid abgebaut ist. Im umgebenden Bentonit gilt die Annahme, dass der Montmorillonit vollständig zu nicht-quellenden Fe-Silikaten wie Cronstedtit, Berthierin und Chlorit (Schätzung der Massenbilanz) umgewandelt wird. Es wird erwartet, dass durch diese Umwandlung die ursprünglichen Porositäts- und hydraulischen Leitfähigkeitseigenschaften bewahrt werden, aber der Quelldruck auf null zurückgeht. Diese veränderte Zone wird vermutlich 0.45 m mächtig sein und erstreckt sich bis zur Bentonitzone, die durch die Interaktion mit dem Betonausbau verändert wurde.

Ähnlich verhält es sich bei einer pessimistischen Annahme betreffend der Veränderung in der Bentonitverfüllung und der hydraulischen Barriere am Kontakt mit dem Betonausbau, die 100'000 Jahre nach Verschluss auf 0.2 m Mächtigkeit (35 Vol.-% des Bentonits) geschätzt wird. Die Porosität und hydraulische Durchlässigkeit dieser Zone werden in Bezug zum anfänglichen Zustand bis auf den Quelldruck (aufgrund des fehlenden Montmorillonits) vermutlich unverändert bleiben. Die mineralogische Zusammensetzung dieser Zone wird wahrscheinlich durch eine Abfolge von Calcit, C(-A)-S-H-Phasen, Ca-Zeolithen, Sepioliten sowie Saponiten charakterisiert, wobei sich C-S-H-Phasen am Kontakt zum Zement und mit zunehmender Distanz Minerale wie Zeolithe und Tone bilden. Eine Zone in welcher Ca- und Na-Ionen im Montmorillonit ausgetauscht sind, wird mit einigen Dezimetern den mineralischen Ausfällungs- und Auflösungsreaktionen vorausgehen. Entsprechende Schätzungen für einen OPC-Betonausbau weisen darauf hin, dass die Menge der veränderten Bentonitmasse um einen Faktor 2.5 erhöht wird und die Schichtmächtigkeit von alteriertem Bentonit um einen Faktor zwischen 2.5 und 3 (~ 60 Vol.-% des Bentonits) für die betrachteten Tunneldurchmesser zunehmen wird.

Bei einer pessimistischen Abschätzung wird der Betonausbau 100'000 Jahre nach Verschluss in Hinsicht auf seine physikalischen Eigenschaften völlig degradiert und durch eine Zone von Ettringit, Calcit und Tobermorit ersetzt werden.

Der Zustand der Bentonit-Barriere eine Million Jahre nach Verschluss wird mit dem Zustand der Barriere nach 100'000 Jahren vergleichbar sein, wenn auch mit einer erhöhten Menge an kristallinen Abbauprodukten aus Ton und Zement.

Es wird erwartet, dass sich die Wechselwirkung eines Kupferbehälters mit Bentonit auf einen begrenzten Kationenaustausch im Montmorillonit (Cu mit Na) beschränkt, was keinen Einfluss auf die sicherheitstechnischen Eigenschaften des Bentonits hat.

Résumé

Dans le concept de stockage géologique de la Nagra pour les éléments combustibles usés et les déchets de haute activité vitrifiés, la bentonite – en tant que composante des barrières ouvragées et matériau de remblayage des galeries – joue un rôle important pour la sûreté du dépôt, ceci notamment en raison de sa faible conductivité hydraulique et de ses propriétés de gonflement. Ces caractéristiques doivent perdurer tout au long de la période considérée dans les analyses de sûreté. Bien qu'il soit possible d'utiliser les analogues naturels pour démontrer la stabilité de la bentonite dans l'environnement d'un dépôt en couches géologiques profondes, certains processus sont toutefois susceptibles d'affecter ses performances sur le long terme, comme par exemple les gradients de température en rapport avec la chaleur dégagée par les colis de déchets, mais aussi les interactions chimiques avec des matériaux instables du point de vue thermodynamique (le ciment et l'acier).

Le présent rapport est consacré aux interactions potentielles, dans un dépôt géologique pour éléments combustibles usés et déchets de haute activité situé dans les argiles à Opalinus, de différents composants des barrières ouvragées avec la bentonite: conteneur en acier, éléments de soutènement (revêtement en béton, treillis d'armature et cintres en acier, etc.), mais aussi éléments en relation avec l'exploitation du dépôt (rails). Ces interactions non-linéaires entrainent des réactions telles que transport de fluides, échanges d'ions, dissolution et transformations minérales, qui sont fortement liées les unes aux autres et induisent des modifications des propriétés physiques de la bentonite, telles que la pression de gonflement, la perméabilité et la porosité. Même si, du point de vue chimique, la bentonite n'interagit pas de la même manière avec l'acier et les matériaux cimentaires, les modifications s'effectueront selon une échelle de temps comparable du fait que les principaux processus (dissolution de la montmorillonite dans un environnement alcalin, formation de zéolithes et de phyllosilicates) se déroulent à la même vitesse. Bien que l'on étudie ces modifications sur une période de un million d'années, il est possible que l'évolution du champ proche se fasse plus rapidement, en raison de contraintes de transfert de masse (valeurs de porosité s'abaissant jusqu'au niveau zéro) ou de bilans massiques (réactifs épuisés). Du fait de la durée de certains de ces processus, ils ne peuvent pas tous être étudiés par le biais d'expériences de laboratoire conventionnelles. Ceci signifie que les résultats de simulations transport/réaction publiées ont joué un rôle important dans l'évaluation des principales caractéristiques sur les périodes prises en compte dans l'analyse de sûreté.

Cette étude suggère que, si l'on estime de manière optimiste l'altération de la bentonite sur 100 000 ans, limitée par des contraintes de transfert de masse (valeurs de porosité s'abaissant jusqu'au niveau zéro), il se formera une fine couche d'altération (0.05 m d'épaisseur, 1 % du volume total de bentonite) autour du conteneur, produite en partie par la redistribution thermique des minéraux et des solutés aqueux, et par l'interaction du conteneur en acier avec la bentonite. Cette fine zone sera caractérisée par une porosité et une pression de gonflement nulles (la montmorillonite sera complètement altérée), mais sa conductivité hydraulique sera restée la même (on suppose que des fissures éventuelles compenseront l'impact de la baisse de porosité). Du point de vue minéralogique, on considère que cette zone consistera en une fine couche de calcite, de gypse / anhydrite et de magnétite autour du conteneur, la montmorillonite de la bentonite altérée étant remplacée par des silicates de fer tels que la cronstedtite, la berthièrine et la chlorite. Cette zone altérée interne sera entourée par un anneau de 0.68 m (92 % du volume total) de bentonite intacte.

L'interaction potentielle des structures métalliques autres que le conteneur avec la bentonite est relativement faible. Même si, pour la transformation de la montmorillonite en chlorite, on utilise une contrainte de bilan massique sans limites cinétiques ou de transfert de masse, seulement

2 % du volume total de bentonite autour du conteneur seraient transformés à l'issue d'une réaction avec ces structures. Si l'on retire les rails avant la fermeture du dépôt, ce chiffre s'abaisse à 1 % du volume total.

A la limite extérieure de la bentonite, l'altération du remblayage et du scellement proche du revêtement en béton est, de manière optimiste, estimé à 0.02 m d'épaisseur (4 % du volume total) 100 000 ans après la fermeture du dépôt (il faut remarquer que cette évaluation n'est pas réaliste du fait qu'il n'y pas de béton à l'interface du scellement). On estime que la conductivité hydraulique de cette zone aura diminué par rapport à l'état initial. La porosité et la pression de gonflement de cette zone vont probablement tomber à zéro sur une période allant de quelques centaines à un millier d'années en raison de l'altération de la montmorillonite. La composition minéralogique de cette zone sera probablement caractérisée par une séquence de calcite, des minéraux C-(A)-S-H, des zéolithes de calcium, des argiles de type sépiolite et saponite, les minéraux C-S-H étant localisés dans la zone la plus proche de l'interface avec le ciment, et tandis que d'autres minéraux tels que les zéolithes et les argiles apparaitront dans la zone proche du conteneur.

Le revêtement en béton lui-même peut se dégrader (transformation de la portlandite et de gel C-S-H en ettringite), entrainant une augmentation significative de la porosité. Les simulations de réaction / transport indiquent que sur 100 000 ans, la porosité pourra augmenter de quelques pourcents, en se basant sur une évaluation optimiste de la dégradation.

Il n'y a pas de conteneurs à proximité du scellement. En revanche, on trouve des cintres et un treillis d'armature, des tirants d'ancrage et des rails – tous ces éléments étant en acier. Sur la base des contraintes de bilan massique décrites plus haut pour la transformation de mont-morillonite en chlorite, on estime qu'un maximum de 5 % du volume de bentonite pourrait être transformé en silicates non gonflants. Si l'on retire les rails avant la fermeture, ce chiffre s'abaisse à 4 % du volume total.

Pour obtenir une évaluation pessimiste de l'altération de la bentonite 100 000 ans après la fermeture du dépôt, on pose comme hypothèse que le processus de corrosion a conduit à la dégradation complète du conteneur en oxyhydroxydes de fer et que, dans la bentonite qui l'entoure, la montmorillonite s'est complètement transformée en silicates de fer non gonflants, tels que la cronstedtite, la berthièrine et la chlorite (évaluation du bilan massique). On considère que suite à cette transformation, ni la porosité, ni la conductivité hydraulique de la bentonite ne seront affectées; en revanche, la pression de gonflement tombera à zéro. On estime que cette zone altérée aura une épaisseur de 0.45 m et s'étendra jusqu'à la zone de bentonite altérée par l'interaction avec le revêtement en béton.

De même, toujours selon une estimation pessimiste, on considère que le remblayage et le scellement en contact avec le revêtement en béton auront encore une épaisseur de 0.2 m (35 % du volume total de bentonite) 100 000 ans après la fermeture du dépôt. On estime que, dans cette zone, la porosité et la conductivité hydraulique originales ne seront pas modifiées, mais qu'en raison de la transformation de la montmorillonite, la pression de gonflement deviendra nulle. La composition minéralogique de cette zone sera probablement caractérisée par une séquence de calcite, des minéraux C-(A)-S-H, des zéolithes de calcium, de la sépiolite et de la saponite. Les minéraux C-S-H se formeront dans la zone la plus proche du ciment, tandis que les autres minéraux tels que les zéolithes et les argiles seront présents dans une zone plus éloignée. Une zone d'échange d'ions (Ca – Na), de quelques dizaines de cm d'épaisseur, se formera dans la montmorillonite à l'avant de la zone de réactions de dissolution-précipitation minérales. Dans le cas d'un revêtement en béton OPC, on estime que la masse de bentonite

altérée augmentera d'un facteur de 2.5, l'épaisseur des zones d'altération étant multipliée par un facteur allant de 2.5 à 3 pour les diamètres de galeries considérés (~ 60 % du volume total de bentonite).

100 000 ans après la fermeture du dépôt, on considère – de façon pessimiste – que le revêtement en béton aura perdu toutes ses capacités physiques en raison de sa dégradation. Toutefois, il est possible que subsiste une zone comportant de l'ettringite, de la calcite et de la tobermorite.

On estime que, un million d'années après la fermeture du dépôt, la barrière de bentonite sera dans un état similaire à celui qu'elle avait atteint au bout de 100 000 ans, avec toutefois des produits cristallins de dégradation de l'argile et du béton en plus grandes quantités.

On prévoit que les interactions entre un conteneur en cuivre et la bentonite se limiteront à de faibles quantités d'échange de cations dans la montmorillonite (Cu – Na), ce qui n'entrainera pas de modifications des caractéristiques importantes pour la sûreté du dépôt sur l'ensemble de sa durée de vie.

Table of Contents

List of Tables

List of Figures

1 Introduction

Bentonite is important as a near-field buffer and backfill for a SF/HLW repository in Opalinus Clay in Switzerland (Nagra 2002). Desirable properties of this material include (Nagra 2002, Leupin & Johnson 2014):

- low hydraulic conductivity ($< 10^{-11}$ m s^{-1})
- chemical retention of radionuclides
- sufficient density (saturated density > 1650 kg m^{-3})
- sufficient swelling pressure (> 0.2 MPa)
- mechanical support (buffer must be sufficiently viscous to avoid canister sinking)
- sufficient gas transport capacity
- minimise microbial activity
- resist mineral transformation
- suitable heat conduction.

Intrinsic to these properties is that they should be preserved in the long-term, i.e. over safety-relevant timescales (up to a million years). Although evidence from natural analogues can be used to demonstrate the potential stability of bentonite in the repository environment in the long-term (e.g. Miller et al. 2000 and references therein), there are a number of processes which could potentially perturb its long-term performance:

- the decay heat of waste packages will impose temperature gradients on the EBS in the short- to medium-term, potentially accelerating any disequilibrium reactions between natural (groundwater, rock) and engineered barriers (canister metals, rock bolts, support arches, concrete tunnel linings etc).
- Some engineering materials (steel, cement/concrete) are thermodynamically unstable in the geological/repository environment and their degradation could cause chemical reaction at interfaces with bentonite.
- Bentonite is a natural geological material, but there may be chemical disequilibrium with ambient groundwater, leading to cation exchange and possible transformation of mont-morillonite through slow dissolution-precipitation processes to other clays/sheet silicates such as illite, saponite, beidellite etc.

Although there may be mass action, mass balance and kinetic drivers for alteration reactions, ultimately, these reactions are controlled to a large degree by the transport properties of the host rock and the bentonite.

However, uncertainties regarding the definitive location of a repository for HLW/SF in Switzer-land, the depth, and the associated stress situation at the disposal site, mean that substantial support for disposal tunnels might be needed (Leupin & Johnson 2014). Emplacement tunnels in the Opalinus Clay may therefore need to be supported with rock bolts and mesh which have a limited lifetime (reference design) or rock bolts and liner (alternative support concept) (see Figure 1). In either case, the lifetime of the support is designed to provide stable conditions during construction and operation (up to several years). Tunnel support has only an operational safety/feasibility requirement and does not contribute to long-term safety. Nonetheless, the measures taken should not violate the safety principles, which include compartmentalisation and minimising detrimental interactions (such that other components of the disposal system can achieve their functions).

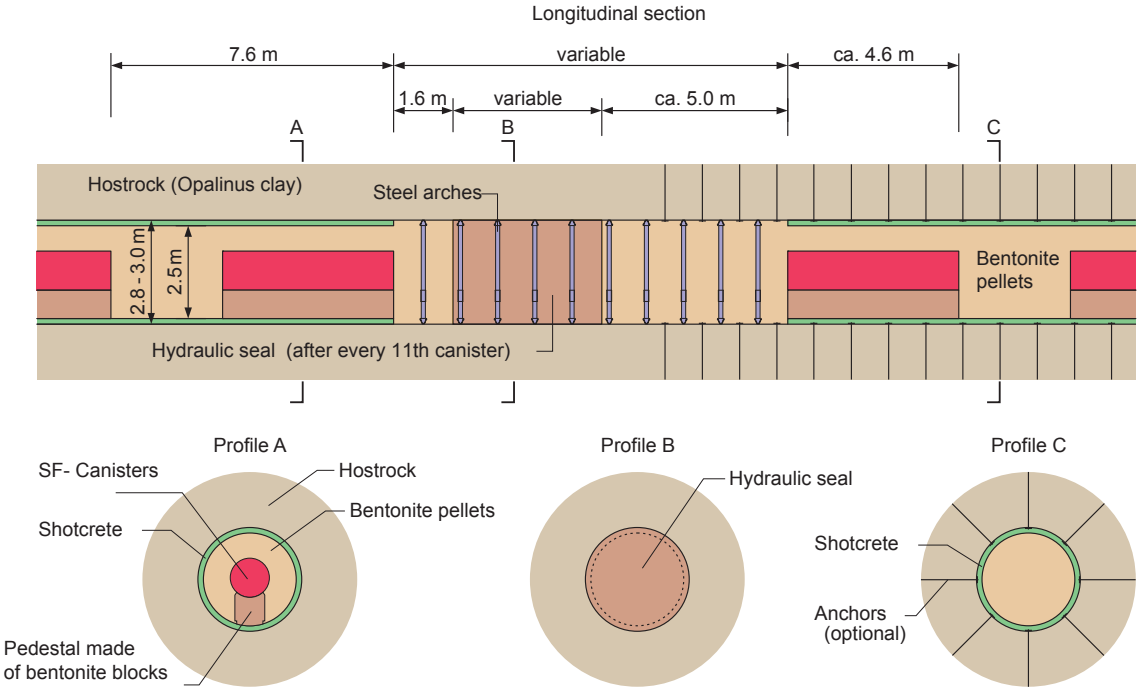

Fig. 1: Schematic diagram of the near-field design of the Swiss SF/HLW based on Nagra (2010) that was used in this study as a conceptual basis for investigating the long-term evolution of the safety relevant functions of bentonite buffer.

From Nagra.

The report presented here includes and extends the previously-reported analysis of the interaction of bentonite with the concrete tunnel liner (Savage et al. 2010b), to include interaction effects from the supporting steel mesh and support arches, and also interactions with canister metals. The effects of the thermal output of the wastes upon bentonite stability have also been evaluated. The principal focus of this report has been on the perturbation of the following safety-relevant properties:

- porosity
- hydraulic conductivity
- swelling pressure
- mineralogical composition.

Following this Introduction, Section 2 discusses key reactions in the alteration process, and Section 3 considers the geometry of the Nagra near-field concept, along with volumes and compositions of barrier components. Sections 4, 5 and 6 consider interactions due to the thermal period, due to interactions with concrete, and due to interactions with metals, respectively. A Summary/Conclusions section comprises Section 7. Appendix A considers the impacts upon potential alternative near-field designs.

2 Key Processes in the Evolution of the Bentonite Buffer

Key processes in the potential long-term alteration of bentonite with engineered structures are the following:

- resaturation and swelling
- ion exchange
- mineral dissolution and precipitation
- mass transport.

These processes are discussed in detail below. Other processes which may have a (lesser) impact would include:

- radiation
- gas and water transport
- microbial activity
- any volume changes associated with metal corrosion.

In this section consideration is also given to potential uncertainties regarding estimating the magnitude and nature of alteration.

2.1 Resaturation and swelling

Resaturation of bentonite may be a slow process due to the slow wetting by groundwater through the concrete liner at the contact with the Opalinus Clay and competing evaporation of water at the interface with the waste packages during the thermal period (Nagra 2002).

At low water saturations, the fraction of water held in interlayer water in montmorillonite is high (represented by high suctions in simple capillary pressure models) and negligible amounts of water exist in all other liquid forms. As water saturation increases, the amount of water in the other forms increases. At high saturations is there a significant amount of liquid water in the free porosity (depending upon the compaction density). Swelling of compacted bentonite is thought to be primarily caused by the effect of (step-wise) water filling the interlayer sites and effectively increasing grain volume, although some limited swelling may occur from water molecules entering the clay double-layers.

Smectite clays can absorb water into clay inter-layers with the most important parameters being the surface charge density of the clay (swelling decreases with increasing charge density), and the charge and solvation behaviour of the inter-layer cations (swelling is greatest for ions such as sodium). Two categories of swelling are generally observed: *innercrystalline swelling* caused by the hydration of the exchangeable cations in the dry clay, and *osmotic swelling*, resulting from concentration gradients in ion concentrations between clay surfaces and pore water (Madsen & Müller-von Moos 1989).

Innercrystalline swelling is attributed to the formation of molecular layers of interlayer water, but is in fact more closely associated with the solvation stages of the interlayer cations themselves (Skipper et al. 2006). The hydration energy is much greater than the bond between the clay layers and pressures of more than 100 MPa can result (Madsen & Müller- von Moos 1989). The cation-clay interaction strongly depends upon the charge locus, with tetrahedral charge sites

(which are closer to the interlayer) leading to more strongly-bonded inner sphere complexes (Hensen & Smit 2002). Wyoming (MX-80) smectites are *beidellitic montmorillonites* (octahedral > tetrahedral charge). Hydration occurs stepwise, with a maximum of four water layers possible. Initially, water is absorbed on external surfaces and once a monolayer capacity is reached, the interlamellar space opens to form a monolayer hydrate (Cases et al. 1992).

As originally pointed out by Grauer, osmotic swelling (and models thereof) is insignificant where bentonite water contents are less than 30 % (about two interstitial water layers in the montmorillonite structure), in other words, in most repository conditions (Grauer 1986). Osmotic swelling operates over larger distances than innercrystalline swelling and in sodium montmorillonite can result in total separation of clay layers. Because the interlayer ions are fixed for electrostatic reasons, water is taken up into the interlayer spaces to balance concentration, provided there is a higher concentration in the interlayer spaces. Osmotic swelling depends to a large extent on the electrolyte concentration and the valency of the dissolved ions. Innercrystalline swelling depends only slightly on these factors.

Note also that resaturation will occur from the Opalinus Clay through the concrete liner, such that the bentonite will be hydrated by a hyperalkaline fluid. Moreover, the eventual bentonite pore fluid will be conditioned by reaction with the concrete liner.

2.2 Ion exchange

The exchange of interlayer cations in montmorillonite could lead to changes in physical properties, especially swelling pressure. Although Ca-exchanged bentonites generally have similar swelling properties as Na-bentonites at given dry densities (e.g. Karnland 2010), the swelling pressures of K- or Mg-exchanged bentonites are lower (Müller-von Moos et al. 1990).

In smectite clays such as montmorillonite, clay layers bear a permanent negative charge compensated by counterions located between them (interlayer space). These counterions are the origin of two features of clay behaviour: swelling, and cation exchange. The former refers to the entrance of water into the clay, while the latter involves the replacement of natural counterions like Na^+ by other ions initially in the aqueous solution in contact with the mineral, and the concomitant release of Na^+ to the solution. Studies have shown that, under a given set of conditions, various cations are not equally replaceable and do not have the same replacing power. In principle, the following law of replacement applies (e.g. Pusch 2002b):

$$Li < Na < K < Ca < Mg < NH_4$$

This implies preferential replacement of e.g. Na^+ by Ca^{2+} rather than *vice versa*. According to the current paradigm for ionic exchange in clays, specific interactions between the ions and the clay surface, or the hydration properties of ions in the clay interlayer, are the driving force for ion exchange (Rotenberg et al. 2009). These microscopic features are then thought to weigh in favour of the interactions of clay interlayers with larger cations. However, considering only the properties of the clay to infer properties of cation exchange can lead to erroneous conclusions since it is the hydration free energy difference, i.e. the contribution of the water phase, that leads to an overall exchange of small ions for larger ones (e.g. Na^+ for Cs^+) (Rotenberg et al. 2009).

Compaction may also affect cation exchange by reducing the activity of water and thereby reducing the hydration of aqueous species (e.g. Wang et al. 2003). Cations with a low hydration tendency, such as caesium, therefore accumulate in the interlayer space, whereas highly hydrated cations such as sodium tend to accumulate in the bulk water where water is easily available for hydration (Van Loon & Glaus 2008).

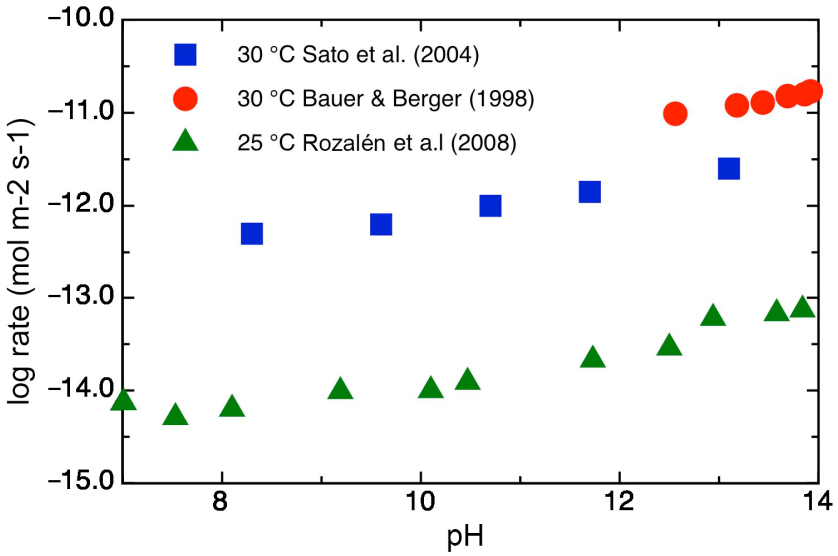

Fig. 2: Summary of near-room temperature experimental studies of montmorillonite dissolution at neutral to alkaline pH and under far-from-equilibrium conditions at high water/clay ratios.

Data are from Bauer & Berger (1998), Rozalén et al. (2008) and Sato et al. (2004).

The evolution of the cation exchange composition of bentonite in a repository for SF/HLW in Opalinus Clay has been modelled by Wersin and co-workers (Curti & Wersin 2002, Wersin 2003, Wersin et al. 2004) who suggest some exchange of Ca from the Opalinus groundwater for Na on interlayer sites in montmorillonite, but with Na remaining the dominant cation.

2.3 Mineral dissolution and precipitation

Although often ignored in models of bentonite pore fluid evolution (e.g. Curti & Wersin 2002, Wersin 2003, Wersin et al. 2004), montmorillonite will undergo dissolution of the aluminosilicate framework under disequilibrium conditions, with concomitant precipitation of secondary minerals (e.g. Savage et al. 2010a, 2011). Although these processes may be undetectable in laboratory experiments, in the long-term they have the potential to modify pore fluid compositions and the mineralogical composition of bentonite, especially where thermal and chemical gradients exist (e.g. Savage et al. 2010a, 2011).

These reactions are excluded from models of bentonite evolution because of their slow nature (e.g. Arcos et al. 2006), but are accelerated by increasing temperature and pH (e.g. Figure 2). Although the data in Figure 2 show considerable variation (across three orders of magnitude at equivalent pH), reaction rates are in the order of 10^{-14} to 10^{-11} mol m^{-2} s^{-1}. With regard to reaction with concrete leachates, it may be seen that there is a significant dependence upon pH (OH-), broadly described by a rate being proportional to [H+] - 0.3. This implies that the rate of dissolution of montmorillonite is a factor of 8 greater at pH 11 than at pH 8 (ambient pH of

bentonite pore fluids) and a factor of 4 greater at pH 13 than at pH 11. Increasing temperature also increases rates such that dissolution of montmorillonite is roughly two orders of magnitude greater at 70 than at 25 °C (Sato et al. 2004).

However, this is a pessimistic (and unrealistic) scenario, i.e. that dissolution of montmorillonite occurs under far-from-equilibrium conditions at large fluid/solid ratios in compacted bentonite. In reality, the rate of dissolution would be slowed orders of magnitude by rapid approach to equilibrium in the compacted state (i.e. very low fluid/solid ratio). As a contrast to the studies of montmorillonite dissolution in dispersed, high water/clay systems, Yamaguchi et al. (Yamaguchi et al. 2007) studied the alteration of clay in compacted bentonite-sand mixes at alkaline pH and variable temperature. Extrapolating their data to pH 10 at 25 °C results in an apparent rate of ~ 10^{-18} mol m^{-2} s^{-1} (i.e. approximately 50'000 times less than the rate in dispersed systems).

Nevertheless, clay dissolution-precipitation reactions need to be accounted for explicitly in models of long-term behaviour since the slow transformation of montmorillonite in bentonite may change its safety-relevant properties.

2.4 Mass transport

Physicochemical processes in bentonite will be limited by slow diffusive transfer of water and solutes through the bentonite. Effective diffusion coefficients for solute transport through bentonite are very low, and generally less than 10^{-10} m^2 s^{-1}. Mass transport by diffusion will thus inhibit alteration of bentonite. Moreover, dissolution-precipitation reactions may affect the porosity distribution in the bentonite, and hence diffusion rates, leading to strongly-coupled non-linear interactions. Replacement of montmorillonite by solids of greater molar volume (e.g. zeolites) may thus inhibit chemical reactions through limitation of mass transport.

2.5 Uncertainties

Most of the conclusions described in this report are based upon the results of relevant reaction-transport simulations, because of their capacity to incorporate effects of mass transport on the overall magnitude of alteration. A typical alteration profile from one of these calculations is shown in Figure 3. Simple scoping calculations involving mass balance or kinetic constraints produce highly pessimistic estimates of alteration (see for example the previous report on this subject – Savage et al. 2010b). Although it is believed that such data provide the most realistic appraisal of long-term bentonite alteration, there are a number of uncertainties relating to:

- a lack of relevant experimental and analogue data to ground-truth such simulations
- a limited number of simulations related to bentonite behaviour in Opalinus Clay
- isothermal boundary condition used in most reaction-transport simulations rather than an evolving temperature field. These conditions cannot adequately simulate mass transfer due to thermal gradients
- reaction transport simulations can indicate the magnitude of redistribution of silica due to thermal gradients but cannot relate changes to cementation (loss of swelling) effects.
- there are currently no reported studies simulating the interactions of compacted MX-80 bentonite with fluids typical of low pH cements, although there are some investigations of the interactions of FEBEX bentonite with $Ca(OH)_2$ solutions (e.g. Michau 2005)

- thermodynamic and kinetic data for some key solids such as montmorillonite, iron-silicates such as berthierine, zeolites, and C-(A)-S-H solids are relatively poorly-defined (e.g. Savage et al. 2007)
- there are poorly-understood couplings between chemical and physical properties, e.g. how permeability is affected by changes in porosity (e.g. Kosakowski et al. 2009).

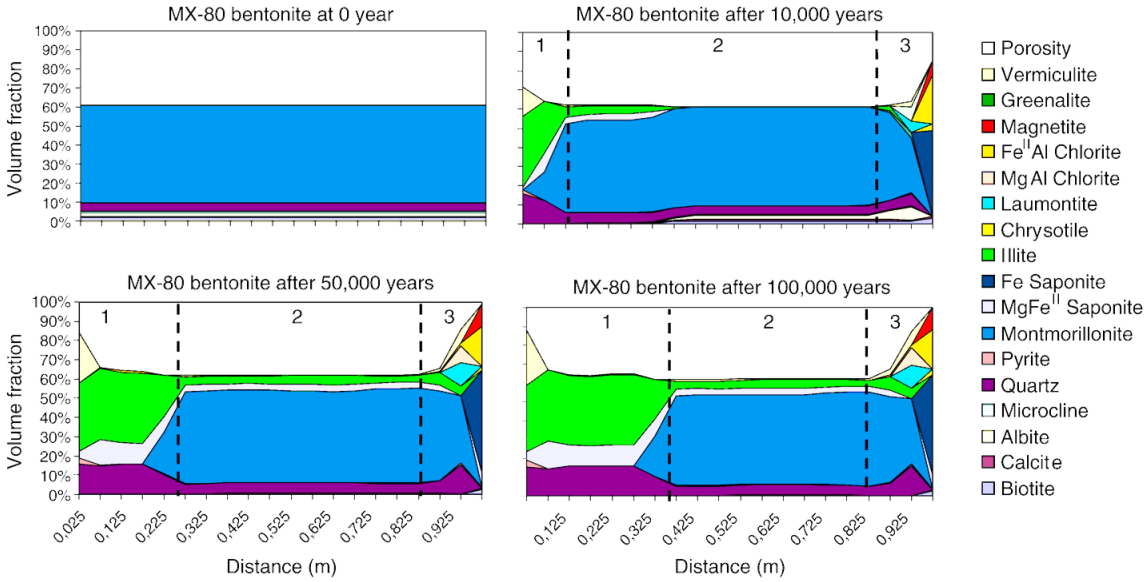

Fig. 3: A typical mineralogical alteration profile from a reaction-transport simulation.

The figure shows the interaction of a steel canister (right margin) and a 1m thickness of MX-80 bentonite (main Figure) and a mudstone groundwater (left margin) at 100 °C after different elapsed times. From Marty et al. (2010).

Currently, there is considerable debate about the nature of porosity in compacted bentonite particularly regarding whether different pore types exist (e.g. Bradbury & Baeyens 2003) or whether bentonite properties are adequately described by a single porosity type (e.g. Birgersson & Karnland 2009). This debate is outside the scope of the report presented here, but suffice it to say that porosity considered here is envisaged as total porosity without prejudice to these two contrasting theories.

3 Input Constraints: Geometry, Volumes, Compositions, T-H evolution

This Section lists fundamental data regarding near-field geometry, inventories and compositions of materials and thermal evolution for analysis presented in Sections 4 – 6. Some of these data have been reported previously (Savage et al. 2010b).

3.1 Geometry

The requirements for the repository near-field including a concrete liner are illustrated in Figure 1 and Figure 4. These show a 15 cm thick concrete liner around a cylindrical section tunnel of approximately 2.5 m internal and 2.8 m external diameters. After anticipated slow rock creep with time, these diameters are expected to be reduced to 2.3 and 2.5 m, respectively.

This cylindrical tunnel contains 4.6 m-long HLW/SF canisters of either 1.05 (HLW) or 0.94 (spent fuel) m diameter, spaced 3 m apart, surrounded by compacted or pelletized MX-80 bentonite of 1450 kg m^{-3} dry density (swelling pressure ~ 4.5 MPa if rigidly confined). Canisters will be constructed of either thick-walled (~ 15 cm) carbon steel or a composite canister fabricated from a copper shell with a cast iron insert (Johnson & King 2003)

After every ten canisters, there is a 10.6 m length of sealing element which consists of compacted MX-80 bentonite of 1650 – 1750 kg m^{-3} dry density (a mean value of 1700 kg m^{-3} is adopted here = 10 – 20 MPa) filling the tunnel as far as the Opalinus Clay, preventing the liner acting as a fast pathway (Figure 1). Here, ten steel arches help support the tunnel in the absence of the concrete liner (Figure 1). Dimensions of a tunnel cross-section are shown in Figure 4.

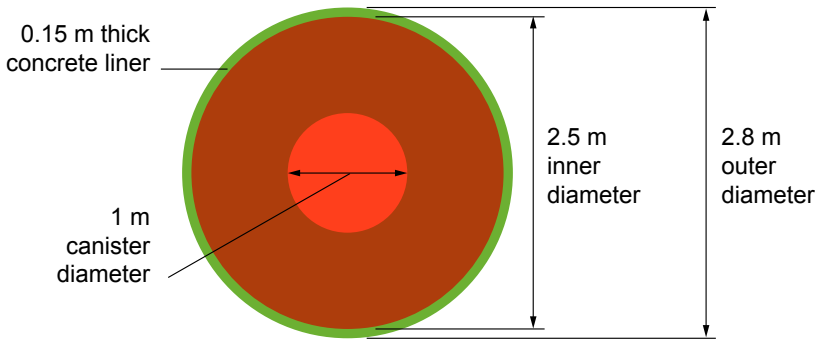

Fig. 4: Dimensions of the outer and inner tunnel sections and canister (not to scale).

Note that after deformation due to rock creep, the inner diameter becomes 2.3 m (Nagra 2002). Modified from Savage et al. (2010b).

3.2 Volumes, masses and surface areas

3.2.1 Concrete

The volumes of concrete in the tunnel liner for a nominal 1 m length of tunnel for both pre- and post-creep conditions are defined in Table 1. A reference canister of 1 m diameter has been assumed to simplify calculations.

3.2.2 Bentonite

The volumes of bentonite for both pre- and post-creep conditions for a 1 m nominal tunnel length are defined in Table 2. A reference canister diameter of 1 m has been assumed.

3.2.3 Metals (canister, reinforcement arches and other structures)

Reference canister dimensions of 1 m diameter by 4.6 m long for both cast steel and composite copper/iron canisters have been assumed to simplify calculations (Table 3). For the steel canister, a total averaged steel mass of 23'000 kg has been assumed[1].

The needed engineered structures to support an emplacement tunnel were estimated based on the planning of the FE-demonstration experiment at the Mont Terri underground rock laboratory. The actual implemented engineered support might differ from the planning (Daneluzzi et al. 2014). Table 4 gives an overview how these numbers were derived for the present study.

Steel reinforcement arches are envisaged to support the tunnel liner around the sealing element with an emplacement density of one arch per metre of tunnel based on the FE demonstration experiment at the Mont Terri Underground Rock Laboratory. Reinforcement steel mesh is used throughout the tunnels, with an emplacement density of 29 kg per metre of tunnel. Steel anchors and anchor plates might also be used throughout, with a total emplacement density of 32.1 kg per metre of tunnel. Steel rails might be used throughout the tunnels to enable canisters to be emplaced at a density of 81.5 kg m^{-1} of tunnel. Some of these engineered structures may be removed prior to tunnel closure. Table 5 summarises these data.

3.3 Compositions of materials

3.3.1 Bentonite

Nagra intends to use pure MX-80 in the form of compacted blocks of 1450 kg m^{-3} dry density as a pedestal-type support for canisters in their near-field design, together with a higher density form (1650 – 1750 kg m^{-3}) as a sealing element between sequences of canisters (Figure 1). The backfill around the canisters will be granular bentonite, comprising ~ 80 % by volume of dense granules (~ 2100 – 2200 kg m^{-3}) and 20 % powder. At emplacement, it will have a dry density of 1450 kg m^{-3} for the buffer and 1650 – 1750 kg m^{-3} for the sealing element. The mineralogical composition of MX-80 is shown in Table 6.

[1] New design studies indicate a total mass (empty) of 17 tons for SF canisters (and 6.4 tons for HLW canisters) (Patel et al. 2012) while earlier design studies by Johnson & King (2003) calculated a total mass (empty) of 26 tons for a SF canister.

Bentonite density is usually expressed as the density of the (oven-dried) dry material (ρ_d). The criterion for the clay density in the near-field is usually expressed as saturated density (ρ_{sat}). The density at saturation can be expressed as (SKB 2006):

$$\rho_{sat} = \rho_d + \left(1 - \frac{\rho_d}{\rho_s}\right)\rho_w \quad (1)$$

where ρ_s is the mineral density (2750 kg/m^{-3}) and ρ_w is the density of water (1000 kg m^{-3}). The calculated saturated density using this method is 1923 kg m^{-3} for the bentonite buffer and 2082 kg m^{-3} for the sealing element (Table 5). The calculated porosity values are 47 (buffer) and 38 % (sealing element).

Tab. 1: Volumes of concrete in the tunnel liner for a nominal 1m length of tunnel.

The tunnel dimensions are defined in Figure 4. Volumes quoted are for both pre- (concrete liner I) and post- (concrete liner II) creep conditions, defined by $\pi r^2 h$, where $\pi = 3.1416$, r = tunnel radius, and h = height (tunnel length).

Tunnel element	**Volume**	**Dimensions**	**Net Volume** [m^3]
Concrete liner I (pre-creep)	Outer tunnel volume – inner tunnel volume	Outer = 1 m length × 1.4 m radius (= 6.16 m^3) Inner = 1 m length × 1.25 m radius (= 4.91 m^3)	1.25
Concrete liner II (post-creep)	Outer tunnel volume – inner tunnel volume	Outer = 1m length × 1.25 m radius (= 4.91 m^3) Inner = 1 m length × 1.15 m radius (= 4.15 m^3)	0.76

Tab. 2: Volumes of bentonite buffer for a nominal 1 m length of tunnel.

The tunnel and canister dimensions are defined in Figure 4. Volumes quoted are for both pre- (canister buffer I) and post-(canister buffer II) creep conditions, defined by $\pi r^2 h$, where $\pi = 3.1416$, r = tunnel radius, and h = height (tunnel length).

Tunnel element	**Volume**	**Dimensions**	**Net Volume** [m^3]
Canister buffer I (pre-creep)	Inner tunnel volume – canister volume	Inner = 1 m length × 1.25 m radius (= 4.91 m^3) Canister = 1 m length × 0.5 m radius (= 0.79 m^3)	4.12
Canister buffer II (post-creep)	Inner tunnel volume – canister volume	Inner = 1 m length × 1.15 m radius (= 4.15 m^3) Canister = 1 m length × 0.5 m radius (= 0.79 m^3)	3.36

Tab. 3: Net volume, surface area and mass for steel and copper canisters.

For the steel canister, a total steel mass of 23'000 kg has been assumed. For the copper canister, a size of 4.6 long by 1.0 m diameter and 0.15 m wall thickness has been assumed. The densities of steel and copper are 7850 and 8960 kg m^{-3}, respectively.

Canister	**Total Volume**	**Net (Metal) Volume** [m^3]	**Total Surface area** [m^2]	**Mass** [kg]
Steel	3.61	1.00	16.02	23000
Copper	3.61	1.00	16.02	8960

Tab. 4: Estimation of the engineered structure to support an emplacment tunnel based on the planning of the FE-demonstration experiment at the Mont Terri underground rock laboratory.

Element	**Calculation**	**Wight per tunnel meter [m']**	**Comment**
Arch (TH 25-profile)	25 kg/m' × π × 2.96 m	232.5 kg	Tunnel diameter (FE-tunnel): 2.96 m
Reinforcement steel mesh (K 169)	3.08 kg/m^2 × π × 3.00 m	29 kg	
Anchor	*7850 kg/m^3 × π × 0.011^2 m^2*	*7.45 kg (per anchor)*	*Diameter: 22 m Length 2.5 m Density: 7'850 kg m^{-3}*
Anchor plate	*per anchor*	*3.14 kg*	
Anchor nut	*per anchor*	*0.1 – 0.2 kg*	
Total weight anchor per tunnelmeter	10.7 kg/m^2 × π × 3 m	32.1 kg	Assumption: 1 anchor per m^2
Rail (Profile S33)	*33.47 kg/m' × 2*	*ca. 67 kg*	
Railway sleeper	*22.7 kg + Anchor = ca. 23 kg*	*11.5 kg*	*Every 2 meters*
Nuts	*3 kg × 2 = 6 kg*	*3 kg*	*Every 2 meters*
Total weight track system		ca. 81.5 kg	

Tab. 5: Masses of additional engineering elements per metre of tunnel.

Structure	**Location**	**Mass** [kg m^{-1}]
Steel arches	Sealing element only	232.5
Steel mesh	throughout	29.0
Steel anchors and plates	throughout	32.1
Rails	throughout	81.5
	Total canister zone	142.6
	Total sealing element	375.1
	Total canister zone less rails	61.1
	Total sealing element less rails	293.6

Tab. 6: Composition of MX-80 bentonite for dry densities of 1450 kg m^{-3} (buffer) and 1700 kg m^{-3} (sealing element) in accord with the most recent design for the near-field (Leupin & Johnson 2014).

MX-80 mineralogical data are from Arcos et al. (2008). Mineral molecular weight data are from the EQ3/6 database thermo.com.V8.R6.230 (Wolery 1992). Note that this composition is slightly different from that described by Bradbury & Baeyens (2003) in that it contains slightly more montmorillonite (87 versus 75 %) and less quartz (5.2 versus 15.2 %).

				Buffer Dry density = 1450 kg m^{-3}			**Sealing Element** Dry density = 1700 kg m^{-3}		
Minerals	wt.-%	Mol wt. [g]	vol.- %	kg m^{-3}	Moles per m^3	vol.-%	kg m^{-3}	Moles per m^3	vol.-%
Na-Montmor	87.00	367.02	86.51	1261.50	3437	50.42	1479.00	4030	53.72
Feldspar (+ mica)	7.00	262.22	7.27	101.50	387	4.24	119.00	454	4.52
Quartz	5.20	60.08	5.34	75.40	1255	3.11	88.40	1471	3.31
Gypsum	0.70	172.17	0.83	10.15	59	0.48	11.90	69	0.51
Pyrite	0.10	119.98	0.05	1.45	12	0.03	1.70	14	0.03
Totals	**100.00**	**-**	**100.00**	**145.00**	**-**		**1700.00**	**-**	
		Water		472.73	26262	41.72	381.82	21212	37.91
		Totals		**1922.73**		**100.00**	**2081.82**		**100.00**

There is a corrrelation between the dry density and swelling pressure for MX-80, which depends upon the salinity of the saturating groundwater at densities less than ~ 1500 kg m^{-3} (Figure 5). This figure indicates that the swelling pressure of the bentonite buffer and sealing element should be approximately 4.5 and 12 MPa, respectively (in dilute groundwater).

SKB has shown that a relationship also exists between dry density and hydraulic conductivity for compacted MX-80 (Figure 6). This figure indicates that the hydraulic conductivity of the bentonite buffer and sealing element should be ~ 5×10^{-14} and ~ 10^{-14} m s^{-1}, respectively (in dilute groundwater).

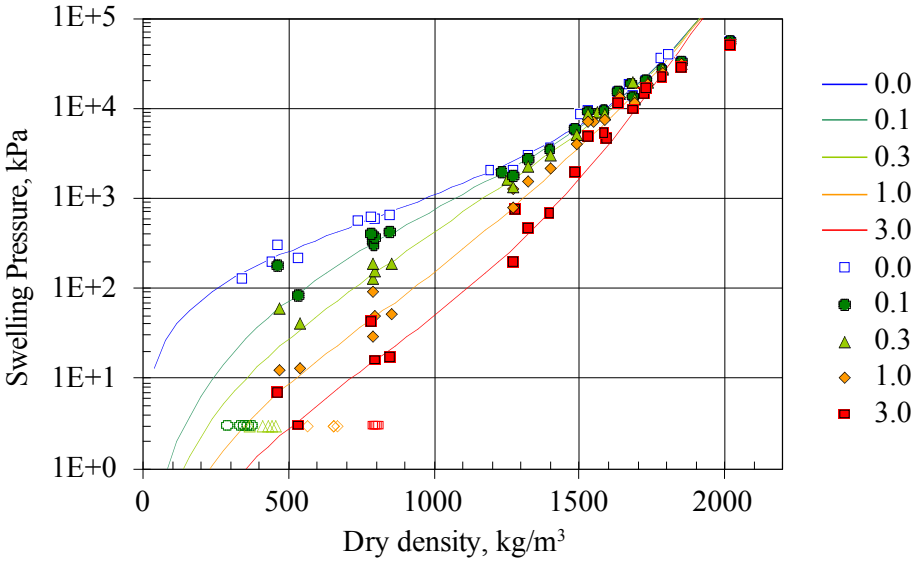

Fig. 5: Measured (squares) and calculated (lines) swelling pressure versus clay dry density for different concentrations in a NaCl solution in equilibrium with the Na-montmorillonite.

The legend shows external solution concentration in mole/L. From SKB (2006).

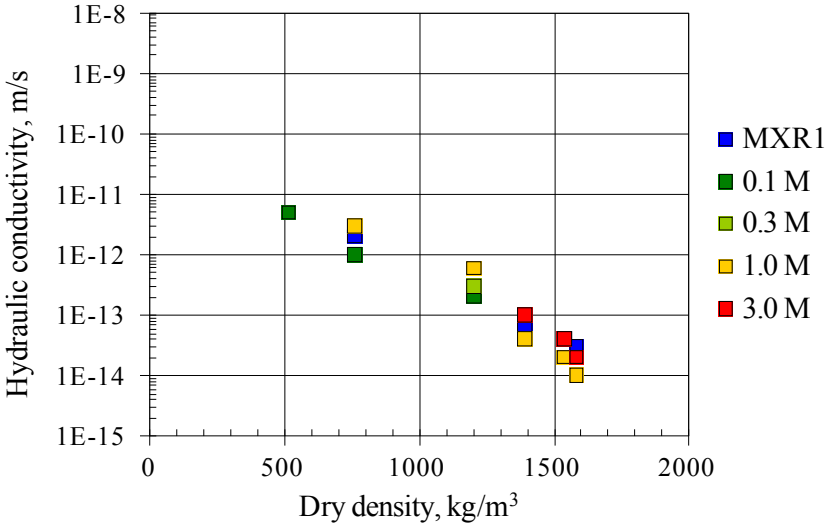

Fig. 6: Hydraulic conductivities of MX-80 exposed to NaCl solutions of differing molality (0.1 – 3.0 mole/L).

From SKB (2006).

3.3.2 Cement and concrete

Nagra intends to use a low pH cement (SR-LPC) for the concrete in the tunnel liner (Leupin & Johnson 2014). Such low-pH cements are obtained by replacing significant amounts of Portland cement with silica fume, *inter alia*. The addition of silica fume lowers the pH of the pore solution by suppressing the formation of free portlandite (which would buffer pH to approximately 12.5), and lowers the Ca/Si ratio of C-S-H gel to approximately unity.

The composition of the candidate concrete using SR-LPC is shown in Table 7. CEM I cement forms ~ 7 wt.-% of the total, which compares with roughly 17.5 wt.-% in typical OPC (Ordinary Portland Cement) concrete (e.g. Karlsson et al. 1999). The measured density of SR-LPC is 2260 – 2285 kg m^{-3} (Savage et al. 2010b). The oxide and normative clinker compositions of the cement component in SR-LPC (CEM I 52.5 N) are presented in Table 8.

The pH of pore fluids from the SR-LPC mix is 12.3 – 13 after 7 days, which decreases to 11.9 – 12.2 and 11.4 – 11.8 after 28 and 90 days, respectively (Savage et al. 2010b). The portlandite content is approximately 0.5 wt.-% after 7 days leaching by water which subsequently decreases to below the detection limit of 0.2 wt.-%. Leaching tests give increasing concentrations of potassium from 0.7 – 0.9 wt.-% (7 – 90 days) and sodium 0.2 – 0.4 wt.-% (in both cases after 7 – 90 days).

The degradation of a cement with x mol of Na_2O, y mol of K_2O, and z mol of CaO may produce a maximum of $n = 2(x + y + z)$ mol of OH^- (e.g. Gribi et al. 2008):

$$x\mathrm{Na_2O} + y\mathrm{K_2O} + z\mathrm{CaO} + n/2\mathrm{H_2O} \Rightarrow 2x\mathrm{Na^+} + 2y\mathrm{K^+} + z\mathrm{Ca^{2+}} + n\mathrm{OH^-} \quad (2)$$

This equation, together with the data in Table 6 and Table 7 have been used to calculate the total amounts of OH- potentially released from kilogram and cubic metre quantities of SR-LPC and OPC concretes (OPC composition as defined by Karlsson et al. 1999) and are shown in Table 9. It may be seen from Table 8 that SR-LPC concrete will release 3833 moles of OH- per cubic metre of concrete in comparison with 9646 moles of OH^- from OPC concrete (i.e. roughly 40 % of that in OPC).

3.3.3 Canisters, support arches

For the calculations considered here, steel present as a canister material and as engineering structures is treated as consisting of 100 % iron. Similarly, copper which may be used as a canister shell is assumed to be 100 % copper.

Tab. 7: Raw composition of low pH cement concrete.

The measured density is 2260 – 2285 kg m^{-3} (mean 2272.5 kg m^{-3}). From Savage et al. (2010b).

Components	**Mass** [kg]
Water	200 – 221
Cement (CEM I 52.5 N)	210
Silica fume	140
Sand	1624
Gravel	659
Superplasticiser	4.2
Accelerator	10.5 – 14.7
Total	2848 – 2873

Tab. 8: Chemical composition of the CEM I 42.5 N cement component in SR-LPC concrete.

From Lothenbach & Winnefeld (2006).

Composition			**Normative Phase Composition**		
	g kg^{-1} cement	Mol kg^{-1} cement		g kg^{-1} cement	Mol kg^{-1} cement
SiO_2	197	3.278	**Alite**	550	2.41
Al_2O_3	47	0.461	**Belite**	150	0.87
Fe_2O_3	26.7	0.167	**Aluminate**	79	0.29
CaO	632	11.270	**Ferrite**	81	0.17
MgO	18.5	0.461	**CaO**	4.6	0.082
SrO	0.7	0.007	**$CaCO_3$**	44	0.44
K_2O	11.2	0.119	**$CaSO_4$**	42	0.31
Na_2O	0.8	0.013	**K_2SO_4**	16	0.09
CaO (free)	4.6	0.082	**Na_2SO_4**	0.96	0.007
CO_2	19.3	0.439	**SrO**	0.7	0.007
SO_3	33.5	0.418	**K_2O**	2.6	0.027
			Na_2O	0.4	0.006
			MgO	19	0.46
			SO_3	1.2	0.014

Tab. 9: Inventory of Na_2O, K_2O and CaO and hydroxyl ions in SR-LPC concrete as defined by equation (2) and data in Table 7.

This assumes 7.3 wt % CEM I in SR-LPC concrete (Table 6), and 17.5 wt % CEM I in OPC concrete (e.g. Karlsson et al. 1999). The densities of SR-LPC and OPC concrete are 2272.5 (Savage et al. 2010b) and 2400 kg m^{-3} (Karlsson et al. 1999), respectively.

	Mol Na_2O kg^{-1} concrete	**Mol K_2O kg^{-1} concrete**	**Mol CaO kg^{-1} concrete**	***n*OH^- kg^{-1} concrete**	***n*OH^- m^{-3} concrete**
SR-LPC	0.0009	0.0087	0.8332	1.6866	3833
OPC	0.0023	0.0208	1.9865	4.0192	9646

3.4 Thermal and hydraulic evolution

The thermal evolution of a repository for spent fuel, high-level waste (HLW) at a depth of 650 m in the Opalinus Clay formation in northern Switzerland has been evaluated by Senger & Ewing (2008) via T-H-M modeling using TOUGH2 (Pruess et al. 1999). The disposal system considered by them consisted of a detailed 3-D model of spent fuel and HLW, encapsulated within steel canisters emplaced within horizontal tunnels, with the space between the canisters and the surrounding rock backfilled with bentonite. Waste emplacement tunnels were assumed to be spaced 40 m apart.

Their results show that the surface temperatures reach a maximum value of ~ 130 °C within a few years after emplacement for spent fuel canisters. The results of the calculation are shown in Figure 7. It may be seen from this figure that the significant thermal pulse lasts for 100 - 200 years at most.

However, Senger & Ewing (2008) note that the temperatures within the bentonite depend strongly on the assumptions regarding the thermal conductivity of the bentonite. The peak temperatures ranged between 118 and 150 °C at the top of the canister for thermal conductivities of dry bentonite of 0.2 and 0.6W/mK, respectively. The thermal conductivities for both bentonite pellets and bentonite blocks were assumed by Senger & Ewing (2008) to increase linearly with saturation to a maximum value of 1.35 W/mK at full saturation, although it should be noted that other authors have shown that the correlation of thermal conductivity with bentonite saturation state is non-linear (e.g. Figure 8).

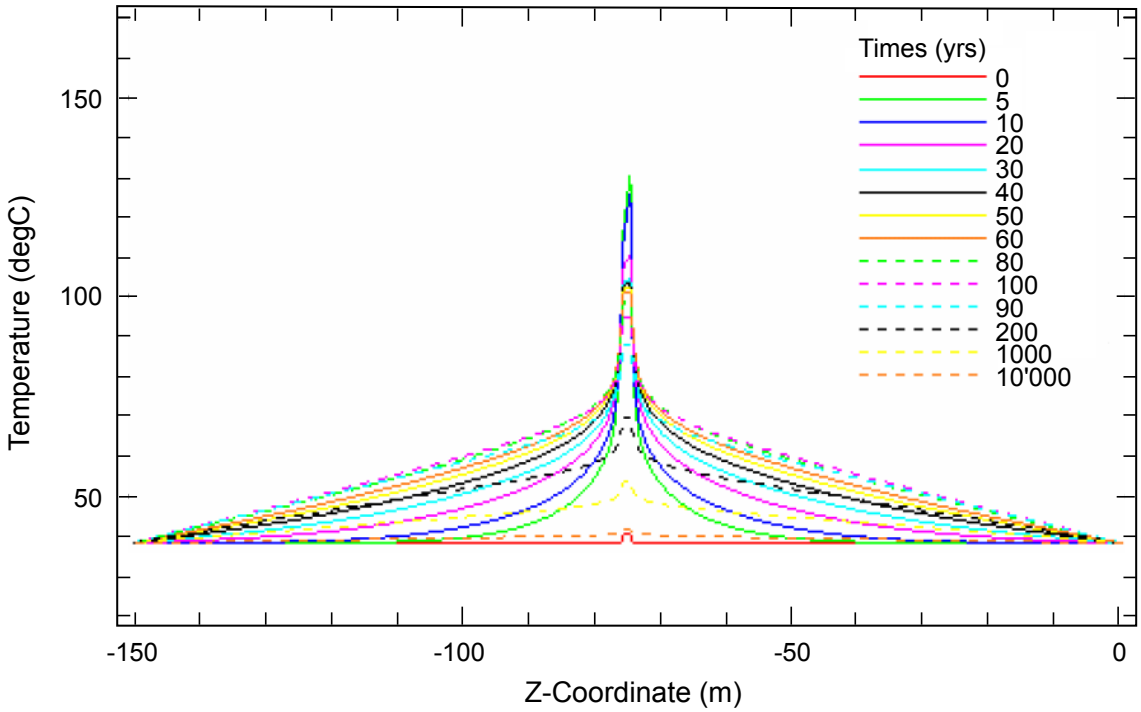

Fig. 7: Vertical profile of temperature along the center line through the disposal cell (x = 0) at different times for a reference case R0.

From Senger & Ewing (2008).

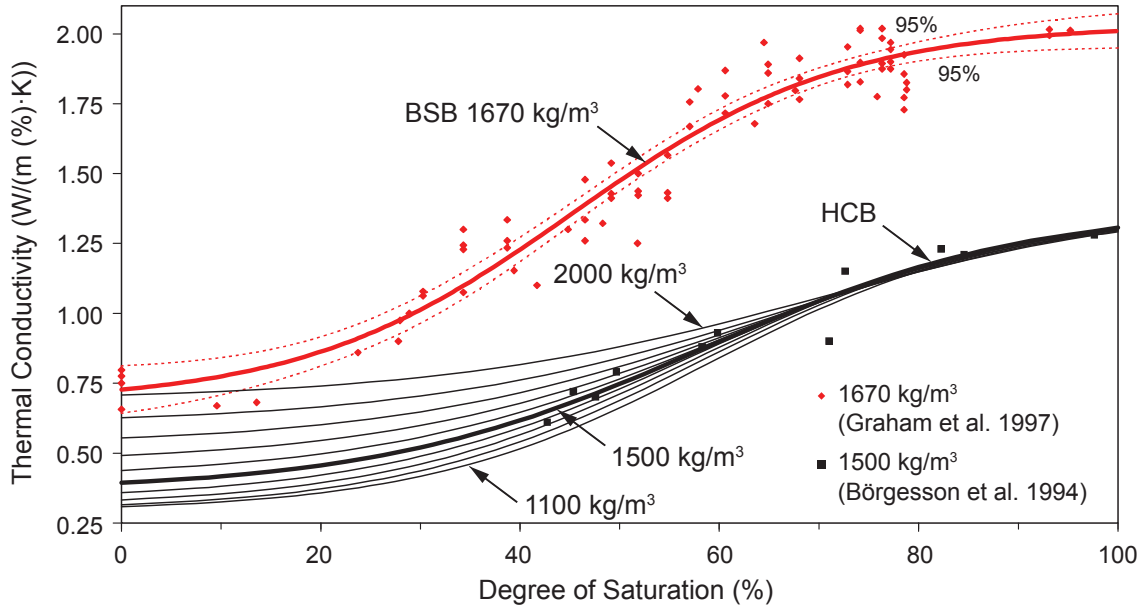

Fig. 8: Thermal Conductivity of 50:50 wt.-% Bentonite-Sand Buffer (BSB) and estimated range of values for Highly Compacted Bentonite Clay (HCB).

Label units are dry densities. From Man & Martino (2009).

4 Impacts due to the Thermal Period

Decay heat from SF and HLW canisters will increase temperatures within and around the repository in the Opalinus Clay for relatively short periods of time. The maximum temperatures achieved in the various disposal system components, and the time dependency of the temperatures, are determined principally by the heat output of the wastes, the selected repository layout and the thermal properties of the bentonite backfill and the surrounding rock (Nagra 2002, Senger & Ewing 2008). In developing the current repository design and layout, Nagra's principal constraint has been the desire to limit the maximum temperature experienced by the outer half of the bentonite barrier to less than approximately 130 °C. This is to preclude significant thermal alteration that might degrade its swelling and hydraulic properties (Nagra 2002).

This thermal gradient is imposed upon that for resaturation of the bentonite. High temperatures near the canisters will initially cause water vapour to migrate away from the canister surfaces. Resaturation of the emplacement tunnels and pressure build-up in the tunnel near-field are controlled by complex process couplings, including thermally induced fluid flow, evaporation of pore water, and air/vapour flow (Senger & Ewing 2008). Senger & Ewing also note that for the same water inflow conditions, the time for reaching full saturation of the bentonite is relatively insensitive to the permeability of the bentonite; both pellets and blocks reach full saturation at approximately the same time, about 80 years (Senger & Ewing 2008). However, uncertainties with regard to the coupled processes, which include bentonite compaction and swelling, self-sealing, salt precipitation, and potential changes in the material parameters (permeability, thermal conductivity, and tortuosity for vapour diffusion) will affect saturation rate (Senger & Ewing 2008).

Gradients in temperature and humidity during the period leading up to bentonite saturation and beyond may lead to the redistribution of mass, alteration of the montmorillonite clay content, and potentially to the cementation of mineral grains within the bentonite. As heat is released from waste packages, processes involved in the evolution of the bentonite buffer include thermally induced distribution of initial pore water in the clay during the early thermal phase. On the outer part of the buffer, water is taken up from the Opalinus Clay-water interface, with potential swelling of the bentonite in this region. On the inner part of the buffer, next to the canister, moisture content decreases (desiccation), with potential shrinkage. Chemically within the bentonite, there may be the dissolution of montmorillonite and other minerals and precipitation of chemical compounds so that mass is redistributed according to dependence of mineral solubility with temperature (see discussion below).

Water taken up from the surrounding Opalinus Clay will induce dissolution of clay minerals and quartz, along with trace minerals, such as gypsum, halite (NaCl), and carbonates. Interaction with the clay fraction and other silicate impurities will cause only slight changes in porewater composition in the short-term, but these may be instrumental in potential cementation effects in the medium to long-term. Ion exchange and protonation/deprotonation reactions occurring at the montmorillonite surfaces will also affect the composition of the porewater.

Hydrothermal experiments carried out by SKB with Wyoming bentonite heated to 150 – 200 °C have shown that cooling may lead to the precipitation of silica in various forms (SKB 2010, p. 126). The precipitation could cause cementation effects, including a strength and stiffness increase, which has been demonstrated in several laboratory investigations (Pusch & Karnland 1988). In the Buffer Mass Test at the Stripa underground laboratory (90 °C maximum temperature), the buffer was analysed with respect to the distribution of silica, but no definite conclusion could be drawn regarding possible enrichment in the coldest part. However, the study of

cooling-related precipitation of silica was confirmed by a coupled modelling study of the Kinnekulle bentonite analogue (Pusch et al. 1998). Results from the LOT and ABM tests at the Äspö Underground Laboratory show that carbonates and sulphates precipitate near the heater (Karnland et al. 2009, Kumpulainen & Kiviranta 2011).

Although illitisation has been the focus with respect to long-term alteration of montmorillonite in bentonite (e.g. Karnland & Birgersson 2006), other reactions, such as beidellitisation or saponitisation *inter alia*, could occur through interaction of bentonite with groundwater. However, evaluation of these other potential reactions has tended to receive relatively little interest.

In general terms, the illitisation reaction can be written as (e.g. Karnland & Birgersson 2006):

$$K^+/Ca^{2+}/Na^+\text{-smectite} + K^+ + (Al^{3+}) \rightarrow \text{illite} + \text{silica} + Ca^{2+}/Na^+$$

So for the reaction to occur, an increase in clay layer charge and an introduction of potassium ions are required. The activity and the precipitation rate of silica in, and from, the aqueous phase can also affect illitisation. The precise mechanism and rate of reaction are still under debate despite more than four decades of research (mainly allied to hydrocarbon exploration) (e.g. Meunier & Velde 2004, McCarty et al. 2009). Nevertheless, using available rates of reaction, the calculated conversion of smectite to illite under chemical conditions relevant to the Opalinus Clay and at temperatures less than 130 °C is likely to be minor (Nagra 2002).

Natural analogues provide examples of the extent and rate of conversion from smectite to non-expandable minerals. Detailed descriptions of the Ordovician (~ 455 Ma) Kinnekulle bentonite (in Sweden), which still contains about 25% smectite after a heating sequence much like the one expected in a HLW repository, seems to validate the working model that is presently used in smectite transformation (Pusch 2002a).

Results of a field test in a clay host rock at the Mont Terri underground laboratory investigating thermal effects upon bentonite are reported by Plötze et al. (2007). In this experiment, a heater was installed in a borehole in the Opalinus Clay and the host rock was backfilled with blocks of compacted bentonite. A constant temperature of 100 °C was maintained over 18 months. Plötze et al. (2007) report only very minor changes to the physical and mineralogical properties after this time period, which may reflect the relatively short duration of this test.

Pusch et al. report more dramatic changes to FoCa bentonite in a heater test carried out in fractured hard rock (granite) at the Stripa underground laboratory in the 1980s (Pusch et al. 1993). Fo-Ca bentonite consists of interlayered smectite/kaolinite and kaolinite with minor amounts of quartz, feldspar, hematite, gypsum, pyrite and calcite. Test parcels consisting of pre-fabricated bentonite blocks (~ 2000 kg m^{-3} at full water saturation) surrounded a steel canister with an electrical heater which maintained a constant temperature at the steel-buffer interface of about 170 °C (i.e. 50 °C higher than that considered here). The temperature at the buffer-rock interface was about 80 °C. Experiments were carried out in two separate boreholes: one for a period of 8 months, and the other for about 4 years. In the 4-year test, amorphous silica, and possibly also amorphous calcium silicates, were found to have precipitated throughout the clay annulus. The amounts precipitated were not determined quantitatively, but were observed to increase generally toward the hotter canister-buffer boundary. Amorphous silica was especially abundant over a region extending 6 – 8 mm into the bentonite from the canister surface, where *in situ* temperatures were inferred to have been between 150 and 180 °C. Neoformed anhydrite was also present in this zone, and the original dioctahedral smectite had been partially altered to

trioctahedral clay (saponite or stevensite). A key finding of the Stripa tests is that the entire thickness of the buffer had been cemented to some extent by precipitation of silica and anhydrite, and that this had altered the rheological behaviour of the clay. The ductility and swelling capacity of the clay near the canister were completely lost, and the hydraulic conductivity had increased by three orders of magnitude. Although the FoCa clay is different in terms of its composition from MX-80 and the temperatures it was exposed to were substantially higher (150 – 170 °C versus < 130 °C in Nagra's concept), these results highlight the need to be able to accurately control the temperature in the vicinity of the canisters.

There are a few modelling studies dealing with the long-term evolution of the bentonite-groundwater system in clay during the thermal period (e.g. Fritz et al. 2006, Montes-H et al. 2005a, Montes-H et al. 2005b, Montes-H et al. 2005c, Marty et al. 2010), but only one considering Opalinus Clay specifically (Benbow et al. 2000). The latter was also conducted using a temperature gradient, whereas other studies employed a constant near-field temperature.

4.1 Key reactions

The most important processes are:

- Saturation of the bentonite, driven by slow wetting at the interface with Opalinus Clay and the tunnel liner and drying from the thermal output of the waste packages.
- Fast exchange of cations (such as Ca^{2+}) in groundwater for cations (principally Na^{+} in MX-80 bentonite) in interlayer sites in montmorillonite. These exchange reactions advance in front of mineral dissolution-precipitation reactions (e.g. Fernández et al. 2009).
- Thermally-driven dissolution of montmorillonite and other minerals present in bentonite, such as quartz, feldspars, pyrite, carbonates and gypsum. Re-precipitation will occur according to temperature-dependent solubility (silicates in cooler zones and sulphates, carbonates in warmer zones). The net change in porosity across the entire alteration zone may be trivial (re-distribution of mass). The precipitation of solids (especially silica) may lead to cementation of clay grains and loss of swelling pressure.
- Potential thermally-accelerated transformation of montmorillonite through dissolution-precipitation reactions to illite, beidellite, saponite etc.

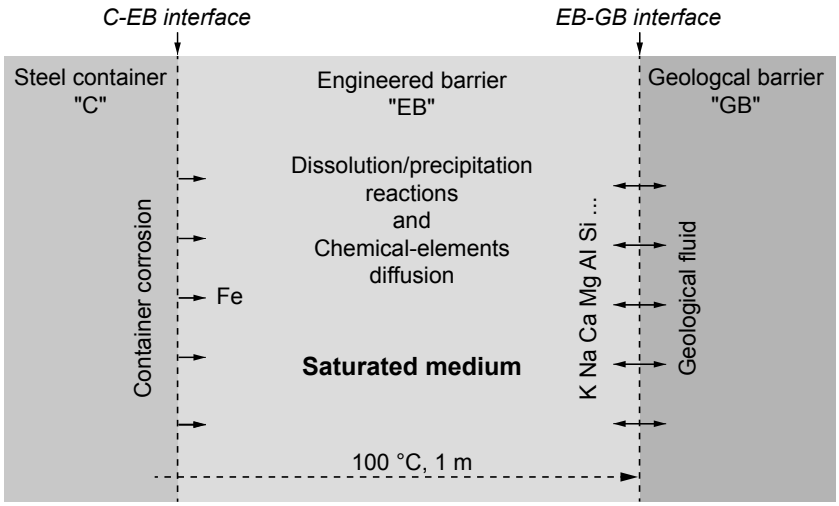

Fig. 9: Schematic representation of the typical geometry and solute diffusion in a computer simulation of EBS evolution.

From Montes-H et al. (2005b).

4.2 Extent of alteration

Definition of the extent of bentonite alteration due to thermal processes is complex because there are a number of mineralogical alteration fronts which are relevant to safety:

- Dissolution/destruction of montmorillonite, leading to loss of swelling pressure and potential changes in porosity and hydraulic conductivity.
- Redistribution of silica, carbonates and sulphates which could lead to a redistribution of porosity and changed hydraulic conductivity. Cementation of clay grains could affect swelling pressure by hindering hydration of interlayer cations (e.g. Laine & Karttunen 2010). However, Wersin et al. (2007) noted that no significant cementation occurs below 110 °C, and that there is only slight cementation at 130 °C, with significant cementation only occurring at temperatures of 150 °C and above.
- Ion exchange in montmorillonite which could lead to changes in swelling pressure.

Also with regard to the results of reaction-transport simulations, it may be impossible to distinguish between reactions driven by thermal processes alone and those driven by chemical gradients, e.g. across metal-bentonite interfaces.

However, the results of reaction-transport simulations (Fritz et al. 2006, Montes-H et al. 2005a, Montes-H et al. 2005b, Montes-H et al. 2005c, Marty et al. 2010) will be used here to define three metrics to define the potential extent of bentonite alteration due to thermal processes (Table 9):

- The extent of total loss of montmorillonite.
- The extent and degree of partial conversion of montmorillonite to non-swelling sheet silicates such as illite.
- The extent and degree of redistribution of silica, defined by peaks in quartz and/or amorphous silica.

These simulations have a geometry similar to that shown in Figure 9, with a canister, bentonite annulus and a far-field mudstone boundary condition. Although all the simulations were carried out at elevated temperature (50 – 100 °C), only one was carried out in a temperature gradient.

It may be seen from Table 10 that the largest total extent of montmorillonite loss is 0.1 m of annulus around the canister after 10 ka and the greatest degree of illitisation is an increase from 1 to 5 %, 0.5 m from the canister after 50 ka.

Tab. 10: Extents of porosity change, montmorillonite loss, illitisation of montmorillonite and reprecipitation of silica.

These extents are estimated by coupled reaction transport modelling of the thermal evolution of a bentonite-based HLW EBS in a clay host rock.

T [°C]	**Porosity change** [%]	**Extent of montmorillonite loss** [m]	**% illite change;** extent [m]	**% silica change;** extent [m]	**Source**
Gradient (105 → 38)	-	-	-	5 → 5.1; 0.9	[1]
Constant (100)	30 → 29	0.1 @ 10 ka	5 → 5; 0.1	5 → 10; 0.1	[2]
Constant (100)	30 → 0 at contact with canister	0.05 @ 50 ka	1 → 5; 0.5	10 → 20; 0.05	[3]
Constant (100)	39 → 0 at contact with canister	0.05 @ 100 ka	2 → 5; 0.6	5 → 10; 0.1	[4]

[1] Benbow et al. (2000). [2] Montes H et al. (Montes-H et al. 2005a, b, c). [3] Fritz et al. (2006). [4] Marty et al. (2010).

Tab. 11: Summary of estimated changes to bentonite properties due to thermal processes at 100 ka for both optimistic and pessimistic scenarios.

Optimistic values are based upon the smallest extent of alteration predicted by reaction-transport simulations listed in Table 9; pessimistic values are based upon the greatest extent of alteration predicted by reaction-transport simulations listed in Table 9.

EBS Component	**Buffer**		**Sealing element**	
Scenario	*optimistic*	*pessimistic*	*optimistic*	*pessimistic*
Alteration zone thickness	0.05 m	0.1 m	None	None
Porosity	Zero from canister to 0.05 m; unchanged in remainder	Zero from canister to 0.1 m; unchanged in remainder	Unchanged throughout	Unchanged throughout
Hydraulic conductivity	Increased (× 10) from canister to 0.05 m; unchanged in remainder	Increased (× 100) from canister to 0.1 m; unchanged in remainder	Unchanged throughout	Unchanged throughout
Swelling pressure	Zero at 0 – 0.05 m from canister; unchanged in remainder	Zero at 0 – 0.1 m from canister; unchanged in remainder	Unchanged throughout	Unchanged throughout
Mineralogy	Gypsum, anhydrite and carbonates deposited on canister; silicates (montmorillonite, quartz) reduced in abundance near canister. Amorphous silica precipitated in cooler zones (on concrete liner)		Minor amorphous silica precipitation.	

4.3 Potential changes to safety relevant properties

Potential changes to safety-relevant properties (porosity, hydraulic conductivity, swelling pressure and mineralogical composition) for optimistic and pessimistic estimates at 100 ka after closure are summarised in Table 11. These data are based on the results of reaction-transport simulations of EBS evolution at elevated temperatures in clay host rocks (Table 10).

4.3.1 Porosity

It is difficult to separate the effects of thermal processes and those due to chemical gradients at the interface between the metal canister and the bentonite regarding porosity changes. However, three of four simulations in Table 10 indicate that there will be a complete filling of porosity at the canister-bentonite interface which will thus limit alteration of the bentonite. To reflect a certain amount of porosity decrease due to silicification/anhydrite precipitation (as shown in some in situ tests), in Table 11, this zone is taken to extend to 5 cm from the canister-bentonite interface for an optimistic estimate and to 10 cm for a pessimistic estimate at 100 ka after closure.

The porosity of the sealing element is expected to be unchanged.

4.3.2 Hydraulic conductivity

Pusch et al. (1993) report an increase in hydraulic conductivity of three orders of magnitude for samples of FoCa bentonite adjacent to the heater in a test carried out at the Stripa underground laboratory, presumably due to embrittlement and fracturing of the bentonite. Temperatures were somewhat higher (170 °C) in this test than that expected in a repository in Opalinus Clay however. Here, a ten-fold increase of hydraulic conductivity in bentonite adjacent to canisters is assumed for an optimistic case and a hundred-fold increase for a pessimistic case at 100 ka after closure (Table 10).

The hydraulic conductivity of bentonite in the sealing element is expected to be unchanged (Table 11). See section 6.1.3 for the impacts due to interactions with metals on the hydraulic conductivity.

4.3.3 Swelling pressure

The results of available computer simulations indicate that there is removal of montmorillonite 0.05 to 0.1 m from the interface with the canister (Table 10) which would lead to zero swelling pressure in that volume (Table 11). These estimates are compatible with measurements made by Pusch et al. (1993) on samples of altered bentonite adjacent to the heater during in situ tests at the Stripa underground laboratory where the ductility and swelling capacity of the strongly-altered FoCa clay near the canister surface were completely lost.

The swelling pressure of bentonite in the sealing element is expected to be unchanged (Table 11). See section 6.1.3 for the impacts due to interactions with metals on the swelling pressure.

4.3.4 Mineralogy

Data from reaction-transport simulations suggest that thermal effects will enhance the redistribution of silicates, sulphates and carbonates. The solubility of silicates (clays, quartz, feldspar) increases with increasing temperature so that these minerals will tend to be removed adjacent to the immediate canister zone and reprecipitated (especially as amorphous silica) in cooler parts of the EBS. By contrast, the solubilities of sulphates (gypsum, anhydrite) and carbonates (calcite, dolomite, siderite) decrease with increasing temperature such that these minerals will tend to precipitate in hotter zones. Although the groundwater in the Opalinus Clay is relatively rich in sulphate and carbonate, some of this will be removed due to precipitation of ettringite and calcite as the groundwater diffuses through the concrete liner. The thermal period may encourage minor growth of illite.

The mineralogical observations from various URL heater tests (Pusch et al. 1993, Karnland et al. 2009, Kumpulainen & Kiviranta 2011) lend support to these conclusions.

In the sealing element, there may be minor precipitation of amorphous silica (Table 11).

5 Impacts due to Interactions of Bentonite with Cement/Concrete

Cement-clay interactions have been studied extensively (at different temperatures) in the last ten years, through laboratory experiments (e.g. Johnston & Miller 1984, Madsen 1998, Ichige et al. 1998, Kubo et al. 1998, Fujiwara et al. 1998, Vigil de la Villa et al. 2001, Ramírez et al. 2002, Nakayama et al. 2004, Yamaguchi et al. 2004, Yamaguchi et al. 2007), computer simulations (e.g. De Windt et al. 2001, Savage et al. 2002, Gaucher et al. 2004, Watson et al. 2007, Marty et al. 2009, Watson et al. 2009, Traber & Mäder 2006), and a few relevant analogue investigations (e.g. Tinseau et al. 2006, Arcilla et al. 2009, Honrado et al. 2009, Savage et al. 2010a). It should be noted that most, if not all these studies, have considered the interaction of OPC-type cement with bentonite, and not formulations of low pH cements. There are some useful reviews extant, especially from a PA perspective (e.g. Takase 2004, Gaucher & Blanc 2006, Savage et al. 2007, Alexander & Neall 2007, Savage & Benbow 2007, Gribi et al. 2008, Savage 2009).

These studies have highlighted that cement-bentonite interactions are strongly non-linear, with a complex interplay between fluid transport, clay ion exchange and dissolution, secondary mineral growth, and consequent changes in physical properties (porosity, permeability, swelling pressure) of the bentonite (Figure 10). This behaviour means that it is difficult to predict long-term behaviour and materials properties from short-term experimental data. Potential impacts upon long-term properties of clay through interaction with cement have thus been assessed previously either by using simple bounding assumptions, such as limitation by mass balance, kinetics, and/or mass transport, or by coupled modelling of reaction and transport processes. The potential impact of the use of a concrete tunnel liner in the Nagra near-field concept has been evaluated previously (Savage et al. 2010b).

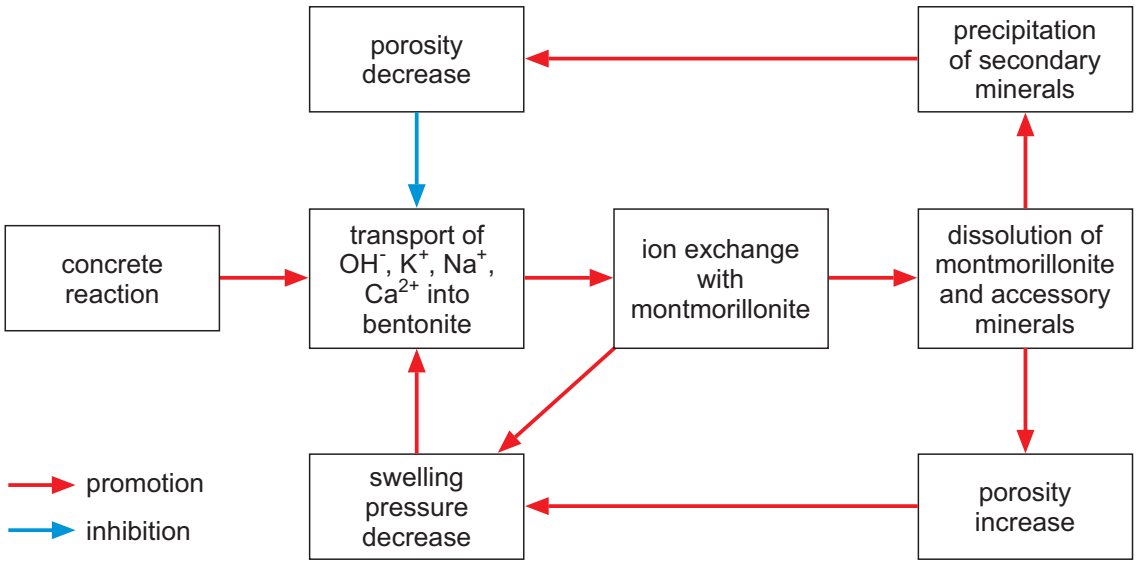

Fig. 10: Cement-bentonite interaction as a coupled non-linear system.
After Takase (2004).

5.1 Key reactions

The most important processes are:

- Diffusive transport of cement pore fluids into bentonite/clay, with mixing and reaction with clay pore fluids. Sharp gradients in pH (and $_{P}CO_2$) across the Opalinus Clay-concrete interface encourage the precipitation of carbonates (e.g. aragonite and calcite), and hydroxides (e.g. brucite), leading to decreased porosity (e.g. Watson et al. 2009).
- Fast exchange of cations in cement pore fluids (principally K and Ca) for cations (principally Na^+ in MX-80 bentonite) in interlayer sites in montmorillonite, leading to a potential change in swelling pressure. These exchange reactions advance in front of mineral dissolution-precipitation reactions (e.g. Fernández et al. 2009).
- Fast protonation-deprotonation reactions at clay edge sites. Typically, such sites can neutralise 55 moles of hydroxyl ions per cubic metre of MX-80 bentonite (at 2000 kg m^{-3} water-saturated compaction density).
- Slow dissolution of montmorillonite and other minerals present, such as quartz, feldspars, pyrite, and gypsum. Multiple reaction fronts may form and propagate due to different dissolution and precipitation rates, with later fronts overriding those formed earlier. The overall evolution thus forms a complex porosity structure, with porosity changes within both the concrete and clay. The net change in porosity across the entire alteration zone may be trivial (re-distribution of mass).
- Precipitation of secondary minerals such as clays, hydroxides, carbonates, calcium (aluminium) silicate hydrates, and aluminosilicates, such as zeolites and feldspars (e.g. Savage et al. 2007). These minerals may form in a zonal fashion, with relatively more siliceous zeolites more likely to form at lower pH (distal regions of migrating cement pore fluids), whereas C-(A)-S-H, illite, feldspars, and the more aluminous zeolites are more likely to form at higher pH and hence, the more proximal regions.

5.2 Extent of alteration

To a large extent, the potential changes in safety-relevant properties of the bentonite correspond directly to the extent of the front of alteration defined by the removal of montmorillonite through dissolution-precipitation processes.

Savage (Savage et al. 2010b) examined potential mass balance controls on the extent of interaction of a concrete tunnel liner with bentonite in the Nagra near-field concept through consideration of the following mass balance (relevant at pH > 10):

$$\begin{aligned} Na_{.33}Mg_{.33}Al_{1.67}Si_4O_{10}(OH)_2 + 2H_2O + 4.68OH^- \Rightarrow \\ 0.33Na^+ + 0.33Mg^{2+} + 1.67Al(OH)_4^- + 4HSiO_3^- \end{aligned} \quad (3)$$

It thus takes 4.68 moles of OH^- to dissolve one mole of montmorillonite, assuming no other OH^--consuming or -generating reactions occur (e.g. the dissolution of other minerals in bentonite, or the precipitation of new minerals), and that no dilution of OH^- in groundwater occurs. The mass of dissolved montmorillonite (kg) can be calculated (e.g. Gribi et al. 2008):

$$\text{dissolved montmorillonite} = \frac{\text{mass of concrete} \times n\text{OH}^- \times M}{4.68} \quad (4)$$

with nOH^- being the amount of OH^- released per kg of concrete (Table 9) and M being the molar mass of montmorillonite (M = 0.367 kg mol^{-1}).

Using equation (4), and the amount of SR-LPC concrete in a 1 m section of tunnel of initial (pre-creep) geometry from Table 2 (1.25 m^3 = 2841 kg), 432 kg of bentonite could be destroyed by reaction if all the OH^- ions from the concrete are considered to dissolve the clay content of the bentonite alone. This amount represents 7 wt.-% of the total bentonite of the canister buffer in a 1 m length of tunnel. The corresponding amount for OPC concrete would be 1087 kg (18 wt.-%). Calculations for post-creep tunnel conditions are identical to these values since the mass of concrete remains the same.

However, a more realistic estimate of the extent of alteration is based on the results of reaction-transport simulations, with greatest emphasis placed upon those studies employing both reaction kinetics and fluid compositions typical of low pH cements (e.g. Savage et al. 2002, Ueda et al. 2007, Watson et al. 2007). However, it should be noted that these studies do not address the behaviour of compacted MX-80 bentonite and instead, focus on bentonite-sand mixes envisaged for the Japanese programme for the disposal of HLW and TRU.

Notwithstanding this limitation, the results of published model simulations summarised in Table 13 indicate a very limited zone of alteration of compacted bentonite – of the order of 2 cm with cement pore fluids of pH $\leq$ 11. The pessimistic value chosen in Table 12 is 0.2 m and is that estimated by for MX-80 with OPC without consideration of kinetics (Gaucher et al. 2004).

Reaction of the sealing element of compacted bentonite with cement pore fluids is likely to be much less than that associated with the buffer, primarily due to its location with regard to the liner. Pore fluids from the concrete liner would have to migrate laterally to degrade the seal. Data in Table 12 are (very pessimistically) assumed to be the same as those for the buffer.

5.3 Potential changes to safety-relevant properties

Here, the information relating to the alteration of clay by the use of a concrete liner is synthesised in terms of potential changes to a number of PA-relevant properties at 100 ka after closure (porosity, hydraulic conductivity, swelling pressure, and mineralogical composition). These conclusions are presented in a summary Table (Table 12) for this topic.

The conclusions in Table 12 are based upon the results of reaction-transport modelling because the coupled, non-linear nature of cement-bentonite interaction (e.g. Figure 10) renders scoping calculations based either on simple mass balance or kinetic constraints of limited use, because of the gross pessimism associated with those assumptions (e.g. Savage et al. 2010b).

To try to address these uncertainties, conclusions in Table 12 are presented in terms of what might be considered to be optimistic or pessimistic.

5.3.1 Changes to porosity

A recent review of laboratory experimental and analogue data of cement-clay interfaces (Savage 2009) noted that systems dominated by diffusion produce porosity decreases in the clay, regardless of pore fluid type (e.g. Fernández et al. 2009, Tinseau et al. 2008). Moreover, reaction-transport simulations of clay with calcic cement pore fluids (i.e. those typical of low-pH cements) all show decreasing porosity with time such that porosity decreases to zero at some distance/time within the simulation. Typically, this time is a few hundred or a thousand years (Table 13). However, this concerns local porosity change and may be limited to one grid cell within a model system.

Optimistic values of porosity are therefore taken to be zero (at some point within the mineralogically-altered zone) in Table 12, whereas pessimistic values are assumed to be unchanged from initial values.

Tab. 12: Summary of estimated changes to bentonite properties at 100 ka after closure.

Optimistic values are based upon the smallest extent of alteration predicted by reaction-transport simulations listed in Table 13; pessimistic values are based upon the greatest extent of alteration predicted by reaction-transport simulations listed in Table 13. For an SR-LPC concrete liner under pre-creep conditions. Note that this Table considers the effects of hyperalkaline alteration in isolation from other perturbations evaluated in this report (see Section 7 for a synthesis).

EBS Component	**Buffer**		**Sealing element**	
Scenario	*Optimistic*	*Pessimistic*	*Optimistic*	*Pessimistic*
Alteration zone thickness, m	0.02	0.20	0.02	0.20
Porosity	Zero at 0 – 0.02 m from liner	Unchanged	Zero at 0 – 0.02 m from liner	Unchanged
Hydraulic conductivity	Decreased	Unchanged	Decreased	Unchanged
Swelling pressure	Zero at 0 – 0.02 m from liner; as initial with greater distance	Zero at 0 – 0.20 m from liner; as initial with greater distance	Zero at 0 – 0.02 m from liner; as initial with greater distance	Zero at 0 – 0.20 m from liner; as initial with greater distance
Evolution of pH plume	Unperturbed bentonite properties 0.73 m radius around can	Unperturbed bentonite properties 0.55 m radius around can	-	
Mineralogy	Calcite, C-S-H minerals, Ca-zeolites, saponite, hydrotalcite		Calcite, C-S-H minerals, Ca-zeolites, saponite, hydrotalcite	

Tab. 13: Summary of some cement-clay reaction-transport simulations (at 25 °C) carried out over the last ten years.

Note that most simulations predict alteration depths (defined by total removal of montmorillonite) in the range 0.01 to 0.2 m. The much larger depth predicted by ref [2] reflects the much lower initial content of montmorillonite in the starting (natural) clay than in MX-80 bentonite. Despite differences in initial porosity, all simulations except one predict complete porosity filling at some distance along the alteration profile.

Solid	**Initial pH**	**Kinetics**	**Porosity Feedback**	**Products**	**Alteration depth** [m]	**Porosity** [%]	**Ref.**
Bentonite + sand	11.3	Yes	Yes	CSH minerals, Ca-zeolite, celadonite, calcite	0.1 @ 3.2 ka	40 → 0 @ 3.2 ka	[1]
Claystone	13.2	No	Yes	CSH minerals, sepiolite, Ca-zeolite, illite	0.6 @ 10 ka	15 → 0 @ 2.5 ka	[2]
MX-80 (1800 kg m^{-3})	12.5	No	No	Illite, zeolites, CSH minerals, saponite, chlorite	0.2 @ 100 ka	?	[3]
Opalinus Clay	13.5	Yes	No	Illite, calcite, CSH minerals, zeolites, sepiolite	0.1 @ 50 ka	11 → 0 @ 0.1 ka	[4]
Bure clay	13.2	No	Yes	Illite, analcime, Ca-zeolites	0.15 m @ 25 ka	15 → 2 @ 25 ka	[5]
Bentonite + sand	11	Yes	Yes	Calcite, CSH minerals, Ca-zeolites	0.01 @ 10 ka	40 → 0 @ 10 ka	[6]
Bentonite + sand	10, 10.5, 11, 11.5	Yes	Yes	Calcite, celadonite, Ca-zeolites, CSH minerals	0.015 @ 1 ka (pH 11)	40 → 0 @ 1 ka (pH 11)	[7]
Claystone	12.5	Yes	Yes	Calcite, muscovite, Ca-zeolite	< 0.02 @ 0.015 ka	Porosity decrease	[8]
Bure clay	12.5	Yes	Yes	CSH minerals, calcite, Ca-zeolites, illite, saponite, hydrotalcite	0.01 @ 0.1 ka	15 → 0 @ 0.1 ka	[9]
Generic clay	12.5	No	Yes	CSH minerals, calcite, gibbsite	0.001 @ 0.07 ka	10 → 0 @ 0.07 ka	[10]

[1] Savage et al. (2002). [2] De Windt et al. (2004). [3] Gaucher et al. (2004). [4] Michau (2005) and Traber & Mäder (2006). [5] Trotignon et al. (2007). [6] Ueda et al. (2007). [7] Watson et al. (2007). [8] De Windt et al. (2008). [9] Marty et al. (2009). [10] Kosakowski et al. (2009).

5.3.2 Changes to hydraulic conductivity

Hydraulic conductivity is not calculated in reaction-transport simulations of cement-clay interactions, and where it has been measured in laboratory experiments, it has been carried out under unrealistic conditions (e.g. with circulation of high pH fluids under advective conditions – Savage 2009). Since porosity is predicted to decrease with time due to cement-clay reactions in diffusive transport conditions, an unquantified decrease is quoted in Table 12 as a realistic assessment, with an unchanged value as a pessimistic estimate.

In support of this conclusion, CEA (as part of the EC ECOCLAY II project), studied diffusion in MX-80 bentonite at 1700 and 2000 kg m^{-3} saturated densities, with an evolved (Ca-rich) cement water of pH 12.5 (Michau 2005, Melkior et al. 2004). The bentonite was saturated with

Bure groundwater prior to coupling with a reservoir of cement water. The effective diffusion coefficient for HTO decreased with time, which they interpreted as being due to occlusion of porosity due to cement-clay reaction.

However, it should be noted that any conclusion regarding changes to hydraulic conductivity of the clay should reflect the predicted saturation state of the bentonite with time. Saturation will be controlled by suction processes within the bentonite and the rate of supply of water from the Opalinus Clay (which may be limited). Consequently, any decrease in hydraulic conductivity of the bentonite may be postponed by any delay in re-saturation.

5.3.3 Changes to swelling pressure

Swelling pressure in compacted bentonite is produced by interlayer cation hydration and osmotic effects in montmorillonite (e.g. Savage 2005) and is therefore dependent upon the presence of montmorillonite in the buffer/sealing element. Total removal of montmorillonite from bentonite will thus reduce swelling pressure to zero. Since the extent of the zone of mineralogical alteration is here defined by total loss of montmorillonite, then the swelling pressure of this altered zone is assumed to be zero.

Karnland reports similar swelling pressures for Ca- as compared with Na-bentonite at similar high compaction densities (Karnland 2010). A front of cation exchange of Ca for Na in smectite interlayers moving in advance of fronts of mineral dissolution-precipitation are therefore expected not to perturb bentonite swelling pressures for materials of the density used in the buffer and backfill[2].

5.3.4 Evolution of pH plume near to canister

The discussion above suggests that the plume from a low-pH cement type concrete liner will not contact the waste canister due to changes in mass transport properties of the bentonite as a consequence of decreasing porosity through mineral precipitation. The canister is surrounded by an annulus of 0.75 m of compacted bentonite under pre-creep conditions and 0.65 m under post-creep conditions. Thicknesses of altered bentonite estimated in Table 12 (for SR-LPC) indicate that 0.73 and 0.55 m of unperturbed bentonite properties will exist around the canister for optimistic and pessimistic scenarios, respectively under pre-creep conditions (Table 12). For post-creep conditions, corresponding thicknesses of 0.63 and 0.45 m are calculated.

5.3.5 Changes to mineralogy

Data from reaction-transport simulations show remarkably similar mineral alteration sequences (Table 13). These model sequences are characterised by C-S-H minerals forming nearest the cement contact, and other minerals such as zeolites and clays forming further away (e.g. Savage et al. 2007). This hypothetical sequence of alteration has not been confirmed by laboratory experimental evidence, but this may be a function of the relatively short duration of such experiments and hence the small spatial development of alteration. Evidence from a 125 year-old industrial analogue of clay-cement (OPC) interaction at Tournemire shows a sequence of calcite, gypsum, Na-zeolites, and K-feldspar with increasing distance across a 2-3 cm zone of claystone adjacent to a cement contact (Tinseau et al. 2006). Computer simulations with pore

[2] NB: This conclusion is revised from that reported by Savage et al. 2010b (Savage, D., Walker, C. & Benbow, S.: *An Analysis of Potential Changes to Barrier Components due to Interaction with a Concrete Liner in a Repository for SF/HLW in Opalinus Clay,* Nagra Working Report NAB 10-17).

fluids with pH ≥ 13 contain appreciable proportions of Na/K-bearing minerals such as analcime, K-feldspar, Na/K-zeolites, and illite (e.g. Savage et al. 2002). The lower contents of Na and K in low pH cement grouts will make these minerals less relevant to alteration around a SR-LPC concrete liner.

5.4 Degradation of the concrete liner

Although the principal focus here is the effects of the concrete liner on the bentonite buffer, there are also potential impacts of the Opalinus Clay groundwater on the concrete liner which should be considered. Although most studies of concrete/cement-clay interaction have tended to focus on impacts upon the latter component, some works have also addressed potential long-term changes to the physicochemical properties of the cement/concrete, either through reaction-transport modelling (e.g. Trotignon et al. 2006, Trotignon et al. 2007, Marty et al. 2009, Kosakowski et al. 2009) or through study of the Tournemire analogue (e.g. Tinseau et al. 2006, Tinseau et al. 2008, Gaboreau et al. 2011). These studies show that interaction of cement/ concrete barriers with clay groundwaters tends to lead to:

- increased porosity in the cement/concrete (e.g. from 9 to 15 % over 50 ka in concrete-clay simulations; from 40 to 60 % over 15 years in cement at Tournemire) in a zone up to 0.2 m from the interface with clay due mainly to dissolution of portlandite, C-S-H gel and monosulphoaluminate.
- Replacement of portlandite, C-S-H gel and monosulphoaluminate by ettringite.
- Formation of calcite at the interface with the clay.

The above observations would suggest that the tunnel liner in a deep geological repository in Opalinus Clay would be subject to increases in porosity with time, with concomitant changes in mineralogical composition.

6 Impacts due to Interactions with Metals

6.1 Iron/steel

The potential detrimental effects of the interaction of iron or steel canisters/overpacks with compacted bentonite in waste package buffers was first identified by Nagra in the mid-1980's (Grauer 1986, Grauer 1990). Although this issue remained of concern, little more research was done until Andra and JAEA initiated new experimental and modelling studies in the late 1990's (e.g. Kamei et al. 1999, Guillaume et al. 2003, Neaman et al. 2003, Lantenois et al. 2005, Charpentier et al. 2006, Wilson et al. 2006a, Wilson et al. 2006b, Perronnet et al. 2007, Perronnet et al. 2008, Ishidera et al. 2008, Mosser-Ruck et al. 2010, Fukushi et al. 2010, Lee & Wilkin 2010). Posiva and SKB followed suit in the middle of the last decade, carrying out reviews and experiments as part of their KBS-3H research programme (e.g. Marcos 2003, Smart et al. 2006a, Smart et al. 2006b, Smart et al. 2008, Carlson et al. 2006, Carlson et al. 2007, Carlson et al. 2008, Wersin & Snellman 2008, Milodowski et al. 2009a, Milodowski et al. 2009b, Kumpulainen et al. 2010). This work has been followed up by several modelling studies carried out through different programmes, mainly in the last five years (e.g. Montes-H et al. 2005c, Bildstein et al. 2006, Fritz et al. 2006, Hunter et al. 2007, Hodgkinson et al. 2007, Wersin et al. 2008, Samper et al. 2008, Savage et al. 2010c, Marty et al. 2010, Lu et al. 2011). Studies of archaeological artefacts have also contributed important information on surface coatings and reaction mechanisms of iron corrosion (e.g. Bellot-Guriet et al. 2009, Saheb et al. 2010), but there are no data relevant to effects upon compacted clay. A more thorough review of this issue is in preparation (Bradbury et al. 2014).

6.1.1 Key reactions

Like cement-bentonite reactions, an essential feature of iron-bentonite interactions is that they are strongly coupled in a non-linear fashion (e.g. Figure 11):

- Anaerobic corrosion of steel supplies ferrous ions and hydrogen gas at the interface with bentonite. Sorption of ferrous ions on the clay may act as a 'pump', driving steel corrosion.
- Ion exchange/sorption of Fe^{2+} on clay will retard its migration through the bentonite, but may be linked to long-term mineralogical transformation processes.
- Corrosion of steel may be linked to smectite transformation through chemical reduction of structural Fe^{3+} in the clay and an increase in layer charge.
- Anaerobic corrosion of iron serves to increase pore fluid pH[3], thus accelerating clay dissolution and the tendency for formation of zeolites.
- Transformation of montmorillonite to non-swelling minerals (e.g. berthierine, chlorite) will change the physical properties of the bentonite, potentially reducing swelling capacity.

[3] A generalised anaerobic corrosion reaction is: $Fe + 2H_2O = Fe^{2+} + 2OH^- + H_2$. This reaction thus increases pH, potentially destabilising montmorillonite.

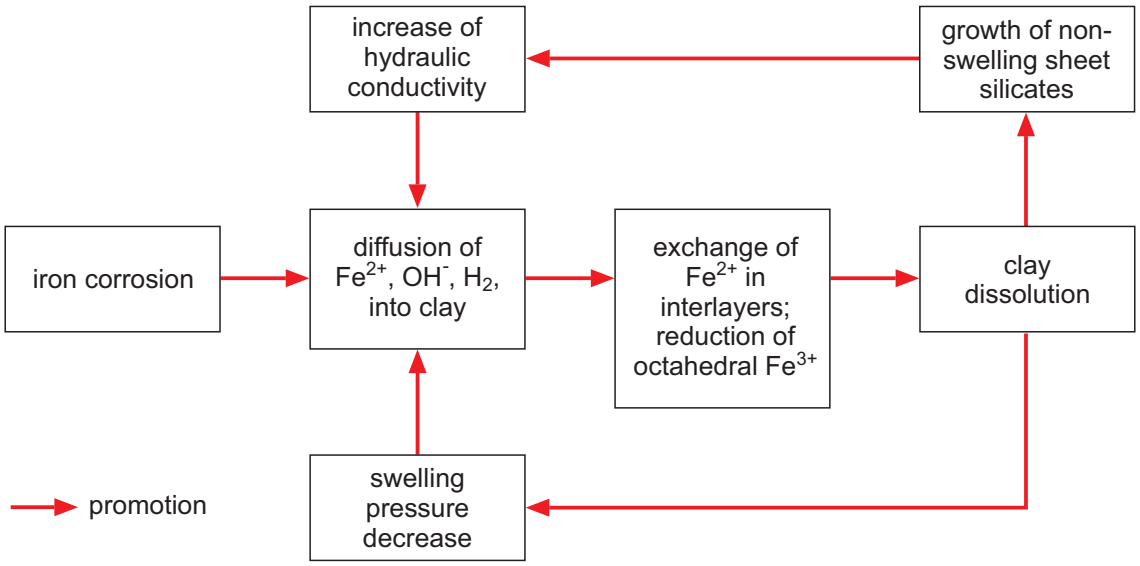

Fig. 11: Iron-bentonite interaction as a non-linear process.

Although mineral transformation of the buffer is expected to proceed slowly, due to the slow steel corrosion rate, slow diffusive migration rate of Fe(II), which is retarded by sorption, and the slow kinetics of the transformation processes, there is evidence from some laboratory experiments that transformation can proceed rapidly, even at relatively low temperatures (Lantenois et al. 2005). Moreover, experiments investigating the corrosion of steel in compacted bentonite (Carlson et al. 2007) have shown that the hydraulic conductivity of bentonite may be substantially increased by steel-bentonite interactions on a relatively short timescale (2 – 3 years).

Laboratory experimental studies of the corrosion of iron in clay show that corrosion product layers are generally thin (< 1 µm) with magnetite, siderite, or 'green rust' occurring depending upon temperature and ambient $_PCO_2$ (Johnston et al. 1985, Allen & Wood 1988, Hermansson 2004, Carlson et al. 2007). However, the results of experiments to characterise the mineralogical products of iron-bentonite interaction are equivocal because the inevitable short-term nature of laboratory experimental studies introduces issues of metastability and kinetics. Factors influencing bentonite alteration include: reaction time, temperature, water/clay ratio, and clay and pore fluid compositions. For example, high temperature experiments (> 250 °C) are dominated by iron chlorite (Cathelineau et al. 2005), whereas lower temperatures produce berthierine, odinite, cronstedtite, or Fe-rich smectite (e.g. Lantenois et al. 2005, Wilson et al. 2006a), depending on initial clay composition and water/clay ratio.

This ambiguity of experimental data has been interpreted as evidence for the relevance of Ostwald step processes in bentonite alteration (Savage et al. 2010c). The models by Savage et al. demonstrate in particular, the potential replacement of initially-forming metastable minerals such as magnetite and odinite, by thermodynamically more stable solids such as berthierine and in the long-term, chlorite.

Experimental results obtained during the EC NF-PRO project on the corrosion of iron/steel in compacted bentonite have challenged the accepted wisdom that steel corrosion would lead to the development of thick corrosion product layers of magnetite/iron oxyhydroxides on canisters. It is clear from experiments with compacted bentonite conducted under NF-PRO (e.g. Carlson et al. 2007) that this is not the case over experimental timescales, in which only thin corrosion product layers develop, with iron diffusing and sorbing readily through the bentonite, driven by the concentration gradient between the internal and external boundary of the bentonite.

Since iron-bentonite interaction is a coupled non-linear problem, it is not always informative to use simple mass balance or kinetic arguments to define the potential magnitude of alteration over the long-term, especially with regard to that around large masses of iron/steel such as waste canisters. Instead, the results of coupled reaction-transport simulations may be more useful to help define the potential extent of alteration. Moreover, the results of these simulations help provide a pointer to other potential changes, such as those to physical properties such as porosity and also mineralogical composition. A summary of these modelling results is presented in Table 14.

All of these simulations rely on a geometry such as that shown in Figure 9 where a thickness of bentonite has an inner boundary condition defined by a corroding iron surface or iron corrosion product and an outer boundary defined by ambient groundwater. There are no simulations published carried out under a temperature gradient. Not all simulations include kinetically-controlled mineral dissolution-precipitation reactions, but most include both ion exchange and clay surface reactions. Some simulations include the effects of changing porosity on transport properties (diffusion coefficient) through Archie's Law.

6.1.2 Thickness of alteration zone

The estimated extent of alteration is an important parameter because it is important in defining the overall distance/thickness of perturbed properties of the bentonite. Here, the alteration extent is defined by the limit of total removal of montmorillonite from the clay at 100 ka after closure, estimated both for that portion of the bentonite surrounding waste packages and that associated with the hydraulic seals (Figure 1).

Canister zone

This refers to the zone of the bentonite between the canister and the concrete tunnel liner. Alteration will proceed mainly around the canister, but also in contact with engineered structures such as the steel mesh, anchors and rails.

For alteration around the canister, a mass balance constraint with respect to the conversion of an idealised sodium montmorillonite ($Na_{0.33}Mg_{0.33}Al_{1.67}Si_4O_{10}(OH)_2$) to chlorite (chamosite[4] – $Fe_5Al_2Si_3O_{10}(OH)_8$) conserving aluminium can be written thus:

$$\text{Montmorillonite} + 4.18\ Fe^{2+} + 6.02\ H_2O \rightarrow$$

$$0.84\ \text{Chlorite} + 0.33\ Na^{+} + 0.33\ Mg^{2+} + 1.50\ SiO_{2\,(aq)} + 7.36\ H^{+} \qquad (5)$$

[4] Chlorites can be quite variable in composition, but those that form in low-temperature sedimentary environments tend to be chamositic (e.g. Grigsby, J.D. 2001: *Origin and growth mechanism of authigenic chlorite in sandstones of the Lower Vicksburg Formation, South Texas*. Journal of Sedimentary Research 71, 27-36).

Therefore, 4.18 moles of Fe^{2+} ions released by steel corrosion are required to alter one mole of montmorillonite to 0.84 moles of chlorite. Consequently, the total mass of steel (iron) in a canister (23'000 kg or 411'817 moles of Fe; Table 3) is sufficient to alter 98'521 moles, or 13.23 m^3 of montmorillonite of 1.34×10^{-4} m^3 molar volume. Since bentonite contains approximately 90 vol.-% montmorillonite at the compaction densities of interest (see Table 5), then this volume of altered montmorillonite equates to an altered bentonite volume of 14.68 m^3.

If this altered volume of bentonite is distributed radially around each 4.6 m long canister (Table 3), then this corresponds to an annulus of altered bentonite of 0.63 m. Since the initial annulus of pristine bentonite around each canister in the disposal tunnel is 0.75 m (Figure 4), then the mass balance assumption results in consumption of 77 % of the total bentonite volume around each canister in the tunnel. This estimate is midway in the range of estimates described by Bradbury et al. (2014) of between 50 and 99 % consumption, depending upon canister type[5].

Bradbury et al. (2014) also evaluate the possibility of conversion of montmorillonite to berthierine (a non-swelling iron-bearing serpentine-like mineral) due to reaction with the steel canister and demonstrates that the amounts of montmorillonite potentially destroyed are roughly three times greater than that for conversion to chlorite. However, it is likely that berthierine is only metastable in this system (e.g. Savage et al. 2010c) and would not be a long-term product of iron-bentonite interaction due to its instability in pore fluids saturated with quartz (Fritz & Toth 1997).

In order to place a timescale on the alteration of montmorillonite to chlorite, it is necessary to consider the steel corrosion rate, and hence the rate of generation of Fe^{2+} for subsequent alteration of bentonite. King reports a long-term anaerobic corrosion rate for carbon steel of 1 to 2 μm yr^{-1} (King 2008), which for the geometry and surface area of a typical waste package (see Table 3), translates into a supply of Fe^{2+} of 0.19 kg yr^{-1} or 3.4 moles yr^{-1} per package (using the mean rate of corrosion of ~ 1.5 μm yr^{-1}). If all this iron is pessimistically assumed to result in conversion of montmorillonite directly to chlorite (as above), then this would take approximately 120'000 years. However, the rate-limiting steps in this reaction are not the rate of supply of iron, but the slow dissolution rate of montmorillonite (Figure 2), even at the slightly elevated pH (~ 10) of pore fluids associated with steel corrosion, and the even slower nucleation and growth of sheet silicates such as chlorite, so that this calculation hugely overestimates the rate of destruction of bentonite.

Although these calculations are informative, they are pessimistic, since there would not only be the slow transformation of montmorillonite to chlorite to consider, but also the physical properties changes in the clay and at the clay-canister interface which would hinder aqueous transport of iron through the bentonite pore space, so that a consideration of a mass transport limitation on clay alteration is more likely. This constraint is most readily assessed using the results of the coupled reaction-transport simulations summarised in Table 14. This Table shows results from simulations carried out at 25, 50 and 100 °C, with a range of bentonite thicknesses (0.4 – 1.0 m), and some with porosity feedback, others without. Different computer codes were used in the simulations (CRUNCHFLOW, QPAC, KIRMAT, etc) with subtly different thermodynamic databases. All simulations included the kinetics of mineral hydrolysis reactions. The results are remarkably consistent, with a maximum extent of montmorillonite removal of only 0.01 – 0.1 m after tens of thousands of years.

[5] Bradbury et al. (2014) considered three different canister types for spent fuel and one type for vitrified waste in their assessment of iron-bentonite interaction.

Most simulations indicate a total clogging of porosity at the canister-bentonite interface at some stage of the evolution, but one study (Bildstein et al. 2006) suggests a porosity increase from 36.5 to 42.5 % and another (Montes-H et al. 2005a, b, c) suggests negligible change (30 to 29 vol.-%).

The results show that the maximum alteration depth of clay is calculated to range from 0.01 to 0.10 m (the latter after after 50'000 years), with alteration being ceased by the filling of porosity at the contact between the canister and the clay at that time. These figures would thus imply an essentially unperturbed annulus of 0.75 m of bentonite unaltered by reaction with the canister.

Tab. 14: Summary of some iron-clay reaction-transport simulations carried out over the last ten years.

Only those simulations including the dissolution-precipitation reactions have been included. The alteration depth is defined as the maximum depth of total removal of montmorillonite.

Clay type; thickness; dry density	**T** [°C]	**Kinetics**	**Porosity Feedback**	**Products**	**Alteration depth** [m]	**Porosity change** [%]	**Ref.**
MX-80; 1 m; 1700 kg m^{-3}	100	Yes	No	Ca-montmorillonite, illite, saponite, laumontite, magnetite, chlorite	0.1 @ 10 ka	30 → 29	[1]
MX-80; 0.8 m; ? kg m^{-3}	50	Yes	Yes	Magnetite, cronstedtite, chamosite, Fe-smectite, siderite, scolecite, saponite	0.1 @ 5 ka	36.5 → 42.5 10 cm from canister; 36.5 → 0 in canister cell	[2]
MX-80; 1 m; 1700 kg m^{-3}	100	Yes	No	Saponite, illite, laumontite, chlorite, magnetite, greenalite, vermiculite	0.05 @ 50 ka	30 → 0 at contact with canister	[3]
MX-80; 0.5 m; 1590 kg m^{-3}	25	Yes	Yes	Magnetite, chlorite, siderite, clinoptilolite	0.01 @ 0.15 ka	42 → 0 at contact with canister	[4]
MX-80; 0.4 m; 1560 kg m^{-3}	25	Yes	Yes	Magnetite, berthierine, cronstedtite	0.09 @ 100 ka	47 → 0 at contact with canister	[5]
MX-80; 0.5 m; 1590 kg m^{-3}	25	Yes	Yes	Magnetite, cronstedtite, berthierine, chlorite, siderite, analcime	-	42 → 0 at interface with canister	[6]
MX-80, 1 m, 1600 kg m^{-3}	100	Yes	Yes	Magnetite, chlorite, saponite, laumontite, greenalite, chabazite, phillipsite, chrysotile	0.05 @ 100 ka	39 → 0 at contact with canister	[7]

[1] Montes-H et al. (2005a, b, c). [2] Bildstein et al. (2006). [3] Fritz et al. (2006). [4] Hodgkinson et al. (2007). [5] Wersin et al. (2008). [6] Savage et al. (2010c). [7] Marty et al. (2010).

Tab. 15: Summary of estimated changes to bentonite properties due to interaction with steel EBS components at 100 ka after closure.

EBS Component	**Buffer**		**Sealing element**	
Scenario	*Optimistic*	*Pessimistic*	*Optimistic*	*Pessimistic*
Alteration zone thickness	0.01 m annulus around canister	0.1 m annulus around canister	1 vol.-% altered	10 vol % altered
Porosity	Zero at canister contact; unchanged in remainder	Unchanged throughout	Unchanged throughout	Unchanged throughout
Hydraulic conductivity	Unchanged throughout	Unchanged throughout	Unchanged throughout	Unchanged throughout
Swelling pressure	Zero at 0 – 0.01 m from canister; unchanged in remainder	Zero at 0 – 0.1 m from canister; unchanged in remainder	Zero in 1 % of volume; unchanged in remainder	Zero in 10 % of volume; unchanged in remainder
Mineralogy	Berthierine, illite, chlorite, magnetite, saponite, Fe-montmorillonite, zeolites in altered zone around canister; unchanged in remainder		Berthierine, illite, chlorite, magnetite saponite, Fe-montmorillonite, zeolites in altered zones adjacent to engineered structures; unchanged in remainder	

Similarly, the potential interaction of other engineered structures in the canister zone with bentonite is relatively minor. Even using the mass balance constraint of conversion of montmorillonite to chlorite outlined above, then only 2 vol.-% of the total bentonite in the canister zone would be transformed by reaction with these structures. Removing the rails prior to closure would reduce this effect to 1 vol.-%.

Sealing element

In this zone, there are no canisters present (see Figure 1), but there are ten steel reinforcement arches, along with steel mesh, steel anchors and steel rails. Using the mass balance constraint described above (conversion of montmorillonite to chlorite), then a maximum of 5 vol.-% of bentonite could be transformed to chlorite. Removing the rails prior to closure would reduce this effect to 4 vol.-%.

6.1.3 Potential changes to safety-relevant properties

The information relating to the alteration of clay by steel/iron is synthesised in terms of potential changes to a number of PA-relevant properties (porosity, hydraulic conductivity, swelling pressure, and mineralogical composition) at 100 ka after closure. These conclusions are presented in Table 15. Both the optimistic and pessimistic figures in Table 15 are based upon the results of reaction-transport modelling.

Changes to porosity

The conversion of montmorillonite to chlorite described above involves a net solid volume decrease of 33 % using molar volumes of 1.34×10^{-4} and 1.06×10^{-4} m^3 for montmorillonite and chlorite (chamosite) respectively, implying an overall increase in porosity due to this reaction. However, the more comprehensive treatment of mass balances in computer simula-

tions of iron-bentonite interaction predict a complete filling of porosity at the canister-bentonite interface due to partial conversion of steel to magnetite at some stage of the evolution of the system (Table 14). Optimistic values of porosity in the canister zone are therefore taken to be zero (at some point within the mineralogically-altered zone) in Table 15, whereas pessimistic values are assumed to be unchanged from initial values.

Porosity in the sealing element zone is taken to be unchanged because of the low percentage of alteration indicated by mass balance calculations.

Changes to hydraulic conductivity

Hydraulic conductivity has been measured in samples of compacted MX-80 bentonite from steel corrosion experiments conducted at 30 and 50 °C for up to 3 years (Carlson et al. 2008). Although these samples had to be reconstituted (clay is separated from the wires/coupons before the measurements), they provide some indication of the potential change (if any) in this parameter. The results of these tests are presented here in Figure 12 which shows that the hydraulic conductivity of clays subjected to the effects of alteration by iron may be greater than samples of pristine MX-80. This is due to a lowering of the montmorillonite/water ratio which determines the magnitude of interactions between water and clay surfaces, and hence hydraulic conductivity (Wersin et al. 2008). Also, any alteration product of montmorillonite can be considered to form isolated grains which have a higher porosity than intact bentonite, thus increasing hydraulic conductivity (Wersin et al. 2008). This difference in hydraulic conductivity increases with decreasing dry density, but at the target dry density for the Nagra engineered barrier system (in excess of 1450 kg m^{-3}), although there is an indication of slightly higher values in the altered samples, it is effectively indistinguishable from pristine MX-80. Without further evidence (e.g. from analogues or *in situ* experiments), it is therefore concluded that the hydraulic conductivity will remain unchanged in both the canister and sealing element zones.

See section 4.3.2 for the potential changes to safety relevant properties due to the cement liner degradation and its impact on hydraulic conductivity.

Changes to swelling pressure

Swelling pressure in compacted bentonite is produced by interlayer cation hydration and osmotic effects in montmorillonite (e.g. Savage 2005) and is therefore dependent upon the presence of montmorillonite in the buffer/sealing element. Total removal of montmorillonite from bentonite will thus reduce swelling pressure to zero. Since the extent of the zone of mineralogical alteration is here defined by total loss of montmorillonite, then the swelling pressure of this altered zone is assumed to be zero (Table 15).

In the zone where montmorillonite is still present, the measurements of swelling pressure on samples of compacted bentonite from steel corrosion experiments, Carlson et al. (Carlson et al. 2008) are pertinent. Their results are presented here in Figure 13. Here, it may be seen that in the zone of dry density of interest (> 1450 kg m^{-3}), the swelling pressure values of altered samples are effectively identical to those of samples of pristine bentonite. Unfortunately, Carlson et al. do not present any conclusions regarding the degree of alteration of the original bentonite in their experiments (Carlson et al. 2008). Therefore it is concluded that swelling pressures in the zone of alteration (in both canister and sealing element zones) where montmorillonite is still present is unaffected by the alteration process.

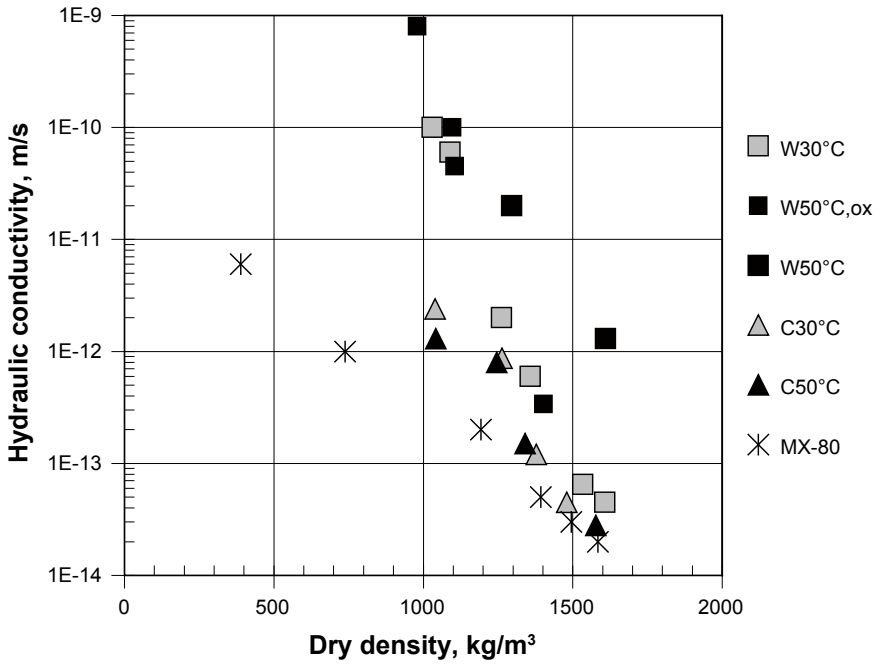

Fig. 12: Measured hydraulic conductivity as a function of reduced clay dry density in compacted clay samples from experiments with corroding steel wires and coupons.

'MX-80' indicates pristine (unaltered) bentonite. 'C' indicates coupon samples, 'W' indicates wire samples, 'W50°C, ox' indicates a slightly oxidised wire from a 50 °C experiment. From Carlson et al. (2008).

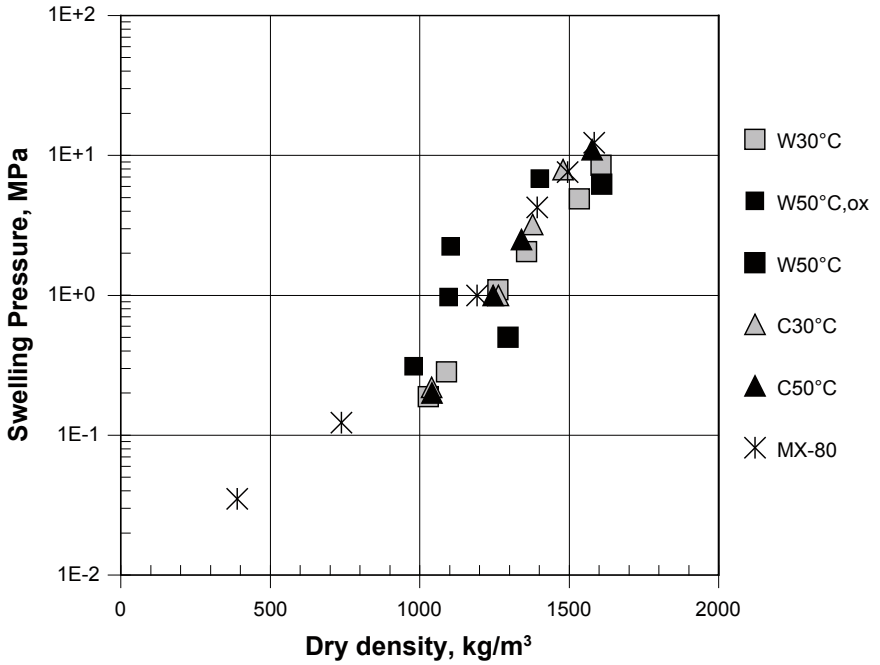

Fig. 13: Measured swelling pressure as a function of reduced clay dry density in compacted clay samples from experiments with corroding steel wires and coupons.

'MX-80' indicates pristine (unaltered) bentonite. 'C' indicates coupon samples, 'W' indicates wire samples, 'W50°C, ox' indicates a slightly oxidised wire from a 50 °C experiment. From Carlson et al. (2008).

See section 4.3.3 for the potential changes to safety relevant properties due to the cement liner deagradtion and its impact on the swelling pressure.

Changes to mineralogy

Despite uncertainties in mineralogical evidence from laboratory experiments, the predicted mineral assemblages resulting from iron/steel-bentonite interaction are relatively consistent (see Table 14). These simulations tend to show minerals such as magnetite, siderite and cronstedtite forming on, or near, the corroding steel surface, with minerals such as berthierine, illite, saponite, chlorite and zeolites (scolecite, clinoptilolite, chabazite, phillipsite, analcime) forming further into the bentonite itself. Unfortunately, there is no directly-relevant published analogue information to help confirm these predictions. Savage et al. (2010c) have argued that information from iron-rich marine sediments gives credence to the idea that odinite and berthierine may form as metastable precursors to chlorite such that a time-sequence of alteration minerals is formed.

6.2 Copper

Under chemically-reducing conditions (as would be expected for pore fluids in any repository in the Opalinus Clay) copper is expected to be immune to corrosion (e.g. King et al. 2001, 2010). Dissolved sulphide species are, therefore, the only corrosive substances that can react with the copper canister after the oxygen in the repository has been consumed. At the proposed repository depth, Opalinus Clay groundwaters have very low sulphide concentrations, mostly much lower than 5×10^{-7} M (Mäder 2009), and the solubility of the sulphide minerals present in the bentonite is, at most, of the same order of magnitude. This means that the corrosion of the copper canister due to sulphides will be controlled by the availability and supply of sulphides from the groundwater and the buffer. Pitting corrosion is unlikely under the chemical conditions of the Opalinus Clay and both Aaltonen & Varis (1993) and Karnland et al. (2000) report no localised corrosion of Cu exposed to compacted clay over periods of up to 2 years. These data indicate that no pitting is to be expected, but that there may be unevenness around the average corrosion depth of roughly the same magnitude as the total corrosion depth. Rosborg & Werme (2008) report an average corrosion rate of less than 0.5 μm per year after 6 years exposure at elevated temperatures. In contrast to other work on the subject, Szakalos et al. (2007) have claimed that copper will undergo corrosion in pure water in the absence of oxygen and cite a new coorosion product, H_xCuO_y as evidence of this process. This study is controversial and is being evaluated through new experimental work. Milodowski et al. (2003) present an analysis of the corrosion of native copper plates that have survived in a water-saturated clay environment for more than 176 million years. Although the native copper is affected by corrosion, the study shows that a significant proportion (30 – 80 % of the original thickness) of the copper sheets is preserved in the saturated compacted clay environment of the Littleham Mudstone, UK. Apart from the recent weathering effects due to exposure at outcrops, petrographical studies demonstrate that most of the observed corrosion and alteration of the native copper is geologically old (i.e. pre-dating sediment compaction) and also occurred before the end of the Lower Jurassic Period. This demonstrates that the native copper can remain stable in a saturated and compacted clay environment for geological timescales well in excess of the timescales considered for safety assessment of a deep geological repository for high-level radioactive wastes.

Despite the importance of copper coexisting with bentonite in the KBS-3 disposal concept employed in the Swedish and Finnish radioactive waste disposal programmes, there is very little published information on potential chemical interactions between the two materials. For

instance, although reports have been written on the interactions between copper corrosion products and MX-80 bentonite (e.g. Wersin et al. 1994, Carlsson 2007), these have focused wholly on the corrosion products of copper, with no mention of potential mineralogical alteration of the bentonite. Karnland et al. have reported migration of copper from copper canister materials into compacted bentonite in the long-term LOT tests at the Äspö underground laboratory (Karnland et al. 2000, 2009) but reported only minor uptake of copper (< 1 % of total exchangeable cation pool) in the bentonite nearest the copper heater employed in the experiment. This suggests that Cu has been incorporated in the bentonite matrix mainly in a form that is not readily soluble or accessible for cation exchange. Montmorillonite alteration processes involving copper have not been reported in the literature.

Nevertheless, copper will exchange for Na^+ in the interlayer sites in montmorillonite (Sposito et al. 1981, Fletcher & Sposito 1989, Zhang & Sparks 1996), with an equilibrium constant (*K*) of 1.35 being reported for Cu/Na exchange, similar to that for other divalent cations such as Ca^{2+} (1.48), Mg^{2+} (1.48), Sr^{2+} (1.48), Zn^{2+} (1.48), Cd^{2+} (1.48) and Co^{2+} (1.48) (Fletcher & Sposito 1989). Since the dissolution rate and solubility of copper is very low under anticipated near-field conditions, even the effects of ion exchange will be minor. Nevertheless, in the absence of any copper-specific data, it is anticipated that copper-montmorillonite is likely to have key properties (hydraulic conductivity, swelling pressure) very similar to those of calcium montmorillonite.

Muurinen et al. (1990) report a diffusion coefficient of 5×10^{-12} m^2 s^{-1} for copper in compacted bentonite at a dry density of 1800 kg m^{-3}.

Potential changes to safety-relevant properties

There is no evidence (experimental or analogue) for the destruction of montmorillonite in bentonite due to its interaction with copper. Moreover, the exchange of copper for sodium in interlayer sites in montmorillonite is likely to be minor (< 1 % of exchangeable cations) because of the low solubility of copper. Consequently, there are no anticipated changes to safety-relevant properties such as porosity, hydraulic conductivity, swelling presssure and mineralogy due to the presence of copper as a canister material.

7 Summary and Conclusions

Potential interactions of bentonite with engineered components (canister metals, concrete tunnel liner, steel support mesh and arches) in a geological repository for SF/HLW in Opalinus Clay have been assessed. These interactions are likely to be strongly non-linear, with a complex interplay between fluid transport, clay ion exchange and dissolution, secondary mineral growth, and consequent changes in physical properties (porosity, permeability, swelling pressure) of the clay. Alteration of the clay due to reaction with other EBS components results in decreasing porosity with time, such that in the long-term, porosity may become totally occluded thus limiting the scale of transformation through mass transport considerations. The time-dependent nature of mineral transformation processes means that not all are readily amenable to study by conventional laboratory experimental procedures. Consequently, the results of published reaction-transport simulations have been important in defining the scale and key properties at PA-relevant timescales.

However, it should be noted that there are no simulations specifically carried out for the conditions of interest described here (compacted MX-80 bentonite surrounding a steel canister with an external boundary of concrete/Opalinus Clay in a temperature gradient). It is recommended that such reaction-transport calculations be carried out in future to better define the potential magnitude of alteration.

In detail, interactions have been assessed with regard to the effects of the thermal output of the wastes, interactions with the concrete tunnel liner and interactions with various metallic engineering components – steel or copper waste canisters and steel supporting mesh, anchors and support arches. Despite the differing nature of the chemical interactions of bentonite with concrete and steel, it is considered that the timescales of alteration will be similar due to the similar rates of key processes in the bentonite (montmorillonite dissolution and the growth of zeolite and sheet silicate minerals at alkaline pH). However, it should be remembered that:

- alteration of the bentonite by concrete occurs from the liner towards the centre of the tunnel and thus alteration fronts proceed in the same direction as resaturating groundwater
- alteration of the bentonite by steel occurs from the canister towards the tunnel liner and thus the onset of alteration may be delayed by the time for full resaturation of the bentonite to occur.

Although these bentonite alteration processes have been evaluated separately in previous sections, here they are synthesised below into combined effects for optimistic and pessimistic scenarios, respectively at a nominal 100 ka after closure. The optimistic and pessimistic estimates are based upon information summarised in Table 16 and are those considered for scenarios where creep of the host rock is ignored.

The interactions of a copper canister with bentonite are predicted to be restricted to minor amounts of cation exchange in montmorillonite (Cu for Na) at all timescales, resulting in no changes to safety-relevant properties over the liftime of the repository.

Tab. 16: Constraints on estimates of the scale of alteration with time.

	Optimistic	**Pessimistic**
Bentonite around canister	Lower estimates from reaction-transport simulations listed in Tables 11, 13, 15	Higher estimates from reaction-transport simulations listed in Tables 11, 13, 15
Bentonite adjacent to concrete liner	Lower estimates from reaction-transport simulations listed in Tables 11, 13, 15	Higher estimates from reaction-transport simulations listed in Tables 11, 13, 15
Concrete liner	Estimates from reaction-transport simulations listed in Section 5.4	Estimates from reaction-transport simulations listed in Section 5.4
Engineered structures	Montmorillonite to chlorite mass balance	Montmorillonite to chlorite mass balance
Sealing element	Montmorillonite to chlorite mass balance	Montmorillonite to chlorite mass balance

7.1 Optimistic estimates of alteration at 100 ka

For the optimistic estimate of alteration at 100 ka after closure, there is a thin (0.05 m; 1 vol.-% total bentonite) alteration layer around the canister, derived partly through thermal redistribution of minerals and aqueous solutes, and partly due to interaction of the steel canister with bentonite (Figure 14). These results in a zone with zero porosity (mainly due to magnetite precipitation on the canister) and zero swelling pressure (montmorillonite totally removed) around the canister, but with an assumed hydraulic conductivity the same as the initial value (a result of zero porosity counterbalanced by potential embrittlement/fracturing in the altered zone). The mineralogical composition of this zone is assumed to consist of a thin layer of calcite, gypsum/ anhydrite and magnetite on the canister, with montmorillonite in the altered bentonite replaced by Fe-silicates such as cronstedtite, berthierine and chlorite. External to this inner alteration zone is an annulus of 0.68 m (92 vol.-%) of unaltered bentonite.

The potential interaction of metallic engineered structures other than the canister with bentonite is assumed to be relatively minor. Even using a mass balance constraint of conversion of montmorillonite to chlorite, then only 5 vol.-% of the total bentonite in the canister zone would be transformed by reaction with these structures. Removing the rails prior to closure would reduce this effect to 2 vol.-%.

At the external margin of the tunnel, alteration of the buffer and sealing element adjacent to the concrete liner is estimated to be 0.02 m thick (4 vol.-% total bentonite). Note that there is no concrete along the sealing element interface, so this estimate is somewhat unrealistic. The hydraulic conductivity of this zone is decreased in comparison with the initial state. The porosity and swelling pressure of the altered bentonite are likely to decrease to zero due to removal of montmorillonite. The mineralogical composition of the altered bentonite is likely to be characterised by a sequence of calcite, C-(A)-S-H minerals, Ca-zeolites, sepiolite and saponite clays, with C-S-H minerals forming nearest the cement contact, and other minerals such as zeolites and clays forming further towards the canister.

The concrete liner itself may degrade via conversion of portlandite and C-S-H gel to ettringite with a consequent increase in porosity. Reaction-transport simulations suggest that this increase is of the order of a few %.

For the sealing element, there are no canisters present (see Figure 1), but there are ten steel reinforcement arches, along with steel mesh, steel anchors and steel rails. Using the conversion of montmorillonite to chlorite mass balance constraint described above, then a maximum of 11 vol.-% of bentonite could be transformed to non-swelling silicates. Removing the rails prior to closure would reduce this effect to 8.5 vol.-%.

7.2 Pessimistic estimates of alteration at 100 ka

This estimate has a thicker (0.1 m; 8 vol.-% total bentonite) alteration layer around the canister, again derived partly through thermal redistribution of minerals and aqueous solutes, and partly due to interaction of the steel canister with bentonite (Figure 15). This results in a zone with zero porosity (due mainly to magnetite precipitation) and zero swelling pressure, again with hydraulic conductivity the same as the initial value.

Alteration of the buffer and sealing element adjacent to the concrete liner is estimated to be 0.2 m (35 vol.-% total bentonite). The porosity and hydraulic conductivity of this zone are estimated to be unchanged with regard to the initial state, but with zero swelling pressure due to removal of montmorillonite. The mineralogical composition is likely to be characterised by a sequence of calcite, C-(A-)S-H minerals, Ca-zeolites, sepiolite and saponite clays, with C-S-H minerals forming nearest the cement contact, and other minerals such as zeolites and clays forming further away. Corresponding estimates for an OPC concrete liner show that the amount of bentonite destroyed is increased by a factor of 2.5 and alteration thicknesses are increased by a factor of between 2.5 and 3 (~ 60 vol.-% of total bentonite).

The scale of alteration of the clay around the metallic engineered structures and in the sealing element is assumed to be the same as the optimistic estimates.

7.3 Evolution of alteration

It is also pertinent to consider how the scale of alteration may evolve with time. This is discussed below and summarised in Table 17.

7.3.1 State at 1 ka

Table 17 shows estimated alteration effects for 1 ka after closure. This description is based upon an intermediate condition between the initial state and the estimated pessimistic state of alteration at 100 ka described in Table 11, Table 12 and Table 15 and described in Section 7.1.

7.3.2 State at 100 ka

Table 17 shows estimated alteration effects for 100 ka after closure. This description is based upon the pessimistic estimates of alteration at 100 ka described in Table 11, Table 12 and Table 15 and described in Section 7.2 above.

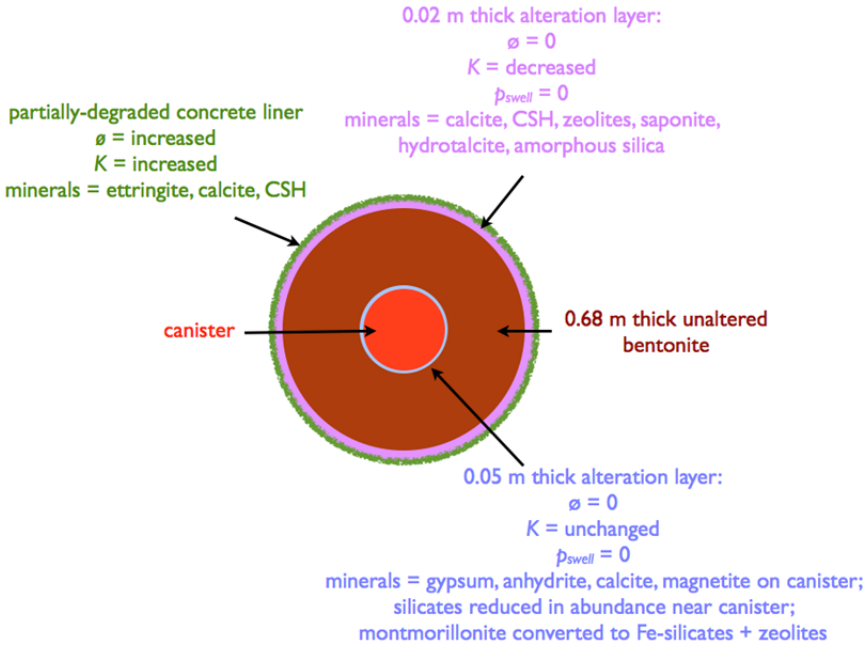

Fig. 14: Schematic illustration of the estimated spatial distribution of bentonite properties changes at 100 ka after closure (optimistic estimate).

The figure shows a disposal tunnel cross-section in pre-creep conditions around a waste canister (canister support not shown).

Not to scale.

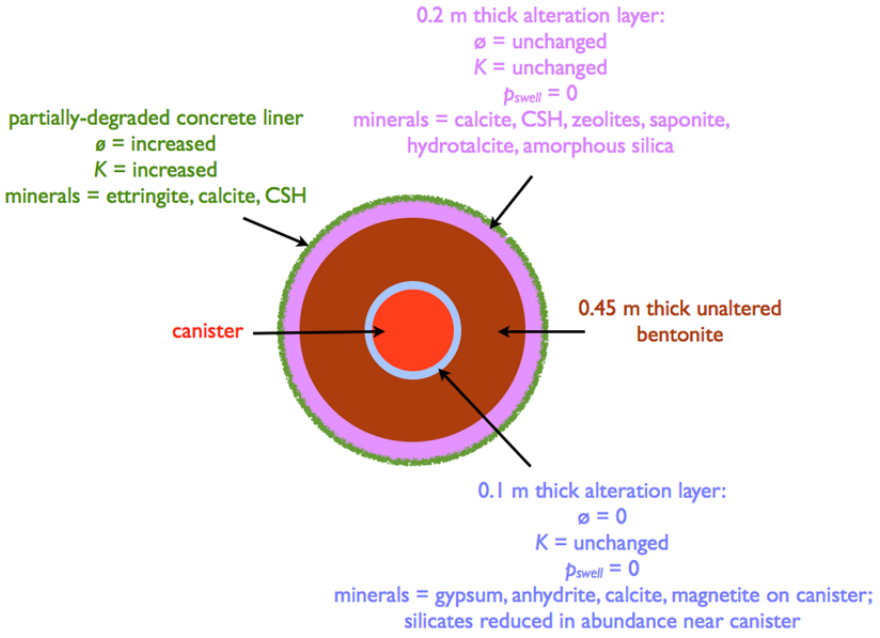

Fig. 15: Schematic illustration of the estimated spatial distribution of bentonite properties changes at 100 ka after closure (pessimistic estimate).

The figure shows a disposal tunnel cross-section in pre-creep conditions around a waste canister (canister support not shown).

Not to scale.

7.3.3 State at 1 Ma

Here, it is assumed that the canister would be completely degraded and beyond this, montmorillonite is considered to be totally converted to non-swelling Fe-silicates such as cronstedtite, berthierine and chlorite (estimated from mass balance considerations). This transformation is expected to preserve the original porosity and hydraulic conductivity of the bentonite, but to decrease swelling pressure to zero. This altered zone is estimated to be 0.45 m thick and to extend to the bentonite zone altered by interaction with the concrete liner.

Alteration of the buffer and sealing element adjacent to the concrete liner is estimated to be the same as that for the state at 100 ka.

The concrete liner itself is likely to have totally degraded at this time.

Tab. 17: Estimates of the evolution of the scale of alteration with time.

	1 ka	**100 ka**	**1 Ma**
Bentonite around canister	0.01 m thick alteration: ø = 0 *K* = unchanged p_{swell} = 0 minerals = gypsum, anhydrite, calcite, magnetite on canister; silicates reduced in abundance near canister; montmorillonite converted to Fe-silicates + zeolites	0.1 m thick alteration: ø = 0 *K* = unchanged p_{swell} = 0 minerals = gypsum, anhydrite, calcite, magnetite on canister; silicates reduced in abundance near canister; montmorillonite converted to Fe-silicates + zeolites	altered bentonite surrounding corroded remains of canister (Fe oxy-hydroxides) ø = unchanged *K* = unchanged p_{swell} = 0 minerals = Fe-silicates + zeolites
Bentonite adjacent to concrete liner	0.01 m thick alteration: ø = 0 *K* = decreased p_{swell} = 0 minerals = calcite, CSH, zeolites, saponite, hydrotalcite, amorphous silica	0.2 m thick alteration: ø = unchanged *K* = unchanged p_{swell} = 0 minerals = calcite, CSH, zeolites, saponite, hydrotalcite, amorphous silica	0.2 m thick alteration: ø = unchanged *K* = unchanged p_{swell} = 0 minerals = calcite, tobermorite, zeolites, saponite, hydrotalcite, amorphous silica
Concrete liner	Partially-degraded *ø* = increased *K* = increased minerals = ettringite, calcite, CSH	Partially-degraded *ø* = increased *K* = increased minerals = ettringite, calcite, CSH	Fully disintegrated minerals = ettringite, calcite, tobermorite
Engineered structures	Minor degradation of adjacent clay	5 vol.-% bentonite converted to non-swelling sheet silicates	5 vol.-% bentonite converted to non-swelling sheet silicates
Sealing element	Minor degradation of adjacent clay	11 vol.-% bentonite converted to non-swelling sheet silicates	11 vol.-% bentonite converted to non-swelling sheet silicates

8 References

Aaltonen, P. & Varis, P. (1993): Long term corrosion tests of OFHC-coppers in simulated repository conditions – final report. Report YJT-93-05. Nuclear Waste Commission of Finnish Power Companies, Helsinki.

Alexander, W.R. & Neall, F. (2007): Assessment of potential perturbations to Posiva's SF repository at Olkiluoto from the ONKALO Facility. Posiva Working Report 2007-35. Posiva Oy, Olkiluoto, Finland.

Allen, C.C. & Wood, M.I. (1988): Bentonite in nuclear waste disposal: a review of research in support of the Basalt Waste Isolation Project. Applied Clay Science 3, 11-30.

Arcilla, C.A., Pascua, C.S., Vargas, E., Honrado, M.L.L., Alexander, W.R., Namiki, K., Fuji, N., Yamakawa, M., Sato, T. & McKinley, I.G. (2009): Reaction pathways for rising hyperalkaline groundwater in a bentonite mine in the Philippines. Geochim. Cosmochim. Acta, Goldschmidt Conference Abstracts: A50.

Arcos, D., Grandia, F. & Domènech, C. (2006): Geochemical evolution of the near field of a KBS-3 repository. SKB Technical Report TR-06-16. Swedish Nuclear Fuel and Waste Management Company, Stockholm.

Arcos, D., Grandia, F., Domènech, C., Fernández, A.M., Villar, M.V., Muurinen, A., Carlsson, T., Sellin, P. & Hernan, P. (2008): Long-term geochemical evolution of the near field repository: Insights from reactive transport modelling and experimental evidences. Journal of Contaminant Hydrology 102, 196-209.

Bauer, A. & Berger, G. (1998): Kaolinite and smectite dissolution rate in high molar KOH solutions at 35 ° and 80 °C. Applied Geochemistry 13, 905-916.

Bellot-Guriet, L., Neff, D., Réguer, S., Monnier, J., Saheb, M. & Dillmann, P. (2009): Raman studies of corrosion layers formed on archaeological irons in various media. Journal of Nano Research 8, 147-156.

Benbow, S., Savage, D., Wersin, P. & Johnson, L.H. (2000): Modelling thermal alteration of bentonite barriers in Opalinus Clay. Silica migration – SiO_2 and smectite kinetics. Unpubl. Nagra Internal Report. Nagra, Wettingen.

Bildstein, O., Trotignon, L., Perronnet, M. & Jullien, M. (2006): Modelling iron-clay interactions in deep geological disposal. Physics and Chemistry of the Earth 31, 618-625.

Birgersson, M. & Karnland, O. (2009): Ion equilibrium between montmorillonite interlayer space and an external solution. Geochim. Cosmochim. Acta 73, 1908-1923.

Börgesson, L., Fredrikson, A. & Johannesson, L-E. (1994): Heat conductivity of buffer materials. SKB Technical Report TR-94-29. Swedish Nuclear Fuel and Waste Management Company, Stockholm.

Bradbury, M.H. & Baeyens, B. (2003): Porewater chemistry in compacted re-saturated MX-80 bentonite. Journal of Contaminant Hydrology 61, 329-338.

Bradbury, M., Berner, U., Curti, E., Hummel, W., Kosakowski, G. & Thoenen, T. (2014): The long term geochemical evolution of the nearfield of the HLW repository. Nagra Tech. Report NTB 12-01. Nagra, Wettingen, Switzerland.

Carlsson, T. (2007): Interactions between copper corrosion products and MX-80 bentonite. NF-PRO RTD2 Deliverable D2.3.11. European Commission.

Carlson, L., Karnland, O., Olsson, S., Rance, A. & Smart, N.R. (2008): Experimental studies on the interactions between anaerobically corroding iron and bentonite. SKB Report R-08-28. Swedish Nuclear Fuel and Waste Management Company, Stockholm.

Carlson, L., Karnland, O., Oversby, V.M., Rance, A., Smart, N., Snellman, M., Vähänen, M. & Werme, L.O. (2007): Experimental studies of the interactions between anaerobically corroding iron and bentonite. Physics and Chemistry of the Earth 32, 334-345.

Carlson, L., Karnland, O., Olsson, S., Rance, A. & Smart, N. (2006): Experimental studies on the interactions between anaerobically corroding iron and bentonite. Posiva Working Report 2006-60. Posiva Oy, Olkiluoto, Finland.

Cases, J.M., Berend, I., Besson, G., Francois, M., Uriot, J.P., Thomas, F. & Poirier, J.E. (1992): Mechanism of adsorption and desorption of water vapor by homoionic montmorillonite. 1. The sodium-exchanged form. Langmuir 8, 2730-2739.

Cathelineau, M., Guillaume, D., Mosser-Ruck, R., Dubessy, J., Charpentier, D., Villiéras, F. & Michau, N. (2005): Dissolution–crystallization processes affecting di-octahedral smectite in presence of iron metal: implication on mineral distribution in clay barriers. *In:* Clays in Natural and Engineered Barriers for Radioactive Waste Confinement, Tours, France, pp. 35.

Charpentier, D., Devineau, K., Mosser-Ruck, R., Cathelineau, M. & Villiéras, F. (2006): Bentonite-iron interactions under alkaline condition: an experimental approach. Applied Clay Science 32, 1-13.

Curti, E. & Wersin, P. (2002): Assessment of porewater chemistry in the bentonite backfill for the Swiss SF / HLW repository. Nagra Tech. Report NTB 02-09. Nagra, Wettingen.

Daneluzzi, R., Burrus, F., Küttel, T., Müller, H.R. & Köhler, S. (2014): Construction of the Emplacement Tunnel for the Full-scale Emplacement (FE) Experiment at Mont Terri Rock Laboratory. Nagra Arbeitsbericht NAB 14-54. Nagra, Wettingen.

De Windt, L., Marsal, F., Tinseau, E. & Pellegrini, D. (2008): Reactive transport modeling of geochemical interactions at a concrete/argillite interface, Tournemire site (France). Physics and Chemistry of the Earth 33, S295-S305.

De Windt, L., Pellegrini, D. & van der Lee, J. (2004): Coupled modeling of cement/claystone interactions and radionuclide migration. Journal of Contaminant Hydrology 68, 165-182.

De Windt, L., van der Lee, J. & Pellegrini, D. (2001): Reactive transport modelling of pH controlling processes in cement/clay systems. *In:* Tenth International Symposium on Water-Rock Interaction, Villasimius, Italy, 1315-1318.

Fernández, R., Mäder, U.K., Rodriguez, M., Vigil de la Villa, R. & Cuevas, J. (2009): Alteration of compacted bentonite by diffusion of highly alkaline solutions. European Journal of Mineralogy 21, 725-735.

Fletcher, P. & Sposito, G. (1989): The chemical modelling of clay/electrolyte interactions for montmorillonite. Clay Minerals 24, 375-391.

Fritz, B., Marty, N., Clément, A. & Michau, N. (2006): Geochemical modelling of the influence of iron corrosion on bentonite stability. *In:* Workshop on Fe-clay interactions in repository environments, a joint initiative by Andra, SKB and Nagra, Basel, 9 – 10 May 2006. Nagra Working Report NAB 06-15, Appendix B12. Nagra, Wettingen.

Fritz, S.J. & Toth, T.A. (1997): An Fe-berthierine from a Cretaceous laterite: Part II. Estimation of Eh, pH and pCO_2 conditions of formation. Clays and Clay Minerals 45, 580-586.

Fujiwara, K., Yokoyama, K., Shimojo, M. & Amaya, T. (1998): The research on the interaction of the cement-bentonite. *In:* Annual Spring Meeting, Atomic Energy Society of Japan, L28, pp. 612 [In Japanese].

Fukushi, K., Sugiura, T., Morishita, T., Takahashi, Y., Hasebe, N. & Ito, H. (2010): Iron-bentonite interactions in the Kawasaki bentonite deposit, Zao area, Japan. Applied Geochemistry 25, 1120-1132.

Gaboreau, S., Pret, D., Tinseau, E., Claret, F., Pellegrini, D. & Stammose, D. (2011): 15 years of in situ cement–argillite interaction from Tournemire URL: Characterisation of the multi-scale spatial heterogeneities of pore space evolution. Applied Geochemistry 26, 2159-2171.

Gaucher, E. & Blanc, P. (2006): Cement/clay interactions – a review: experiments, natural analogues, and modeling. Waste Management 26, 776-788.

Gaucher, E., Blanc, P., Matray, J.M. & Michau, N. (2004): Modeling diffusion of an alkaline plume in a clay barrier. Applied Geochemistry 19, 1505-1515.

Graham, J., Chandler, N.A., Dixon, D.A., Roach, P.J., To, T. & Wan, A.W.L. (1997): The buffer/container experiment: results, synthesis, issues. AECL Report 11746, COG-97-46-I.

Grauer, R. (1990): The chemical behaviour of montmorillonite in a repository backfill: selected aspects. Nagra Tech. Report 88-24E. Nagra, Wettingen.

Grauer, R. (1986): Bentonite as a backfill material in the high-level waste repository: chemical aspects. Nagra Tech. Report 86-12E. Nagra, Wettingen.

Gribi, P., Johnson, L.H., Suter, D., Smith, P.A., Pastina, B. & Snellman, M. (2008): Safety assessment for a KBS-3H spent nuclear fuel repository at Olkiluoto: Process report. SKB Report R-08-36. Swedish Nuclear Fuel and Waste Management Company, Stockholm.

Grigsby, J.D. (2001): Origin and growth mechanism of authigenic chlorite in sandstones of the Lower Vicksburg Formation, South Texas. Journal of Sedimentary Research 71, 27-36.

Guillaume, D., Neaman, A., Cathelineau, M., Mosser-Ruck, R., Peiffert, C., Abdelmoula, M., Dubessy, J., Villiéras, F., Baronnet, A. & Michau, N. (2003): Experimental synthesis of chlorite from smectite at 300 °C in the presence of metallic Fe. Clay Minerals 38, 281-302.

Hensen, E.J.M. & Smit, B. (2002): Why clays swell. Journal of Physical Chemistry B 106, 12664-12667.

Hermansson, H.-P. (2004): The stability of magnetite and its significance as a passivating film in the repository environment. SKI Report 2004:07. Swedish Nuclear Power Inspectorate, Stockholm.

Hodgkinson, D., Savage, D., Watson, C., Watson, S. & Benbow, S. (2007): Coupled system evolution modelling of EBS processes. NF-PRO Deliverable 5-1-10. European Commission, Luxembourg.

Honrado, M.L.L., Pascua, C.S., Vargas, E., Arcilla, C.A., Alexander, W.R., Namiki, K., Fuji, N., Yamakawa, M., Sato, T. & McKinley, I.G. (2009): Smectite and zeolite formation from the pyroclastic deposits of the Aksitero Formation, Philippines. Geochim. Cosmochim. Acta, Goldschmidt Conference Abstracts A547.

Hunter, F.M.I., Bate, F., Heath, T.G. & Hoch, A.R. (2007): Geochemical investigation of iron transport into bentonite as steel corrodes. SKB Technical Report TR-07-09. Swedish Nuclear Fuel and Waste Management Company, Stockholm.

Ichige, S., Ito, M. & Mihara, M. (1998): Alteration of compacted bentonite in alkaline solution. *In:* Annual Spring Meeting, Atomic Energy Society of Japan, L27, pp. 611 [In Japanese].

Ishidera, T., Ueno, K., Kurosawa, S. & Suyama, T. (2008): Investigation of montmorillonite alteration and form of iron corosion products in compacted bentonite in contact with carbon steel for ten years. Physics and Chemistry of the Earth 33, S269-S275.

Johnson, L.H. & King, F. (2003): Canister options for the direct disposal of spent fuel. Nagra Tech. Report NTB 02-11. Nagra, Wettingen.

Johnston, R.M. & Miller, H.G. (1984): The effect of pH on the stability of smectite. AECL Report AECL-8366. Atomic Energy of Canada Limited, Pinawa.

Johnston, R.G., Strope, M.B. & Anantatmula, R.P. (1985): X-ray diffraction/electron microprobe analysis of surface films formed on alloys during hydrothermal reaction with geologic materials. *In:* C.S. Barrett, P.K. Perdecki & D.C. Leyden (eds.): Advances in X-Ray Analysis. Plenum Press, New York, USA, 367-375.

Kamei, G., Oda, C., Mitsui, S., Shibata, M. & Shinozaki, T. (1999): Fe(II)-Na ion exchange at interlayers of smectite: adsorption-desorption experiments and a natural analogue. Engineering Geology 54, 15-20.

Karlsson, F., Lindgren, M., Skagius, K., Wiborgh, M. & Engkvist, I. (1999): Evolution of geochemical conditions in SFL 3-5. SKB Report R-99-15. Swedish Nuclear Fuel and Waste Management Company, Stockholm.

Karnland, O. (2010): Chemical and mineralogical charcterization of the bentonite buffer for the acceptance control procedure in a KBS-3 repository. SKB Report TR-10-60. Swedish Nuclear Fuel and Waste Management Company, Stockholm.

Karnland, O. & Birgersson, M. (2006): Montmorillonite stability with special respect to KBS-3 conditions. SKB Technical Report TR-06-11. Swedish Nuclear Fuel and Waste Management Company, Stockholm.

Karnland, O., Olsson, S., Dueck, A., Birgersson, M., Nilsson, U., Hernan-Hakansson, T., Pedersen, A.K., Nilsson, S., Eriksen, T.E. & Rosborg, B. (2009): Long term test of buffer material at the Äspö Hard Rock Laboratory, LOT project. Final report on the A2 test parcel. SKB Report TR-09-29. Swedish Nuclear Fuel and Waste Management Company, Stockholm.

Karnland, O., Sandén, T., Johannesson, L.-E., Eriksen, T.E., Jansson, M., Wold, S., Pedersen, K., Motamedi, M. & Rosborg, B. (2000): Long term test of buffer material. Final report on the pilot parcels. SKB Technical Report TR-00-22. Swedish Nuclear Fuel Management Company Limited, Stockholm.

King, F. (2008): Corrosion of carbon steel under anaerobic conditions in a repository for SF and HLW in Opalinus Clay. Nagra Tech. Report NTB 08-12. Nagra, Wettingen.

King, F., Lilja, C., Pedersen, K., Pikänen, P. & Vähänen, M. (2010): An update of the state-of-the-art report on the corrosion of copper under expected conditions in a deep geologic repository. SKB Report TR-10-67. Swedish Nuclear Fuel and Waste Management Company, Stockholm.

King, F., Ahonen, L., Taxén, C., Vuorinen, U. & Werme, L. (2001): Copper corrosion under expected conditions in a deep geologic repository. SKB Report TR 01-23. Swedish Nuclear Fuel and Waste Management Company, Stockholm.

Kosakowski, G., Blum, P., Kulik, D.A., Pfingsten, W., Shao, H. & Singh, A. (2009): Evolution of a generic clay/cement interface: first reactive transport calculations utilizing a Gibbs energy minimization based approach for geochemical calculations. Journal of Environmental Science for Sustainable Society 3, 41-49.

Kubo, H., Kuroki, Y. & Mihara, M. (1998): The basic research of the long term degeneration of bentonite by concrete pore water. Geotechnology Bulletin 46/10, 31-34 [In Japanese].

Kumpulainen, S. & Kiviranta, L. (2011): Mineralogical, chemical and physical study of potential buffer and backfill materials from ABM test package 1. Posiva Working Report 2011-41. Posiva Oy, Olkiluoto, Finland.

Kumpulainen, S., Kiviranta, L., Carlsson, T., Muurinen, A., Svensson, D., Sasamoto, H., Yui, M., Wersin, P. & Rosch, D. (2010): Long-term alteration of bentonite in the presence of metallic iron. SKB Report R-10-52. Swedish Nuclear Fuel and Waste Management Company, Stockholm.

Laine, H. & Karttunen, P. (2010): Long-term stability of bentonite: a literature review. Posiva Working Report 2010-53. Posiva Oy, Olkiluoto, Finland.

Lantenois, S., Lanson, B., Muller, F., Bauer, A., Jullien, M. & Plançon, A. (2005): Experimental study of smectite interaction with metal Fe at low temperature: 1. Smectite destabilization. Clays and Clay Minerals 53, 597-612.

Lee, T.R. & Wilkin, R.T. (2010): Iron hydroxy carbonate formation in zerovalent iron permeable reactive barriers: Characterization and evaluation of phase stability. Journal of Contaminant Hydrology 116, 47-57.

Leupin, O. & Johnson, L. (2014): Buffer Requirements for a SF/HLW Repository in Opalinus Clay. Nagra Working Reoirt NAB 13-46. Nagra, Wettingen.

Lothenbach, B. & Winnefeld, F. (2006): Thermodynamic modelling of the hydration of Portland cement. Cement and Concrete Research 36, 209-226.

Lu, C., Samper, J., Fritz, B., Clement, A. & Montenegro, L. (2011): Interactions of corrosion products and bentonite: An extended multicomponent reactive transport model. Physics and Chemistry of the Earth 36, 1661-1668.

Mäder, U. (2009): Reference pore water for the Opalinus Clay and 'Brown Dogger' for the provisional safety analysis in the framework of the sectoral plan – interim results (SGT-ZE). Nagra Working Report NAB 09-14. Nagra, Wettingen.

Madsen, F.T. (1998): Clay mineralogical investigations related to nuclear waste disposal. Clay Minerals 33, 109-129.

Madsen, F.T. & Müller-von Moos, M. (1989): The swelling behaviour of clays. Applied Clay Science 4, 143-156.

Man, A. & Martino, J.B. (2009): Thermal, hydraulic and mechanical properties of sealing materials. NWMO Technical Report NWMO TR-2009-20. Nuclear Waste Management Organization (NWMO), Toronto, Canada.

Marcos, N. (2003): Bentonite-iron interactions in natural occurrences and in laboratory – the effects of the interaction on the properties of bentonite: a literature survey. Posiva Working Report 2003-55. Posiva Oy, Olkiluoto, Finland.

Marty, N.C.M., Fritz, B., Clément, A. & Michau, N. (2010): Modelling the long term alteration of the engineered bentonite barrier in an underground radioactive waste repository. Applied Clay Science 47, 82-90.

Marty, N.C.M., Tournassat, C., Burnol, A., Giffaut, E. & Gaucher, E.C. (2009): Influence of reaction kinetics and mesh refinement on the numerical modelling of concrete/clay interactions. Journal of Hydrology 364, 58-72.

McCarty, D.K., Sakharov, B.A. & Drits, V.A. (2009): New insights into smectite illitization: A zoned K-bentonite revisited. American Mineralogist 94, 1653-1671.

Melkior, T., Mourzagh, D., Yahiaoui, S., Thoby, D., Alberto, J.C., Brouard, C. & Michau, N. (2004): Diffusion of an alkaline fluid through clayey barriers and its effect on the diffusion properties of some chemical species. Applied Clay Science 26, 99-107.

Meunier, A. & Velde, B. (2004): Illite: Origins, evolution and metamorphism. Springer-Verlag, Berlin, Heidelberg.

Michau, N. (2005): ECOCLAY II: Effects of cement on clay barrier performance. Andra Report C.RP.ASCM.04.0009. Andra, Paris, France.

Miller, W., Alexander, R., Chapman, N., McKinley, I. & Smellie, J. (2000): Geological disposal of radioactive wastes and natural analogues. Lessons from Nature and Archaeology. Pergamon, Amsterdam.

Milodowski, A.E., Cave, M.R., Kemp, S.J., Taylor, H., Green, K., Williams, C.L., Shaw, R.A., Gowing, C.J.B. & Eatherington, N.D. (2009a): Mineralogical investigations of the interaction between iron corrosion products and bentonite from the NF-PRO Experiments (Phase 2). SKB Report TR-09-03. Swedish Nuclear Fuel and Waste Management Company, Stockholm.

Milodowski, A.E., Cave, M.R., Kemp, S.J., Taylor, H., Vickers, B., Green, K., Williams, C.L. & Shaw, R.A. (2009b): Mineralogical investigations of the interaction between iron corrosion products and bentonite from the NF-PRO Experiments (Phase 1). SKB Technical Report TR-09-02. Swedish Nuclear Fuel and Waste Management Company, Stockholm.

Milodowski, A.E., Styles, M.T., Werme, L. & Oversby, V.M. (2003): The corrosion of more than 176 million year old native copper plates from a deposit in mudstone in South Devon, United Kingdom. *In:* Corrosion 2003 (NACE International Conference), San Diego, 1-10.

Montes-H, G., Fritz, B., Clement, A. & Michau, N. (2005a): Modeling of transport and reaction in an engineered barrier for radioactive waste confinement. Applied Clay Science 29, 155-171.

Montes-H, G., Fritz, B., Clement, A. & Michau, N. (2005b): Modelling of geochemical reactions and experimental cation exchange in MX80 bentonite. Journal of Environmental Management 77, 35-46.

Montes-H, G., Marty, N., Fritz, B., Clement, A. & Michau, N. (2005c): Modelling of long-term diffusion-reaction in a bentonite barrier for radioactive waste confinement. Applied Clay Science 30, 181-198.

Mosser-Ruck, R., Cathelineau, M., Guillaume, D., Charpentier, D., Rousset, D., Barres, O. & Michau, N. (2010): Effects of temperature, pH, and iron/clay and liquid/clay ratios on experimental conversion of dioctahedral smectite to berthierine, chlorite, vermiculite, or saponite. Clays and Clay Minerals 58, 280-291.

Müller-von Moos, M., Kahr, G., Bucher, F. & Madsen, F.T. (1990): Investigation of Kinnekulle K-bentonite aimed at assessing the long-term stability of bentonites under repository conditions. Engineering Geology 28, 269-280.

Muurinen, A., Olin, M. & Uusheimo, K. (1990): Diffusion of sodium and copper in compacted sodium bentonite at room temperature. *In:* Scientific Basis for Nuclear Waste Management XIII, Boston, USA. MRS Proceedings 176, 641-647.

Nagra (2010): Beurteilung der geologischen Unterlagen für die provisorischen Sicherheitsanalysen in SGT Etappe 2 – Klärung der Notwendigkeit ergänzender geologischer Untersuchungen. Nagra Technischer Bericht. NTB 10-01. Nagra, Wettingen.

Nagra (2002): Project Opalinus Clay Safety Report: Demonstration of disposal feasibility for spent fuel, vitrified high-level waste and long-lived intermediate-level waste (Entsorgungsnachweis). Nagra Tech. Report NTB 02-05. Nagra, Wettingen.

Nakayama, S., Sakamoto, Y., Yamaguchi, T., Akai, M., Tanaka, T., Sato, T. & Iida, Y. (2004): Dissolution of montmorillonite in compacted bentonite by highly-alkaline aqueous solutions and diffusivity of hydroxide ions. Applied Clay Science 27, 53-65.

Neaman, A., Guillaume, D., Pelletier, M. & Villiéras, F. (2003): The evolution of textural properties of Na/Ca-bentonite following hydrothermal treatment at 80 and 300 °C in the presence of Fe and/or Fe oxides. Clay Minerals 38, 213-223.

Patel, R., Punshon, C., Nicholas, J., Bastid, P., Zhou, R., Schneider, C., Bagshaw, N., Howse, D., Hutchinson, E., Asano, R. & King, F. (2012): Canister design concepts for disposal of spent nuclear fuel and high level waste. Nagra Tech. Report NTB 12-06. Nagra, Wettingen.

Perronnet, M., Jullien, M., Villiéras, F., Raynal, J., Bonnin, D. & Bruno, G. (2008): Evidence of critical content in Fe(0) on FoCa7 bentonite reactivity at 80 °C. Applied Clay Science 38, 187-202.

Perronnet, M., Villiéras, F., Jullien, M., Razafitianamaharavo, A., Raynal, J. & Bonnin, D. (2007): Towards a link between the energetic heterogeneities of the edge faces of smectites and their stability in the context of metallic corrosion. Geochim. Cosmochim. Acta 71, 1463-1479.

Plötze, M., Kahr, G., Dohrmann, R. & Weber, H. (2007): Hydro-mechanical, geochemical and mineralogical characteristics of the bentonite buffer in a heater experiment: the HE-B Project at the Mont Terri Rock Laboratory. Physics and Chemistry of the Earth 32, 730-740.

Pruess, K., Oldenburg, C. & Moridis, G. (1999): TOUGH2 user's guide, Version 2. LBNL Report LBL-43134. Lawrence Berkeley National Laboratory, Berkeley, California, USA.

Pusch, R. (2002a): The buffer and backfill handbook Part 2: Materials and techniques. SKB Technical Report TR-02-12. Swedish Nuclear Fuel and Waste Management Company, Stockholm.

Pusch, R. (2002b): The buffer and backfill handbook. Part 1: Definitions, basic relationships, and laboratory methods. SKB Technical Report SKB TR-02-20. Swedish Nuclear Fuel and Waste Management Company, Stockholm.

Pusch, R. & Karnland, O. (1988): Hydrothermal effects on montmorillonite. A preliminary study. SKB Report TR-88-15. Swedish Nuclear Fuel and Waste Management Company, Stockholm.

Pusch, R., Takase, H. & Benbow, S. (1998): Chemical processes causing cementation in heat-affected smectite – the Kinnekulle bentonite. SKB TR-98-25, SKB Report TR-98-25. Swedish Nuclear Fuel and Waste Management Company, Stockholm.

Pusch, R., Karnland, O., Lajudie, A., Lechelle, J. & Bourchet, A. (1993): Hydrothermal field test with French candidate clay embedding the steel heater in the Stripa Mine. SKB Technical Report TR-93-02. Swedish Nuclear Fuel and Waste Management Company, Stockholm.

Ramírez, S., Cuevas, J., Vigil, R. & Leguey, S. (2002): Hydrothermal alteration of "La Serrata" bentonite (Almeria, Spain) by alkaline solutions. Applied Clay Science 21, 257-269.

Rosborg, B. & Werme, L. (2008): The Swedish nuclear waste program and the long-term corrosion behaviour of copper. Journal of Nuclear Materials 379, 142-153.

Rotenberg, B., Morel, J.-P., Marry, V., Turq, P. & Morel-Desrosiers, N. (2009): On the driving force of cation exchange in clays: Insights from combined microcalorimetry experiments and molecular simulation. Geochim. Cosmochim. Acta 73, 4034-4044.

Rozalén, M.L., Huertas, F.J., Brady, P.V., Cama, J., García-Palma, S. & Linares, J. (2008): Experimental study of the effect of pH on the kinetics of montmorillonite dissolution at 25 °C. Geochim. Cosmochim. Acta 72, 4224-4253.

Saheb, M., Descostes, M., Neff, D., Matthiesen, H., Michelin, A. & Dillmann, P. (2010): Iron corrosion in an anoxic soil: comparison between thermodynamic modelling and ferrous archaeological artefacts characterised along with the local in situ geochemical conditions. Applied Geochemistry 25, 1937-1948.

Samper, J., Lu, C. & Montenegro, L. (2008): Reactive transport model of interactions of corrosion products and bentonite. Physics and Chemistry of the Earth 33, S306-S316.

Sato, T., Kuroda, M., Yokoyama, S., Tsutsui, M., Fukushi, K., Tanaka, T. & Nakayama, S. (2004): Dissolution mechanism and kinetics of smectite under alkaline conditions. *In:* International Workshop on Bentonite-Cement Interaction in Repository Environments, Tokyo, Japan, NUMO-TR 04-05, A3-38 – A3-41.

Savage, D. (2005): The effects of high salinity groundwater on the performance of clay barriers. SKI Report 2005:54. Swedish Nuclear Power Inspectorate, Stockholm.

Savage, D. (2009): A review of experimental evidence for the development and properties of cement-bentonite Interfaces with implications for gas transport. Nagra Working Report NAB 09-30. Nagra, Wettingen.

Savage, D. & Benbow, S. (2007): Low pH cements. SKI Report 2007:32. Swedish Nuclear Power Inspectorate, Stockholm.

Savage, D., Arthur, R., Watson, C., Wilson, J. & Strömberg, B. (2011): Testing geochemical models of bentonite pore water evolution against laboratory experimental data. Physics and Chemistry of the Earth 36, 1817-1829.

Savage, D., Benbow, S., Watson, C., Takase, H., Ono, K., Oda, C. & Honda, A. (2010a): Natural systems evidence for the alteration of clay under alkaline conditions: an example from Searles Lake, California. Applied Clay Science 47, 72-81.

Savage, D., Walker, C. & Benbow, S. (2010b): An analysis of potential changes to barrier components due to interaction with a concrete liner in a repository for SF/HLW in Opalinus Clay. Nagra Working Report NAB 10-17. Nagra, Wettingen.

Savage, D., Watson, C., Benbow, S. & Wilson, J. (2010c): Modelling iron-bentonite interactions. Applied Clay Science 47, 91-98.

Savage, D., Walker, C., Arthur, R.C., Rochelle, C.A., Oda, C. & Takase, H. (2007): Alteration of bentonite by hyperalkaline fluids: a review of the role of secondary minerals. Physics and Chemistry of the Earth 32, 287-297.

Savage, D., Noy, D.J. & Mihara, M. (2002): Modelling the interaction of bentonite with hyperalkaline fluids. Applied Geochemistry 17: 207-223, 2002.

Senger, R. & Ewing, J. (2008): Evolution of temperature and water content in the bentonite buffer: detailed modelling of two-phase flow processes associated with the early closure period. Nagra Working Report NAB 08-32. Nagra, Wettingen.

SKB (2010): Buffer, backfill and closure process report for the safety assessment SR-Site. SKB Report TR-10-47. Swedish Nuclear Fuel and Waste Management Company, Stockholm.

SKB (2006): Long-term safety for KBS-3 repositories at Forsmark and Laxemar – a first evaluation. Main report of the SR-Can project. SKB Technical Report TR-06-09. Swedish Nuclear Fuel and Waste Management Company, Stockholm.

Skipper, N.T., Lock, P.A., Titiloye, J.O., Swenson, J., Mirza, Z.A., Howells, W.S. & Fernandez-Alonso, F. (2006): The structure and dynamics of 2-dimensional fluids in swelling clays. Chemical Geology 230, 182-196.

Smart, N.R., F., B., Carlson, L., Heath, T.G., Hoch, A.R., Hunter, F.M.I., Karnland, O., Kemp, S.J., Milodowski, A.E., Pritchard, A.M., Rance, A.P., Reddy, B. & Werme, L.O. (2008): Interactions between iron corrosion products and bentonite. NF-PRO Final Report Serco/TAS/MCRL/19801/C001 Issue 2, Harwell, UK.

Smart, N.R., Carlson, L., Hunter, F.M.I., Karnland, O., Pritchard, A.M., Rance, A.P. & Werme, L.O. (2006a): Interactions between iron corrosion products and bentonite. 24 month report SA/EIG/12156/C001 Issue 1, Serco Ltd, Harwell, UK.

Smart, N.R., Rance, A.P., Carlson, L. & Werme, L.O. (2006b): Further studies of the anaerobic corrosion of steel in bentonite. Mat. Res. Soc. Symp. Proc. 932, 813-818.

Sposito, G., Holtzclaw, K.M., Johnston, C.T. & LeVesque, X. (1981): Thermodynamics of sodium-copper exchange on Wyoming bentonite at 298K. Soil Science Society of America Journal 45, 1079-1084.

Szakálos, P., Hultqvist, G. & Wikmark, G. (2007): Corrosion of copper by water. Electrochemical and Solid-State Letters 10, C63-C67.

Takase, H. (2004): Discussion on PA model development for bentonite barriers affected by chemical interaction with concrete: do we have enough evidence to support bentonite stability? *In:* International Workshop on Bentonite-Cement Interaction in Repository Environments, Tokyo, Japan, NUMO-TR 04-05, A3-172 – A3-177.

Tinseau, E., Gaboreau, S., Bartier, D. & Techer (2008): A 15 years in situ alkaline propagation into the Tournemire argillite: Microstructural and petrological approaches. *In:* Second International Workshop on Mechanisms and Modelling of Waste/Cement Interactions, Le Croisic, France, 76.

Tinseau, E., Bartier, D., Hassouta, L., Devol-Brown, I. & Stammose, D. (2006): Mineralogical characterization of the Tournemire argillite after in situ reaction with concretes. Waste Management 26, 789-800.

Traber, D. & Mäder, U. (2006): Reactive transport modelling of the diffusive interaction between Opalinus Clay and concrete. Nagra Working Report NAB 05-06. Nagra, Wettingen.

Trotignon, L., Devallois, V., Peycelon, H., Tiffreau, C. & Bourbon, X. (2007): Predicting the long-term durability of concete engineered barriers in a geological repository for radioactive waste. Physics and Chemistry of the Earth 32, 259-274.

Trotignon, L., Peycelon, H. & Bourbon, X. (2006): Comparison of performance of concrete barriers in a clayey geological medium. Physics and Chemistry of the Earth 31, 610-617.

Ueda, H., Hyodo, H., Takase, H., Savage, D., Benbow, S. & Noda, M. (2007): Evaluation of the kinetics of cement-bentonite interaction in a HLW repository using the reactive solute transport simulator. *In:* 15th International Conference on Nuclear Engineering, Nagoya, Japan, pp. ICONE15-10566.

Van Loon, L. & Glaus, M.A. (2008): Mechanical compaction of smectite clays increases ion exchange selectivity for cesium. Environmental Science and Technology 42, 1600-1604.

Vigil de la Villa, R., Cuevas, J., Ramirez, S. & Leguey, S. (2001): Zeolite formation during the alkaline reaction of bentonite. European Journal of Mineralogy 13, 635-644.

Wang, Y., Bryan, C., Xu, H. & Gao, H. (2003): Nanogeochemistry: geochemical reactions and mass transfers in nanopores. Geology 31, 387-390.

Watson, C., Benbow, S. & Savage, D. (2007): Modelling the interaction of low pH cements and bentonite. Issues affecting the geochemical evolution of repositories for radioactive waste. SKI Report 2007:30. Swedish Nuclear Power Inspectorate, Stockholm.

Watson, C., Hane, K., Savage, D., Benbow, S., Cuevas, J. & Fernandez, R. (2009): Reaction and diffusion of cementitious water in bentonite: results of 'blind' modelling. Applied Clay Science 45, 54-69.

Wersin, P. (2003): Geochemical modelling of bentonite porewater in high-level waste repositories. Journal of Contaminant Hydrology 61, 405-422.

Wersin, P. & Snellman, M. (2008): Impact of iron on the performance of clay barriers in waste disposal systems: Report on the status of research and development. SKB Report R-08-45. Swedish Nuclear Fuel and Waste Management Company, Stockholm.

Wersin, P., Birgersson, M., Olsson, S., Karnland, O. & and Snellman, M. (2008): Impact of corrosion-derived iron on the bentonite buffer within the KBS-3H disposal concept: the Olkiluoto site as case study. SKB Report R-08-34. Swedish Nuclear Fuel and Waste Management Company, Stockholm.

Wersin, P., Johnson, L.H. & McKinley, I.G. (2007): Performance of the bentonite barrier at temperatures beyond 100 °C: a critical review. Physics and Chemistry of the Earth 32, 780-788.

Wersin, P., Curti, E. & Appelo, C.A.J. (2004): Modelling bentonite-water interactions at high solid/liquid ratios: swelling and diffuse double layer effects. Applied Clay Science 26, 249-257.

Wersin, P., Spahiu, K. & Bruno, J. (1994): Kinetic modelling of bentonite-canister interaction. Long-term predictions of copper canister corrosion under oxic and anoxic conditions. SKB Technical Report 94-25. Swedish Nuclear Fuel and Waste Management Company, Stockholm.

Wilson, J., Cressey, G., Cressey, B., Cuadros, J., Ragnarsdóttir, K.V., Savage, D. & Shibata, M. (2006a): The effect of iron on montmorillonite stability. (II) Experimental investigation. Geochim. Cosmochim. Acta 70, 323-336.

Wilson, J., Savage, D., Cuadros, J., Ragnarsdóttir, K.V. & Shibata, M. (2006b): The effect of iron on montmorillonite stability. (I) Background and thermodynamic considerations. Geochim. Cosmochim. Acta 70, 306-322.

Wolery, T.J. (1992): EQ3NR, a computer program for geochemical aqueous speciation-solubility calculations: Theoretical manual, user's guide, and related documentation (version 7.0). UCRL-MA-110662 PT III. Lawrence Livermore National Laboratory, Livermore, California, USA.

Yamaguchi, T., Sakamoto, Y., Akai, M., Takazawa, M., Iida, Y., Tanaka, T. & Nakayama, S. (2007): Experimental and modeling study on long-term alteration of compacted bentonite with alkaline groundwater. Physics and Chemistry of the Earth 32, 298-310.

Yamaguchi, T., Sakamoto, Y., Akai, M., Takazawa, M., Tanaka, T., Nakayama, S. & Sato, T. (2004): Experimental study on dissolution of montmorillonite in compacted sand-bentonite mixture under Na-Cl-OH pore-water conditions. Posiva WR 2004:25 (also: NUMO TR-04-05). NUMO/Posiva, Tokyo, Japan and Helsinki, Finland, 125-131.

Zhang, Z.Z. & Sparks, D.L. (1996): Sodium-Copper Exchange on Wyoming Montmorillonite in Chloride, Perchlorate, Nitrate, and Sulfate Solutions. Soil Science Society of America Journal 60, 1750-1757.

Appendix A: Consideration of Alternative Near-field Concepts

Introduction

In addition to the near-field design presented in the main body of this report (named variant B in this Appendix), Nagra is considering a number of design alternatives (Figure A-1). In this Appendix, the following two variant designs, which cover a representative range of design alternatives, are discussed:

- a variant with a thicker OPC concrete liner (20 cm thick) and with a supercontainer made of perforated steel similar to that envisaged for the KBS-3H concept in Sweden and Finland (e.g. Smith et al. 2008), containing the compacted bentonite blocks and the waste canister (variant A in Figure A-1), and
- a variant with no concrete liner, but with an upper third of the deposition tunnel reinforced with metal mesh and with anchors (variant C in Figure A-1).

Regarding additional steel engineering structures, the significant differences between the concepts are:

- concept A (supercontainer) has no steel rails or anchors present, but has a 0.01 m thick steel shell between the concrete liner and the bentonite blocks surrounding the canister across all the tunnel section, together with steel reinforcement of the concrete liner itself
- concept B has steel rails, steel mesh between the concrete liner and the Opalinus Clay and steel anchors around the upper third of the deposition tunnel
- concept C has steel rails, together with steel mesh and anchors present between the bentonite and the Opalinus Clay around the upper third of the tunnel section only.

Although variant A contains compacted blocks of bentonite rather than the mix of compacted blocks and pellets in variants B and C, for the evaluations described below, it is assumed that the amounts and properties of bentonite are the same for each variant.

In the discussion below, all dimensions exclude consideration of any post-closure creep of the tunnel.

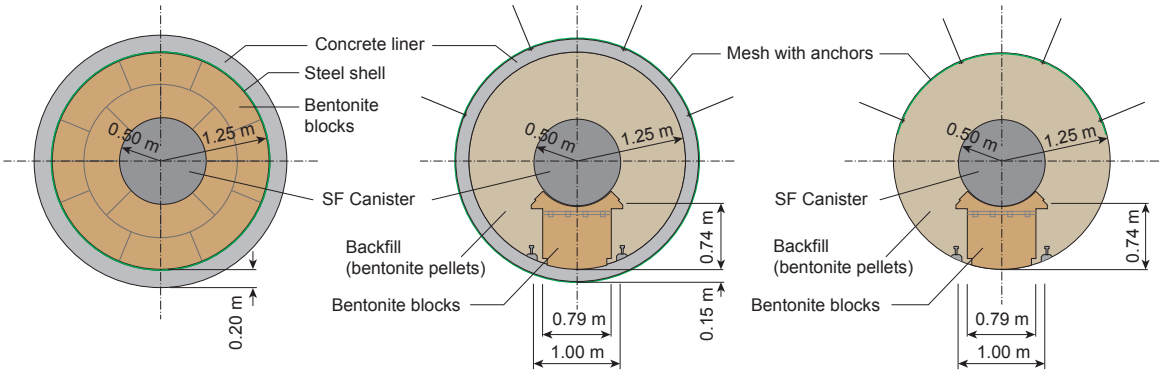

Fig. A-1: Schematic diagram of three different conceivable near-field designs for a SF/HLW repository.

The configuration in the centre (B) is that discussed in the main body of this report.

Impacts due to the thermal period

In the absence of any thermal analysis of the three concept variants, it is assumed that impacts associated with the thermal period for variants A and C are the same as that for variant B described in Section 4 and as summarised in Table 11 of the main report. Information in Table 11 indicates optimistic and pessimistic bentonite alteration zones due to thermal processes of 0.05 and 0.1 m, respectively.

Impacts due to interactions of bentonite with cement/concrete

The discussion of key processes described in Section 5 are relevant here in that the type of bentonite alteration associated with the OPC cement/concrete liner of variant A is anticipated to be similar to that described for the SR-LPC concrete liner of variant B. A (perforated) steel supercontainer between the concrete liner and the compacted bentonite in concept variant A is unlikely to have any significant impact with regard to the type of alteration because of the low solubility of iron at elevated pH. Also it is unlikely that the perforations in the steel would inhibit diffusion of cement pore fluids into the bentonite. However, the greater proportion of cement in OPC concrete (variant A) as compared with SR-LPC concrete (variant B) means that from a mass balance perspective the physical scale of alteration will be greater for variant A.

Table A-1 shows the amounts of concrete and potentially-leachable hydroxyl ions in the concept variants as calculated using the data presented in Table 9 of the main report. It may be seen from this Table that the concrete liner for concept variant A contains more than three times the amount of potentially-leachable hydroxyl ions than concept B.

The amounts of bentonite potentially altered by interaction with concrete pore fluids have been calculated using the mass balance approach adopted in Section 5.2 and as defined by equations (3) and (4) specifically. These equations assume dissolution of the montmorillonite clay component of the bentonite without any precipitation of a secondary solid, such that 4.68 moles of OH- ions are needed to consume each mole of montmorillonite. Using a molecular weight of montmorillonite of 0.367 kg mol^{-1}, the proportion of montmorillonite in bentonite (87 wt.-%; Table 6), and the calculated amounts of OH- released by concrete dissolution defined in Table A-1, then the amounts of bentonite potentially destroyed by reaction with a concrete tunnel liner are shown in Table A-2.

Tab. A-1: Volumes of concrete and inventory of total OH^- in concrete (see Table 9 for definition of total OH^-) in the tunnel liner for a nominal 1 m length of tunnel.

Variant A uses OPC concrete with an assumed 17.5 wt.-% CEM I and variant B contains 7.3 wt.-% CEM I in SR-LPC concrete. There is no concrete liner in variant C. The tunnel dimensions are defined in Figure A-1.

Parameter	**Variant A**	**Variant B**	**Variant C**
Concrete volume [m^3]	1.70	1.25	0
Total OH^- [moles]	16364	4789	0

Tab. A-2: Masses, volume percent and annular thicknesses of bentonite potentially altered by interaction with a concrete tunnel liner for a nominal 1 m length of tunnel using the stoichiometry defined by equation (4) in the main report.

Note that MX-80 bentonite contains 87 wt.-% montmorillonite clay (Table 6) and that the volume of the initial buffer for 1 m tunnel length is 4.12 m^3 (Table 2). The altered annulus (m) is calculated using the formula: annular volume = $\pi (R^2 - r^2)$, where R is the outer radius (= 1.25 m) and r is the inner radius of altered bentonite (calculated). There is no concrete liner in variant C. The tunnel dimensions are defined in Figure A-1.

Parameter	**Variant A**	**Variant B**	**Variant C**
Clay dissolved [kg]	1283	375	-
Bentonite altered [kg]	1475	432	-
Bentonite altered [m^3]	1.017	0.298	-
Vol.-% of total buffer	24.7	7.2	
Altered annulus [m]	0.14	0.04	-

Table A-2 shows that the 432 kg of bentonite potentially altered in variant B (equivalent to 7 wt.-% of the total bentonite volume, or an annulus of 0.04 m of the canister buffer), compares with a figure of 1475 kg of bentonite potentially destroyed (equivalent to ~ 25 wt.-% of the total bentonite volume or an annulus of 0.14 m of the canister buffer) for variant A.

However, as concluded in Section 5 of the main report, these mass balance estimates are likely to be highly pessimistic since reactive-transport simulations and analogue evidence of concrete-clay interaction show that the scale of alteration will be limited by mass transport. In other words, the re-distribution of porosity due to the alteration of bentonite will serve to decrease diffusive transport at the concrete-clay interface, thus limiting the penetration of hyperalkaline fluids into the clay. It is unlikely therefore that the estimates of alteration presented in Table 12 for concept variant B using mass transport constraints would be exceeded by the increased inventory of potentially-leachable hydroxyl ions for concept variant A.

Nevertheless, these mass balance estimates of cement-bentonite interaction presented here provide strong evidence for the relative insignificance of these processes for the integrity of the bentonite buffer over the long-term. These calculations therefore demonstrate that even with a pessimistic mass balance assumption, it it likely that at least 0.56 and 0.66 m of bentonite around the spent fuel canister would remain unaltered considering the interaction with concrete for concepts A and B, respectively.

Impacts due to interactions of bentonite with steel structures

Since the dimensions and the mass of steel in each canister are unchanged from that defined in Table 3 of the main report (23'000 kg), it is assumed that that the conclusions presented in Section 6 remain relevant to the discussion presented in this Appendix. Consequently, data presented in Table 15 concerning optimistic and pessimistic annular thicknesses of 0.01 and 0.1 m of bentonite potentially altered by interaction with the steel canister remain valid.

Table A-3 summarises the amounts of engineered structures in the three concept variants and shows that variant A contains the most steel engineered structures, particularly in the canister zone. Variant C contains the least steel engineered structures. Variants B and C have similar amounts of engineering structures which are approximately three to four times less than those for variant A in the canister zone due to the presence of a steel supercontainer in the latter concept. By contrast, variants B and C have slightly more engineered structures in the sealing element than that for concept A.

Adopting the mass balance in equation (5) of the main report which describes the alteration of bentonite by steel in terms of conversion of montmorillonite to the non-swelling sheet silicate chlorite, then the alteration caused by interactions with the additional steel engineered structures can be calculated in a similar manner. These results are presented in Table A-4 and A-5.

It may be seen from these Tables that potential impacts are relatively minor for all concept variants. Most alteration is associated with concept variant A where approximately 8 vol % of the bentonite may be altered in the canister zone. Least impact is associated with concept variant C where approximately 2 and 5 vol.-% of the bentonite may be altered in the canister and sealing element zones, respectively.

Tab. A-3: Masses of steel engineering elements (kg) in a deposition tunnel for a nominal 1 m length of tunnel as defined in Daneluzzi et al. (2014) adapted for the different variants.

The tunnel dimensions are defined in Figure A-1.

Structure	**Variant A**	**Variant B**	**Variant C**
Steel arches (sealing element only)	232.5	232.5	232.5
Steel mesh	-	29.0	9.7
Supercontainer *	343.2	-	-
Concrete rebar/fibre §	127.5	-	-
Steel anchors and plates	-	32.1	32.1
Rails	-	81.5	81.5
Total canister zone	470.7	142.6	123.3
Total sealing element	232.5	375.1	355.8
Total canister zone less rails	470.7	61.1	41.8
Total sealing element less rails	232.5	293.6	274.3

* The supercontainer has a mass of 1716.2 kg and is 5 m in length (Fries & Winter 2009). Here, this value is divided by a factor of five to produce a kg m^{-1} tunnel value.

§ The range 85 – 170 kg m^{-1} tunnel length is quoted in Fries & Winter (2009). Here, a mean value of 127.5 kg m^{-1} is used.

Tab. A-4: Volumes of bentonite (m^3) potentially altered by interaction with additional steel engineering elements for a nominal 1 m length of deposition tunnel as defined in Table A-3.

The number of moles of Fe^{2+} ions potentially released by corrosion are derived from the masses of steel engineering elements defined in Table A-3 divided by the atomic weight of iron (0.056 kg mol^{-1}). These amounts are used to calculate the number of moles of montmorillonite converted to chlorite through the reaction defined in equation (5) in the main body of the report, whereby 4.18 moles of Fe^{2+} ions released by steel corrosion are required to alter one mole of montmorillonite to 0.84 moles of chlorite. The volume of altered bentonite is then derived from the volume of montmorillonite converted to chlorite (montmorillonite molar volume = 1.34×10^{-4} m^3 mol^{-1}) and the amount of montmorillonite in bentonite (86.5 vol.-%; Table 6).

Structure	**Variant A**	**Variant B**	**Variant C**
Total canister zone	0.31	0.10	0.08
Total sealing element	0.16	0.25	0.24
Total canister zone less rails	0.31	0.04	0.03
Total sealing element less rails	0.16	0.20	0.18

Tab. A-5: Volume percent of bentonite potentially altered by interaction with additional steel engineering elements in a deposition tunnel for a nominal 1 m length of tunnel.

Data shown in Table A-4 are used and the initial amounts of bentonite in the canister and sealing element zones in 1 m length of tunnel being 4.12 and 4.91 m^3, respectively (Table 2).

Structure	**Variant A**	**Variant B**	**Variant C**
Total canister zone	7.6	2.3	2.0
Total sealing element	3.2	5.1	4.8
Total canister zone less rails	7.6	1.0	0.7
Total sealing element less rails	3.2	4.0	3.7

Summary

The potential for alteration of bentonite is different for each of the three concept variants:

- Concept A has both the most concrete and the most amount of additional steel structures and thus has the thickest zones of both alkaline alteration and that associated with interaction with steel engineered structures.
- Concept B has a small amount of concrete and a relatively small amount of additional steel structures and thus has the thinnest zone of alkaline alteration and a thin zone of alteration by interaction with steel engineered structures.
- Concept C has no concrete and has the least amount of additional steel structures and thus has no alkaline alteration and a small thickness of alteration by interaction with steel engineered structures.

The potential alteration is represented schematically in Figure A-2 where it can be seen that the use of a concrete tunnel liner and a steel supercontainer in variant A effectively reduces the annular thickness of unaltered bentonite around the canister to 0.46 m as compared with greater than 0.6 m in the other concept variants.

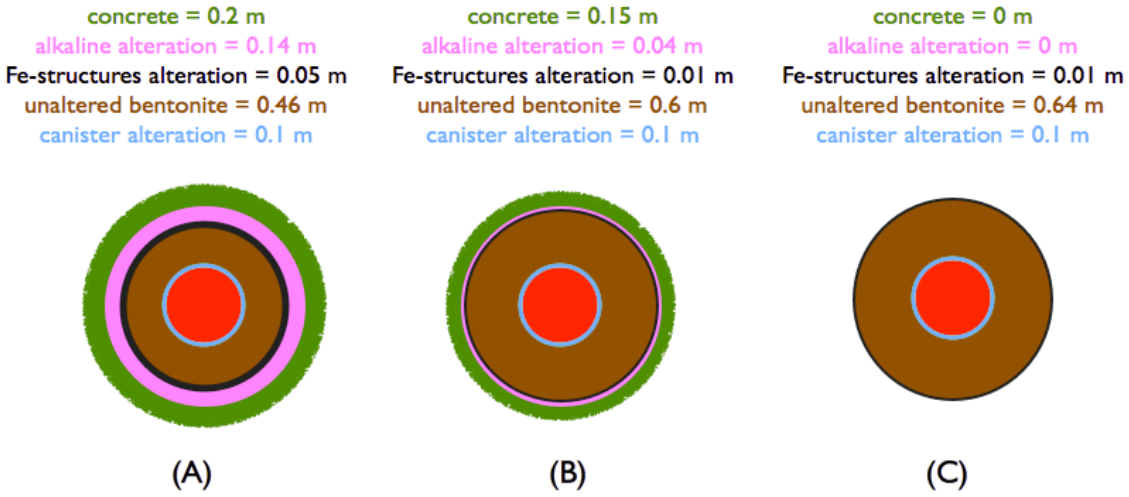

Fig. A-2: Schematic diagram of bentonite alteration associated with each of the three concept variants (broadly to scale).

The alteration associated with the presence of steel engineered structures is pessimistically shown as a black concentric zone inside that for the alkaline alteration. In reality there will be a mixed zone of iron-alkaline interaction rather than two discrete zones. The thickness of alteration associated with interaction of bentonite with the steel canister is the pessimistic estimate from Table 15.

References

Daneluzzi, R., Burrus, F., Küttel, T., Müller, H.R. & Köhler, S. (2014): Construction of the Emplacement Tunnel for the Full-scale Emplacement (FE) Experiment at Mont Terri Rock Laboratory. Nagra Arbeitsbericht NAB 14-54. Nagra, Wettingen.

Fries, T. & Winter, M. (2009): Standortunabhängige Grundlagen Anlagen und Betrieb SGT / SUG 2.3. Alternatives Ausbaukonzept ("Liner Concept") für BE/HAA-Lagerstollen. Nagra Arbeitsbericht NAB 09-07. Nagra, Wettingen.

Smith, P.A., Neall, F., Snellman, M., Pastina, B., Nordman, H., Johnson, L.H. & Hjerpe, T. (2008): Safety assessment for a KBS-3H spent nuclear fuel repository at Olkiluoto: Summary report. SKB Report R-08-39. Swedish Nuclear Fuel and Waste Management Company, Stockhom.

Appendix B: The Effect of Concrete Tunnel Liner Thickness

Introduction

It is pertinent to consider the effects of different thicknesses of concrete tunnel liner upon alkaline alteration of bentonite for concept variant A to ascertain whether a cut-off point exists, i.e. whether there is a certain liner thickness beyond which the bentonite is too thin to perform its safety functions.

Calculations

Here, the same approach as that described in Section 5 and in Appendix A is employed, i.e. a mass balance using equation (4) of the main report and input data for concrete and bentonite compositions from Tables 9 and 6, respectively. The liner is assumed to be constructed from an OPC-type concrete. Tunnel design dimensions are as shown in Figure A-1.

The results of the calculations are tabulated in Table B-1 and shown graphically in Figure B-1. It may be seen from these data that even in the (unlikely) event of the use of a 1 m thick OPC concrete tunnel liner, an annulus of 0.35 m of unaltered bentonite would remain around the canister despite the pessimism of the mass balance approach.

Tab. B-1: Calculation of the annular thickness of alteration of bentonite due to interaction with concrete pore fluids for different thicknesses of concrete tunnel liner for concept variant A (per m of tunnel length).

Concrete annulus [m]	**Concrete vol** [m^3]	**Concrete mass** [kg]	**Total *n*OH^-**	**Montmor destroyed** [kg]	**Bentonite destroyed** [kg]	**Bentonite destroyed** [m^3]	**Bentonite destroyed** [vol.-%]	**Altered bentonite annulus** [m]
0.15	1.25	2838	4787	375	431	0.298	7.2	0.038
0.20	1.70	3855	6503	510	586	0.404	9.8	0.053
0.25	2.16	4908	8279	649	746	0.515	12.5	0.067
0.30	2.64	5997	10115	793	912	0.629	15.2	0.083
0.35	3.13	7121	12012	942	1083	0.747	18.1	0.099
0.40	3.64	8282	13968	1095	1259	0.868	21.1	0.116
0.45	4.17	9477	15985	1253	1441	0.994	24.1	0.134
0.50	4.71	10709	18063	1416	1628	1.123	27.2	0.152
0.55	5.27	11976	20200	1584	1821	1.256	30.5	0.172
0.60	5.84	13279	22398	1756	2019	1.392	33.8	0.192
0.65	6.43	14618	24655	1933	2222	1.533	37.2	0.213
0.70	7.04	15992	26974	2115	2431	1.677	40.7	0.236
0.75	7.66	17402	29352	2302	2646	1.825	44.2	0.259
0.80	8.29	18848	31790	2493	2865	1.976	47.9	0.284
0.85	8.95	20329	34289	2689	3091	2.131	51.7	0.310
0.90	9.61	21846	36848	2889	3321	2.290	55.5	0.337
0.95	10.30	23399	39467	3095	3557	2.453	59.5	0.366
1.00	11.00	24987	42146	3305	3799	2.620	63.5	0.396

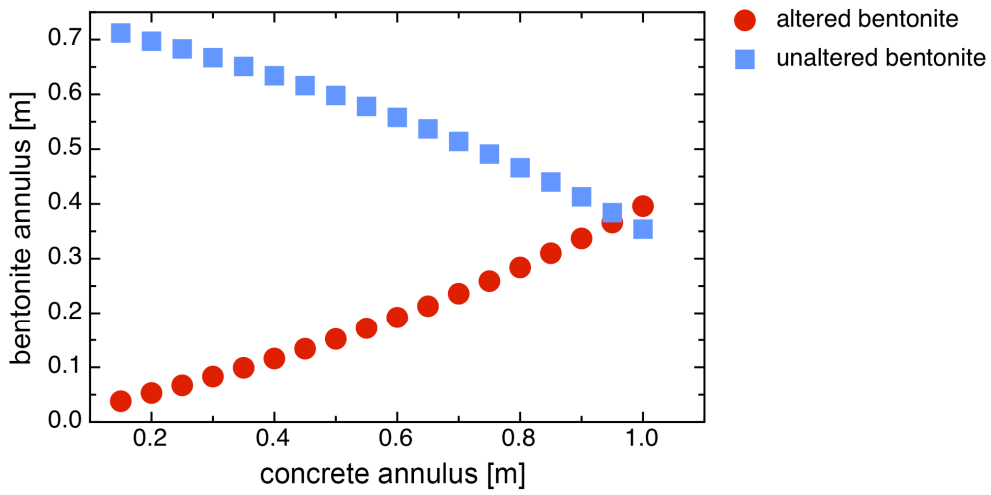

Fig. B-1: Effect of concrete tunnel liner thickness on the thickness of alteration of bentonite.

Conclusions

A mass balance approach to the estimation of alteration of compacted bentonite in contact with an OPC-type concrete tunnel liner for disposal concept variant A shows that even a 1 m thick liner would still preserve an annulus of at least 0.35 m of unaltered bentonite over the long-term evolution of the system.